CONNECTED WATERS INITIATIVE
THE UNIVERSITY OF NEW SOUTH WALES
SCHOOL OF CIVIL AND ENVIRONMENTAL ENGINEERING
WATER RESEARCH LABORATORY

GEOCHEMICAL AND GEOPHYSICAL SAMPLING CAMPAIGN AT MAULES CREEK – DATA REPORT FOR 2006.

Prepared by

Martin Søgaard Andersen
R. Ian Acworth

July 2007

Cotton Catchment Communities CRC

BIBLIOGRAPHIC DATA SHEET

Report No. 229	Report Date: July 2007	ISBN: 0 85824 076 9

Title: GEOCHEMICAL AND GEOPHYSICAL SAMPLING CAMPAIGN AT MAULES CREEK – DATA REPORT FOR 2006

Author(s) Martin Søgaard Andersen
R. Ian Acworth

Sponsoring Organisation Cotton Catchment Communities – CRC

Supplementary Notes

The work reported was carried out under the direction of the Director of WRL.

Abstract

This report describes the preliminary data of a study of surface water groundwater interactions in the Maules Creek catchment, Namoi Valley, NSW, Australia. Physical and hydrochemical processes were studied in the aquifer and streams of the catchment during 2 field campaigns.

In the up gradient part of the study site, zones of groundwater discharge were identified largely based on temperature anomalies and EC variations. Further downstream zones where the stream appears to be recharging the aquifer were identified based on the geology and vertical gradients in hydraulic head as well as electrical conductivity and the chemical signature of water samples. Geological heterogeneity appears to be an important factor in controlling the occurrence of surface water flow and the exchange of water between stream and aquifer. Groundwater extraction probably enhances aquifer recharge from surface water sources.

The results of this study show how a combination of hydrological and natural hydrochemical tracers can be used to unravel surface water groundwater interactions.

Distribution Statement

For general distribution

Descriptors

Groundwater, surface water, hydrochemistry, Murray-Darling Basin, geology, temperature, geophysics

Identifiers

Maules Creek catchment, Namoi Valley, NSW

Number of Pages: 63	Price: On Application.

CONTENTS

Abstract

This report describes the preliminary data of a study of surface water groundwater interactions in the Maules Creek catchment, Namoi Valley, NSW, Australia. Physical and hydrochemical processes were studied in the aquifer and streams of the catchment during 2 field campaigns (August and October 2006) using a combination of geological, hydrological and hydrochemical data encompassing among others: lithological logs; geophysical well logging; stream water levels; aquifer head distributions and hydrographs; water temperature; resistivity imaging, fluid EC; and a suite of hydrochemical parameters in both surface water and groundwater.

In the up gradient part of the study site, zones of groundwater discharge were identified largely based on temperature anomalies and EC variations. Further downstream zones where the stream appears to be recharging the aquifer were identified based on the geology and vertical gradients in hydraulic head as well as electrical conductivity and the chemical signature of water samples. Geological heterogeneity appears to be an important factor in controlling the occurrence of surface water flow and the exchange of water between stream and aquifer. Groundwater extraction probably enhances aquifer recharge from surface water sources.

Electrical conductivity (EC) was found to vary in a complex pattern in the catchment reflecting different sources of water in addition to water rock interactions within the aquifer. Generally EC and major dissolved ions increased in the aquifer along the hydraulic gradient due to leaching of salts from clayey lithologies and weathering of minerals. A redox sequence was observed with anoxic conditions developing along the hydraulic gradient, and in particular near the Namoi River. The variations in EC, major dissolved ion composition, and redox sensitive species were used to identify possible zones of surface water groundwater interactions and flow directions.

The results of this study show how a combination of hydrological and natural hydrochemical tracers can be used to unravel surface water groundwater interactions. The results of this study have implications for understanding stream fed aquifer recharge and in turn for estimating the sustainable extraction of groundwater from the regional aquifer. In addition understanding the hydrochemical processes may give important insights in the possible fate of various organic and inorganic pollutants linked to the infiltration of surface water or discharge of groundwater.

However, the data of this study (except for the groundwater and stream hydrographs) largely represent a given point in time and the complexity of the water exchange between streams and aquifer as a function of time is still poorly documented and far from being quantified or even understood in terms of processes. The temporal variation of the hydrological and the hydrochemical components of the system and their interactions require further study. For example, the direct recharge of precipitation; recharge from surface water streams due to flood events; as well as the human component: groundwater extractions; irrigation return flows and associated deep drainage; and release of dam water.

1. INTRODUCTION

This report contains field data collected during the winter and spring of 2006 (August to October) in the Maules Creek catchment (Groundwater management zones 5 and 11), NSW, Australia (see Fig. 1), as well as lithological and hydrological data from the database of the Department of Natural Resources (DNR, 2006). The report also contains preliminary interpretations and discussion of the hydrochemical, geophysical and hydrogeological data collected. The report should be viewed as work in progress and the interpretations as a first iteration in understanding the hydrological and geochemical processes in the catchment.

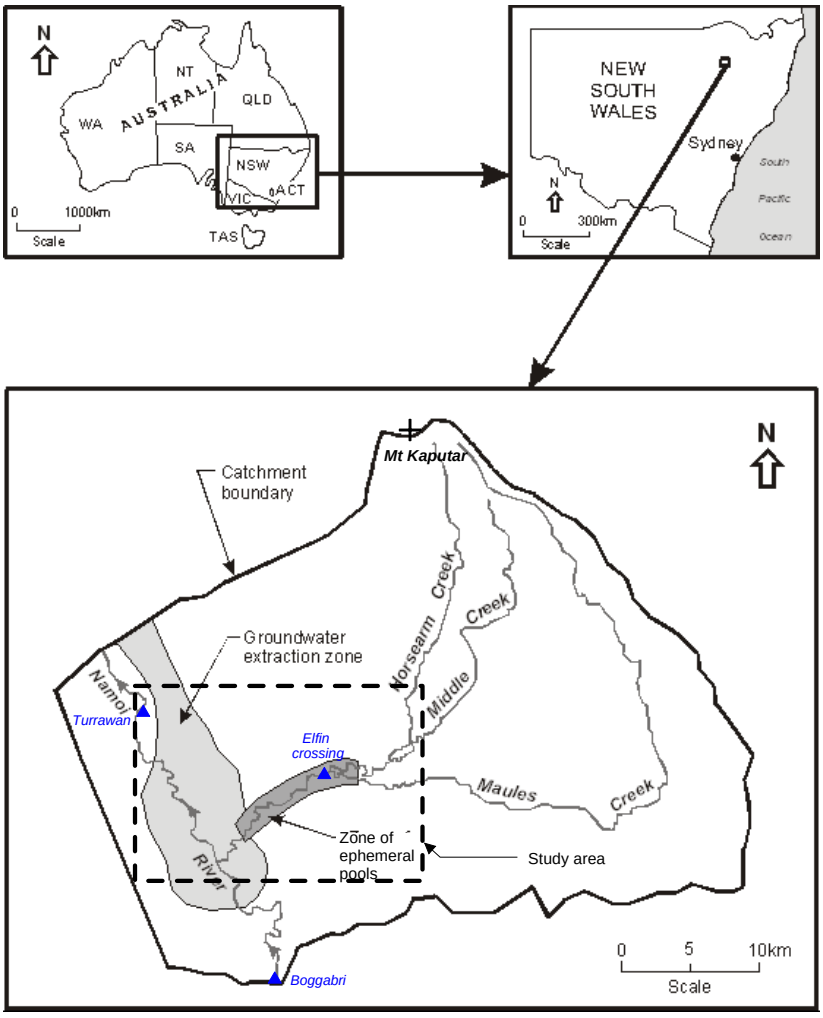

Fig. 1. Location of the study area in the Maules Creek catchment. The zone of groundwater extraction and the zone of ephemeral pools in Maules Creek are also shown. ▲ Denote locations of stream flow gauging stations.

The Maules Creek area was chosen as a study site because surface water flow in Maules Creek (see Fig. 2) appears to be almost exclusively controlled by surface water groundwater interactions (Sinclair *et al.*, 2005). This makes it an excellent site for studying

such interactions as well as a suitable site for developing and testing tools and methodologies for measuring surface water groundwater interactions.

The project was funded by the Cotton Catchment Communities-CRC (CCC-CRC Project No. 2.02.03).

Fig. 2. Pool on Maules Creek near the confluence of Maules Creek and Horsearm Creek. The uncharacteristic blue colour is probably a sign of groundwater discharge.

2. METHODOLOGY

During August 2006 (1st-18th) 28 bore locations containing 46 piezometers (see Fig. 3) in the Maules Creek catchment and an additional seven surface water sites on the Namoi River and Maules Creek were sampled. From 16th to 20th of October well positions and well levels were surveyed. In addition, a detailed survey of surface water electrical conductivity (EC), temperature and water elevations were done along a part of Maules Creek (blue dashed line in Fig. 3). From 23rd to 25th of October three resistivity imaging surveys were carried out: one in the dry creek bed of Maules Creek and two along the Namoi River (green lines in Fig. 3).

2.1 Hydrogeology and Positioning

Positioning of wells and water levels along the creek was obtained by RTK differential GPS using Trimble 5800 equipment. A base station was temporarily positioned on a state survey mark and in radio contact with the second roving GPS unit using a UHF radio. The RTK DGPS precision was generally better than 0.015 m in the horizontal plane and 0.02 m vertically. However, the precision below dense tree cover, especially in the creek bed, was considerably poorer with precisions sometimes in the order of meters. Water levels in wells were obtained by a manual dip meter.

A HACH SensION-156 EC-meter with a 4-pole conductivity probe was used to measure groundwater and surface water electrical conductivity (EC) and temperature.

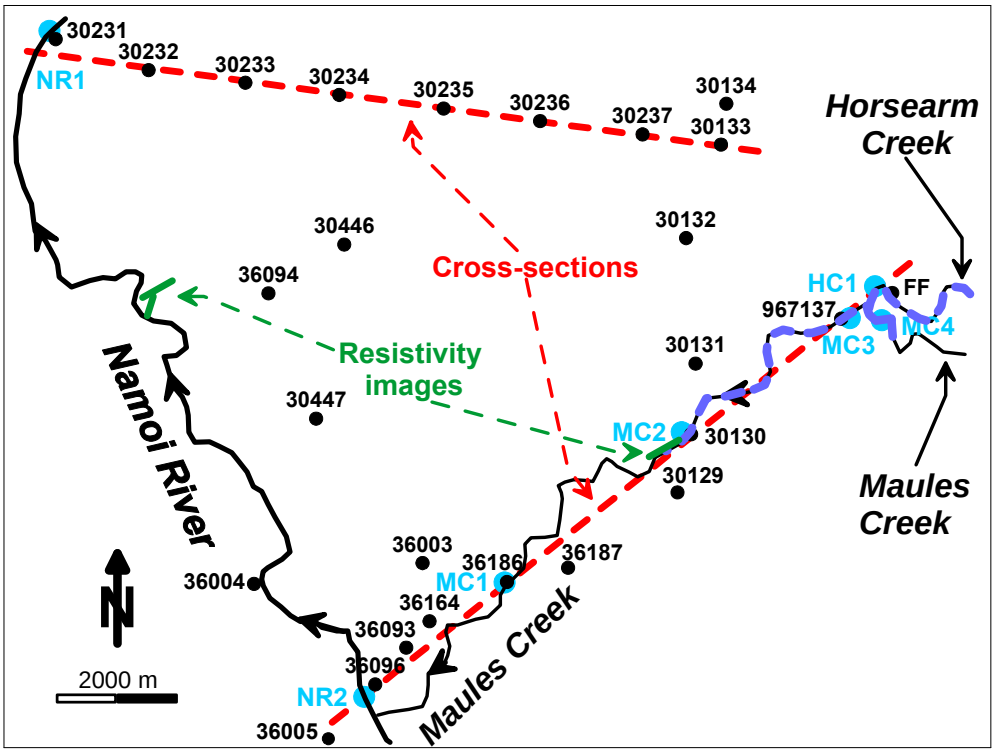

Fig. 3. Study area (location in the catchment see insert in Fig. 1). Black circles are sampled piezometers. Blue dots are surface water locations sampled during August 2006. Blue dashed part of Maules Creek and Horsearm Creek denotes the detailed surface water survey of water elevation and EC during October 2006. The green lines denote location of resistivity profiles.

2.2 Geophysical Methods

Geophysical logs were generally run in the deepest piezometer at each bore location. A Geovista logging system was used to run the logging tools (winch: GV 100 series, model 118). At each site the following logging tools were employed: calliper, natural gamma; and

EM39 (Geonics single spaced EM induction sonde). At selected sites a spectral gamma sonde and a Hydrolab mini sonde (temperature, EC and pH) were employed.

Resistivity imaging of the subsurface was obtained at selected sites in the creek bed by using multi-core cables with and an array of steel electrodes spaced 2.5 m or 5 m apart. The cables were connected to an ABEM LUND ES464 switching unit and to an ABEM SAS4000 Terrameter.

2.3 Water Sampling Methodology

A majority of the sampled bores were observation bores belonging to DNR and drilled between 1970 and 2005 to varying depths between 10 and 110 m. The screened intervals in the piezometers are typically between 1 and 6 m long, averaging 3 m. Generally the piezometers were purged one well volume with a pump placed just below the standing water level in the well. Subsequently a fresh groundwater sample was retrieved from the middle of the screened interval of the bore. Most groundwater samples were retrieved using a Bennett air driven sample pump (Model: 1800-8). For shallow wells (<30 m) the pump intake was lowered to the middle of the screened interval. For deeper wells (> 30 m) the pump intake was extended downwards by adding tubes to the bottom of the pump. In this way samples could be retrieved from as deep as 80 m. Wells deeper than 80 m were sampled at 80 m assuming that the water sampled represents fresh groundwater at the screen. Surface water samples were collected using a tube lowered to mid-water column. Luerlock syringes (60 mL) were used for collecting the samples.

An inline flow-through cell (Sheffield-LFC, Waterra, SLF) was used to obtain values of dissolved oxygen (DO), pH, EC and Eh with minimum contact to the atmosphere and to monitor whether wells were sufficiently purged for sample acquisition. DO and pH were determined using a HACH portable meter (HQ40d) connected to a HACH luminescent (LDO101-03) oxygen probe and a HACH pH electrode (PHC301-03), respectively. A HACH SensION-156 EC-meter with a 4-pole conductivity probe was used to measure electrical conductivity (EC) and temperature. The redox potential (Eh) were measured by an Orion Platinum Redox electrode (model 96-78) connected to a TPS-meter (WP-80).

Groundwater samples were collected directly from the sampling line without contact with the atmosphere using 60 mL Luerlock syringes (pre-rinsed 3-times with sample) and immediately filtered through Satorious minisart (Cellulose Acetate) 0.2 μm disposable filters. Sub-samples for major cations and minor trace elements were preserved in 20 mL PE-vials with 2 % of 5N HNO_3 and stored at 5 °C for later analysis. The PE-vials for

cations were pre-washed in a 10% HNO_3 solution. Sub-samples for anions were frozen in 10 mL PE-vials for later analysis. Samples for Dissolved Organic Carbon (DOC) were acidified with 1% concentrated H_2SO_4 and stored at 5 °C in 40 mL amber glass vials (ALS) for later analysis. Unfiltered samples for stable isotopes (^2H and ^{18}O) were stored inverted at room temperature in pre-rinsed 30 mL McCartney bottles. The samples for stable isotopes are currently being analysed.

2.4 Chemical Field Analysis

Alkalinity was measured in the field shortly after sample retrieval on a filtered 25 mL sub-sample by the Gran titration method (Stumm and Morgan, 1981) using a HACH Digital Titrator Model 16900 and cartridges with 0.16 N H_2SO_4. The pH readings for the titration were measured by a TPS WP-81 pH and temperature meter and a TPS pH gel-electrode.

Ferrous iron (Fe^{2+}) and hydrogen sulfide (H_2S) were determined spectrophotometrically in the field on filtered sub-samples minutes after sample retrieval using a HACH spectrophotometer DR 2800. Fe^{2+} was determined by the Ferrozine method (Stookey, 1970) and H_2S by the Methylene-blue method (Cline, 1967).

2.5 Chemical Laboratory Analysis

Major cations (Na, Ca, Mg and K) and trace elements (Sr, Fe, Mn, Ba, Li and Si) were determined by ICP-OES using a Perkin Elmer, Optima 3000DV. Anions were determined by IC on a Waters 430 Conductivity detector (for Cl, PO_4^{3-} and SO_4^{2-}) and a Waters 484 Tunable Absorbance detector (for Br, NO_2^- and NO_3^-) connected to a Waters 510 HPLC Pump and a Waters U6K Injector. Dissolved Organic Carbon (DOC) was measured on a Shimadzu TOC-5000A (version 4.30) analyser with a 1 min. pre-purging step to remove inorganic carbon (CO_2). A satisfying analysis quality was assessed by calculating the ion balance and comparing total dissolved solids (in meq/L) with EC/100 (Appelo and Postma, 2005). A vast majority of samples had a charge balance error of less than 5 % (see Appendix 1 where all the water chemistry analyses are collated in). Speciation and saturation index calculations were calculated using the code PHREEQC (Parkhurst and Appelo, 1999).

3. RESULTS

3.1 Geology

Cross-sections of the lithology were constructed on the basis of the bore logs (drillers logs – DNR, 2006). Two cross-section transects are shown in Figure 4 (for location see Fig. 3). The cross-sections are subjective interpretations of the geology, since correlations between bores kilometres apart are inferred. There are therefore several equally possible, yet different representations of the distribution of lithologies satisfying the bore log data. The cross-section in Figure 4a is based on the lithology in bores located on both sides of Maules Creek and the creek crosses the cross-section several times, whereas the cross-sections in Figure 4b is within the aquifer about 10 km north of Maules Creek and terminating at the Namoi River.

Cross-section 1 (Fig. 4a) along Maules Creek shows quite variable bedrock topography. The general trend is however, an increasing depth to bedrock westwards towards the Namoi River with a maximum depth of 110 m just east of the river. Part of the seemingly dramatic variation in bedrock elevation in the cross-section is due to the projection of bores on to the cross-section line. E.g. the deep notch at bore 30130 is likely to be oriented along the cross-section plane rather than perpendicular to it, and thus probably represents past erosion by Maules Creek. The bedrock consists of rhyolitic Permian volcanics in the western part of the cross-section (DMR, 1998). In places it appears to be overlain by basalts. Towards the east the bedrock is comprised of the Permian Maules Creek Formation with sandstones, shales and coal measures (DMR, 1998).

a)

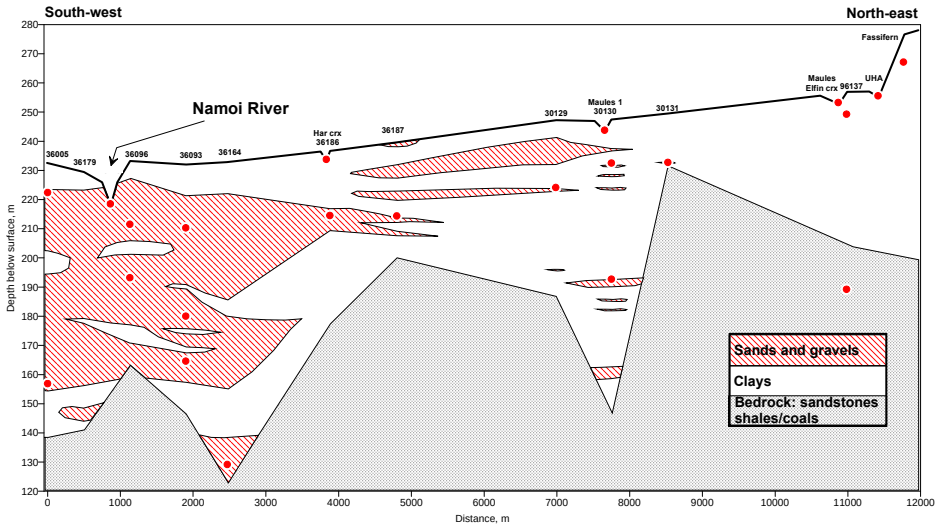

b)

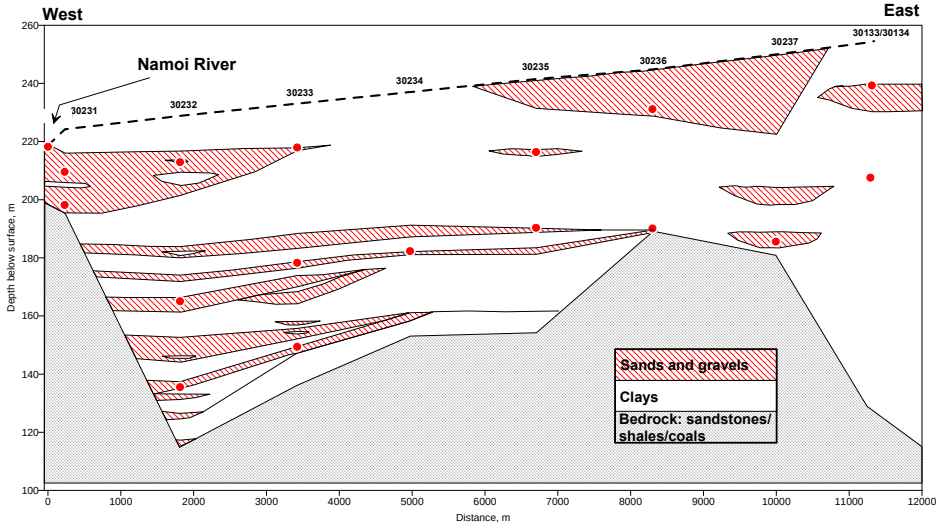

Fig. 4. Geological cross-sections based on lithological bore logs from the DNR database (DNR, 2006). Notches in the surface indicate where Maules Creek and the Namoi River cuts the cross-sections (for Location see Fig. 3). Dots denote the location of piezometer screens. a) Cross-section 1: oriented along Maules Creek b) Cross-section 2: oriented along the Narrabri-Maules Creek road.

Fluvial Quaternary sands, gravels and clays are deposited unconformably on top of the bedrock. In the Quaternary deposits there are generally a shift in texture from a clay dominated lithology in the east to thick deposits of sands and gravels in the west. The thick sequence of sands and gravel below the Namoi River will henceforth be referred to as the Namoi paleochannel. This picture is generally repeated in Cross-section 2 (Fig. 4b) to the north. However, the deposits of sand and gravel toward the west (and the river) are thinner than in Cross-section 1 and separated by several clay layers. In addition the bedrock to the west near the River appears to be the Maules Creek Formation with shales, sandstones and coal measures rather than the volcanic deposits in Cross-section 1.

3.2 Geophysical Results

3.2.1 Well Logging

A number of logging tools were run in most of the monitoring bores during August 2006. Fig. 5 shows some examples (additional logs are shown in Appendix 3). Fig. 5a show a log from bore GW 036164 in the western part of the study (location see Fig. 3).

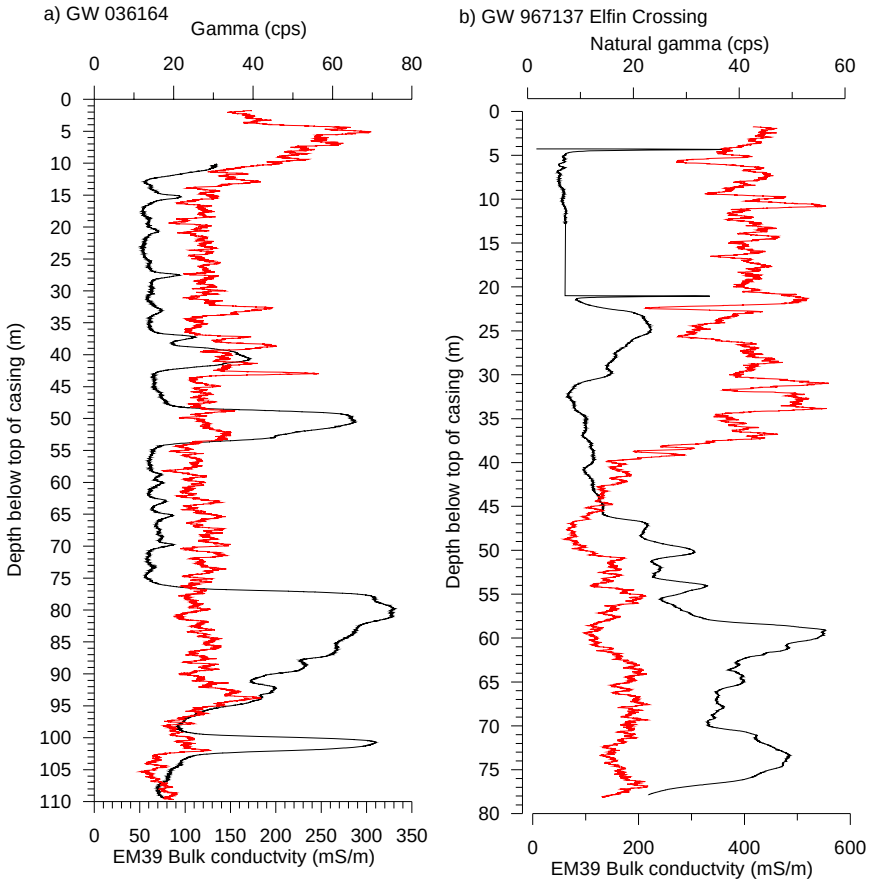

Fig. 5. Examples of geophysical bore logs from monitoring bores. Black lines denotes EM39 logs (mS/m) and red lines denotes natural gamma logs (cps). a) bore GW036164 and b) GW967137 at Elfin Crossing. For locations see Fig. 3 (additional logs see Appendix 3).

For this particular site the electromagnetic induction log (EM39) showed a good response for clay layers (at 40, 50 and 80 m). The gamma log surprisingly appears to have problems distinguishing between the clayey and the sandy and gravely lithologies. An explanation could be that the Quaternary sands and gravels of the Maules Creek Catchment are derived from the volcanic Mt Kaputar complex having very high potassium (K) content (DMR, 2002). The K content in the clay layers and the more coarse alluvium could therefore be comparable. In contrast, the logs from the bore GW967137 at Elfin Crossing (Fig. 5b) show a distinct decrease in the gamma signal at 39 m. In this case the decrease appears to correlate with the interface between the K-rich Quaternary deposits and the seemingly more potassium deprived Permian Maules Creek Formation. However, more work needs to be done on the interpretation of the geophysical logs and correlating them with the geological information from the drillers logs.

3.2.2 Resistivity Imaging

A resistivity image was carried out in the creek bed of Maules Creek (Property of Ian Norrie) starting at (UTM zone 56; 216706.9; 62020.8) and running east (location, see Fig.

3). The image shows (Fig. 6) an upper zone of 2-3 m with a resistivity ranging from 40–770 Ω·m. Below this zone the resistivity drops to between 3 and 40 Ω·m, with some zones/pockets of resistivity up to 100 Ω·m. A lithological interpretation of the image needs validation by bore log-data of which there are none next to the image line. However, the upper high resistivity zone probably represents variably saturated cobbles and gravels occupying the upper 2-3 m of the creek bed in Maules creek. Below this, a qualified guess could be that the low resistivity could indicate a predominantly clayey lithology. This is in accordance with the bore-log from 30130 (a couple of 100s meters away) which show essentially clay in the upper 40 m. It is possible that the higher resistivity zones (up to 100 Ω·m) at depth represent a more sandy/gravely composition. Such zones could be permeable conduits connecting the creek bed to the aquifer below.

Two profiles were carried out on the property of Darren Eather near the Namoi River (UTM zone 55; 783230.5; 6623820.2, see plots in Appendix 4 and Fig. 3 for approximate location). Profile 1 starts at the edge of the Namoi River crosses an elevated floodplain with sparse River Redgums to end at the edge of a wheat field (see Fig. A.4.1 in Appendix 4). The resistivity in the image is ranging between 6-130 Ω·m. In the deeper parts, 10 m below the surface resistivities are between 40-130 Ω·m reflecting predominantly sand and gravel. The upper 10 m seems more heterogeneous with zones of low resistivity (6-40 Ω·m) indicating zones of more clayey lithology. These zones apparently correlate with topographical depressions: sites where clay may accumulate during flooding events. At the time of measurement the river had a fluid conductivity of 439 μS/cm (T = 22.1°C).

Profile 2 (see Fig. A.4.2 in Appendix 4) was carried out on the same property, 200 m further north starting at the eastern edge of a wheat field and running almost due west, to stop about 50 m short of the river. From 0 to 560 m the upper 3 to 7 m of this profile appears to be dominated by rich clay possibly saturated by irrigation water with resistivities from 4 to 40 Ω·m. Below 3 to 7 m the lithology is predominantly sandy/gravely (resistivity ranging between 40-420 Ω·m). However, zones of lower resistivity (~40 Ω·m) indicate a more clayey lithology. It is therefore possible that the sand and gravel layers are hydraulically discontinuous along the plane of the profile. Towards the bottom of the profile the resistivity decreases indicating a more clayey lithology (resistivity < 40 Ω·m). West of the wheat field (+560 m) towards the river clay is again (as in Profile 1) associated with the topographical depression. From 560 to 800 m heterogeneity in the resistivity distribution seems to be elevated with the higher resistivities near the surface (1-5 m) related to areas covered with trees.

In summary, at the Maules Creek site the lithology appears to be predominantly clayey at depth. Cobbles and gravels occupy the upper 2-3 m of the creek bed. In contrast, at the Namoi site, sand and gravels appear to be the dominating lithology at depth (5 to 20 m). Clay seems to be associated with the upper part of the wheat field and topographical depressions in the river plain (4 to 40 Ω·m).

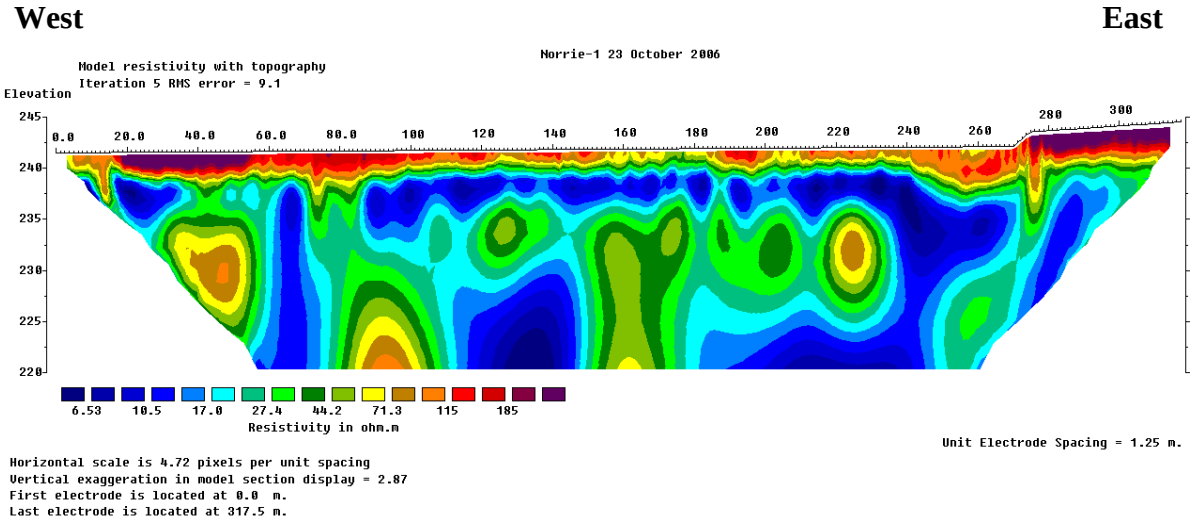

Fig. 6: East-west trending resistivity image in the creek bed of Maules Creek (on Ian Norries property, for location see Fig. 3). Additional images are in Appendix 4.

3.3 Hydrological Data

3.3.1 Flow Gauging Data

Continuous daily flow monitoring is carried out at three sites in the catchment (see Fig. 1 for location). In Maules Creek, measurements have been made since 1972 at a gauging station at Elfin Crossing. Fig. 7a shows stream flow from 24th of February 2006 to 18th of April 2007 encompassing the two field campaigns of this study. The recorded daily discharge shows some rather erratic variations. Particularly conspicuous are the short periods of low flow, which seem hard to explain in terms of hydrologic processes, unless pumping in the order of 4-8 ML/d is done directly from the creek or in the alluvium close to the bank. However, the overall long term decrease from about 8 ML/day in June to zero in mid December is consistent with field observations. On the 6th of August the stream flow was manually assessed at the weir at Elfin crossing to be 6 ML/d, which compares well with the 5 ML/s from the gauging station. During the August sampling campaign the stream flow decreased from 6 to 3 ML/d and for the October campaign the flow was around 2 ML/d.

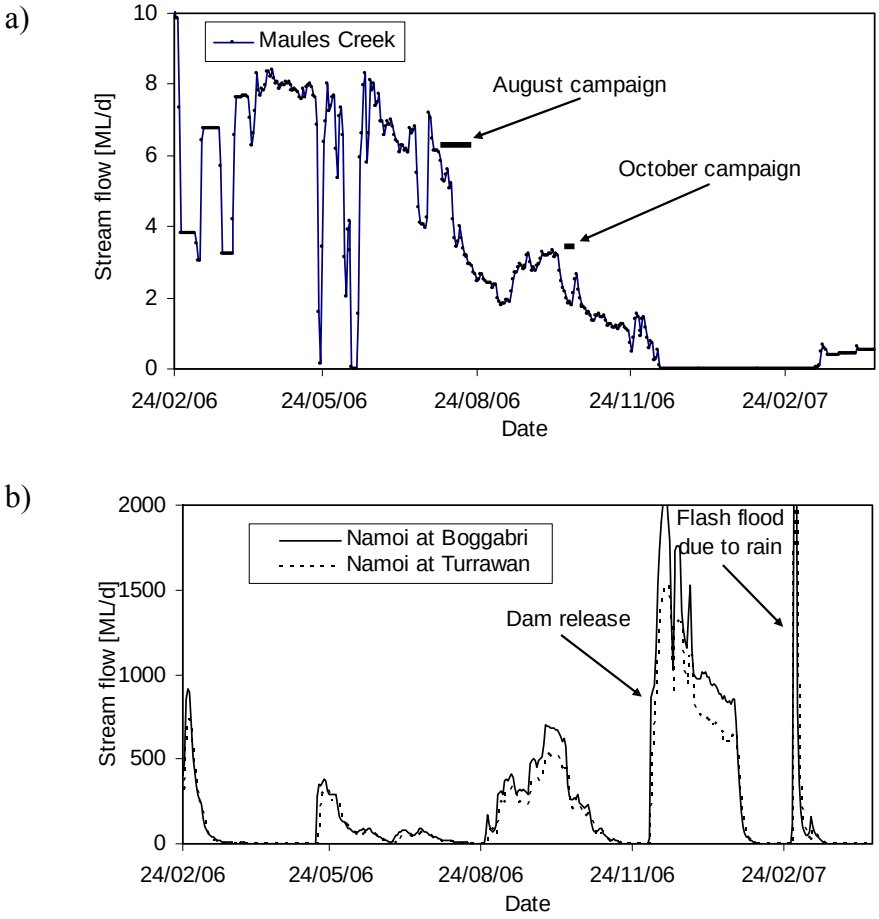

Fig. 7. Stream discharge from 24th of February 2006 to 18th of April 2007 (ML/d) at a) Elfin Crossing in Maules Creek and b) Boggabri and Turrawan in the Namoi River (DNR, 2007). Locations see Fig. 1.

Stream flow of the Namoi River (Fig. 7b) is monitored at two sites in the Maules Creek catchment: upstream at Boggabri (since 1913) and downstream at Turrawan (since 1953). The temporal variations in the Namoi are fundamentally different from Maules creek reflecting that the Namoi is a regulated river where major flow occurrences are often caused by dam releases. However, rapid floods do also occur and appear to move rapidly through the system as seen for the flood in the beginning of March 2007. In contrast, this event seems to have a longer duration in Maules Creek (Fig. 7a), perhaps fed by groundwater derived base flow.

An interesting feature of the stream flow data from the Namoi is the consistently lower downstream flow at Turrawan. This loss between Boggabri and Turrawan must largely be aquifer recharge (and perhaps some surface extraction for irrigation). Bank-storage and subsequent release would produce a delayed base-flow. So bank-storage is probably insignificant, since there does not seem to be evidence of a tail of stream flow at Turrawan compared to Boggabri following major flow events (Fig. 7b).

3.3.2 Creek Water Levels

In the beginning of the August sampling campaign the creek was flowing past the Harparary Crossing (3.5 km upstream of the confluence with the Namoi). The flowing reach was more than 8 km. During the 3 week sampling campaign the flow ceased at Harparary (and several 100 m upstream). Later in October surface flow had receded more than 4 km upstream and the flow rate had diminished significantly at Elfin Crossing compared to August (see insert in Fig. 8a). These observations and the stream flow data of Fig. 7 highlight the dynamic nature of flow in Maules Creek.

In August surface water levels were estimated for 3 sites and compared to levels in nearby piezometers (Fig. 8b). For the upper part of the creek near Elfin Crossing vertical gradients were negligible between the creek and the upper part of the aquifer. This indicates mainly horizontal flow in the creek alluvium with possibly no significant exchange with the deeper aquifer at the time of measurement. However, further downstream near the Harparary Crossing downward head differences of up to -4.4 m were observed (corresponding to a gradient of approx. –0.23 m/m). This, and the downstream termination of flow, indicates that the creek was recharging the aquifer in this part of the reach.

During October 2006 a detailed survey of water levels in the pools and the flowing parts of Maules Creek and Horsearm Creek showed a surface water hydraulic gradient trending to the west-south-west (Fig. 9). For the lower section of the creek containing seemingly stagnant pools a very uniform gradient ($dh/dx = 0.0025$) was observed (Fig. 10). This probably implies that the pools are in hydraulic contact with flow occurring in the sands and gravels of the streambed. In the Horsearm creek the gradient appears steeper (Fig. 10a, open symbols), however, this observation is questionable since the surveying precision was rather poor due to the dense vegetation cover.

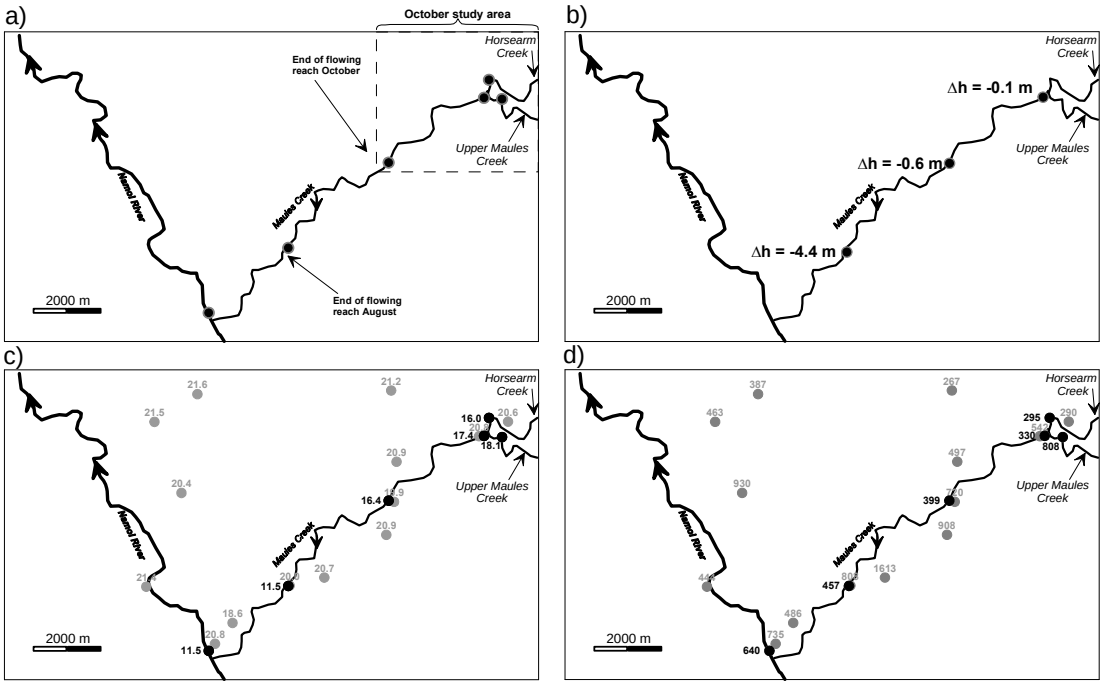

Fig. 8. The Maules Creek study site in August 2006. a) Location of surface water sampling sites. Insert shows area investigated during end of October; b) Vertical head differences (Δh) between surface water and groundwater for three sites (negative for a downward gradient); c) Temperature (°C), black numbers and symbols are for surface water measurements in Maules Creek whereas grey numbers and symbols are for shallow groundwater less than 30 m.b.s.; and d) Electrical conductivity (µS/cm) measured in Maules Creek (same symbol and number colouring as in c)).

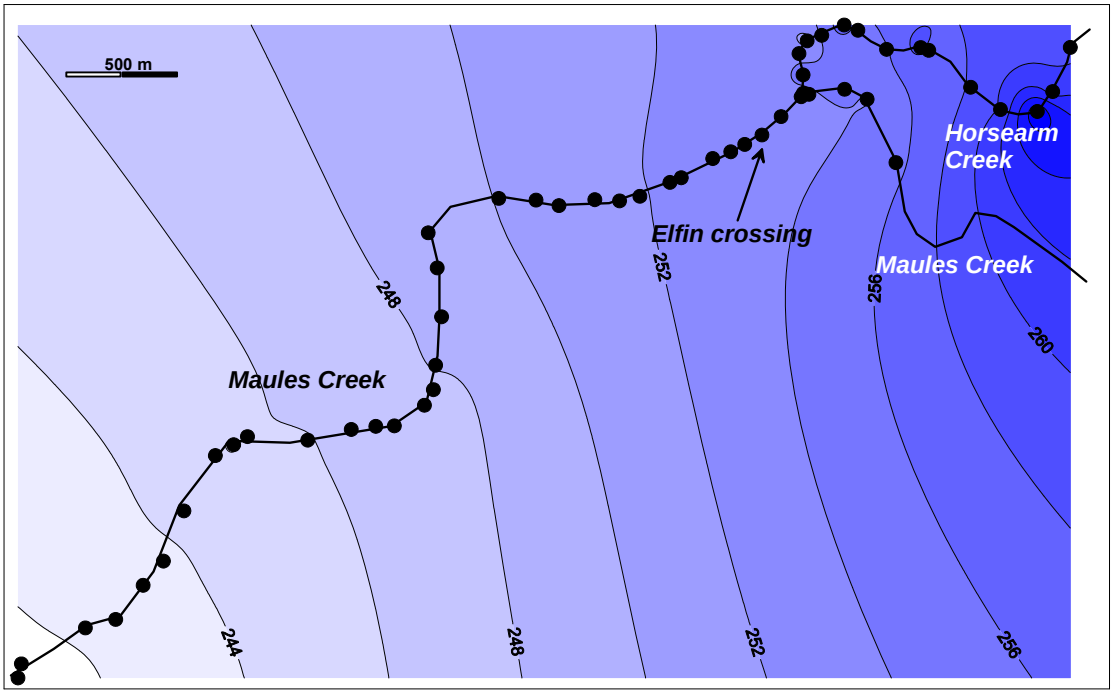

Fig. 9. Contour map of surface water heads (m AHD) in the Maules Creek and its tributary Horsearm Creek measured in October 2006.

3.3.3 Creek Temperature

In August (winter) surface water temperatures were measured at 5 sites along the creek (Fig. 8c) and within the aquifer in selected monitoring wells. In the aquifer the groundwater temperature was very uniform averaging 21.1 °C (std = 0.8, n = 46) reflecting the average annual air temperature of the region (Fig. 8c). In contrast the measured surface water temperatures, even at midday, are generally lower due to the cooler winter air temperatures. In the upper section where the creek starts flowing the surface water temperatures are anomalously high for the season: 16 to 18.1 °C, reflecting the discharge of relatively warm groundwater. Downstream, the surface water temperatures drop to around 11.5 °C, because of the cooling by the low winter air temperatures and no additional groundwater inflow. The measured water temperatures seem to indicate that groundwater is actively discharging in the upper part of Maules Creek and its tributary Horsearm Creek. Later in spring (October), temperature measurements did not give any clues about groundwater discharge as air temperatures were warming up. Surface water temperatures were warmer and varied more erratically (20 to 35 °C) due to the much warmer weather (Fig.10c).

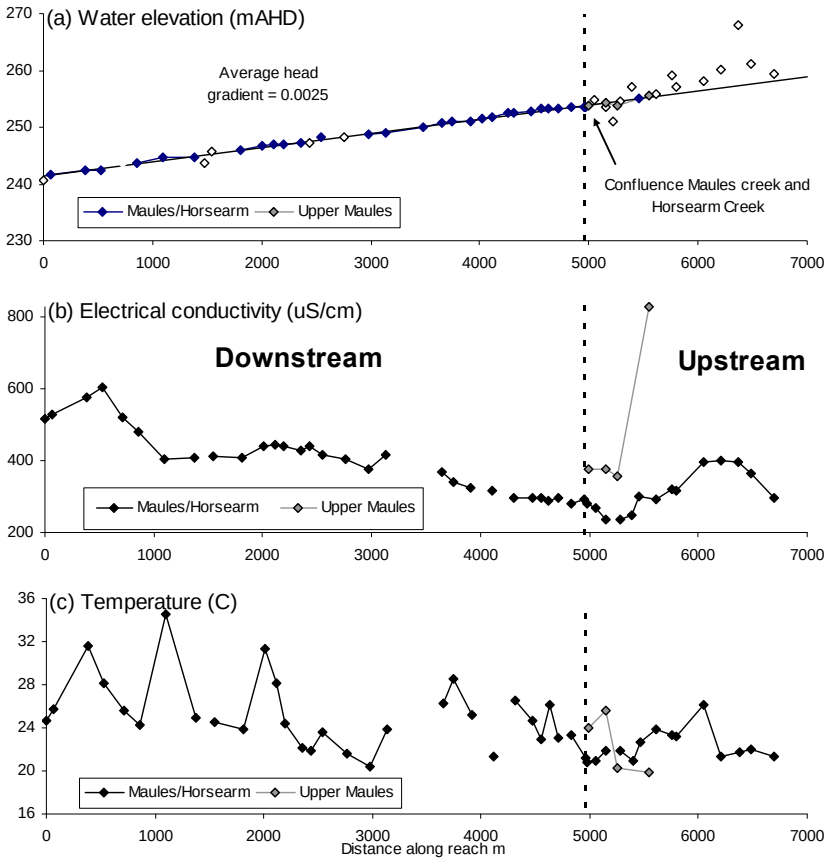

Fig. 10. a) Surface water elevation; b) electrical conductivity (EC) and c) temperature measured in Maules Creek during October 2006. Solid diamonds in a) indicate high precision positioning ($h \leq 0.015$ m, $v \leq 0.02$ m) whereas open diamonds indicate pore precision due to dense tree cover. Grey diamonds indicate measurements in the Maules Creek upstream from the confluence.

3.4 Hydrogeology

3.4.1 Aquifer Water Levels

Water levels in the aquifer were measured in August (1st-18th) and October (16th - 20th) 2006 in relation to the sampling. Figure 11 show the hydraulic head distribution in the upper part of the aquifer (< 30 m) in August. Generally the inferred groundwater flow is westwards, but tending south-west in the southern part paralleling the orientation of Maules Creek. In the deeper parts of the aquifer the flow directions only vary marginally from the upper part (see Appendix 5 and 6 for plots). In general there seems to be a downward head gradient from the upper to the lower part of the aquifer as indicated by cross-section plots of point water heads (Fig. 12a,b). The vertical gradients seem more pronounced in the Maules Creek cross-section (Fig. 12a) than in the Northern cross-section (Fig. 12b). This could possibly be due to infiltration of stream water in the Maules Creek cross-section. The head differences are more clearly seen from head difference calculations at sites with several piezometers situated at different depths (Fig. 13a). In August the downward vertical head difference is up to 5.6 m and generally largest somewhat to the east of the paleochannel (Fig. 13a).

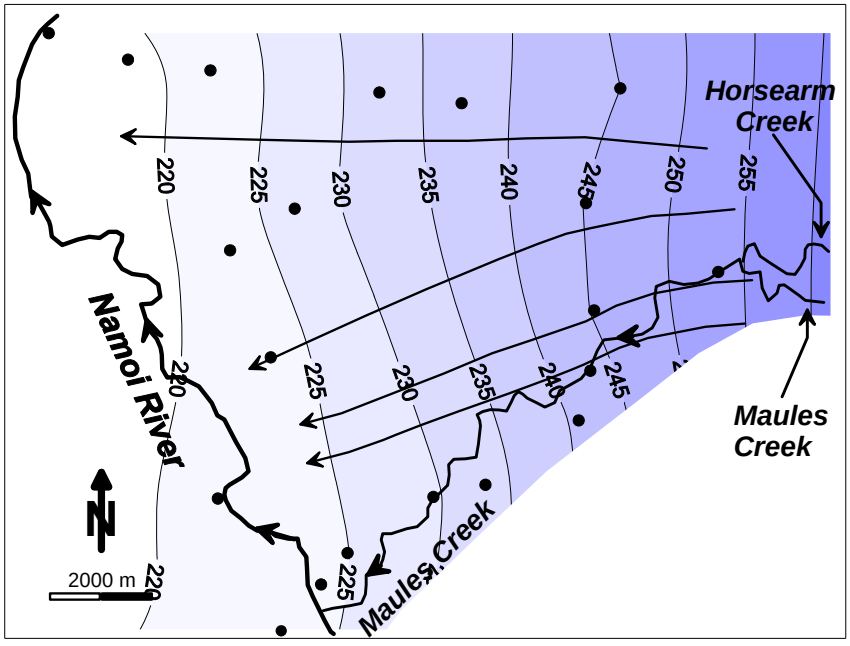

Fig. 11. Hydraulic head distribution (mAHD) in the upper part of the aquifer (< 30 m) in August 2006. Arrows indicate the general flow paths. Additional plots for August and October are shown in Appendix 5 and 6.

The general head distribution in the aquifer and the inferred direction of groundwater flow did not change significantly from August to October (Appendix 5 and 6). However,

drawdowns of up to 8.8 m were observed between August and October presumably due to the onset of groundwater extraction for irrigation during spring (Fig. 14). Locally this extraction of groundwater would significantly change the flow conditions near pumping wells. The drawdown was most pronounced in the western part (Fig. 14) and associated with the Namoi paleochannel. In addition, the maximum downward vertical head gradient has nearly doubled from 5.6 m up to 9.1 m in October (Fig. 13b).

a)

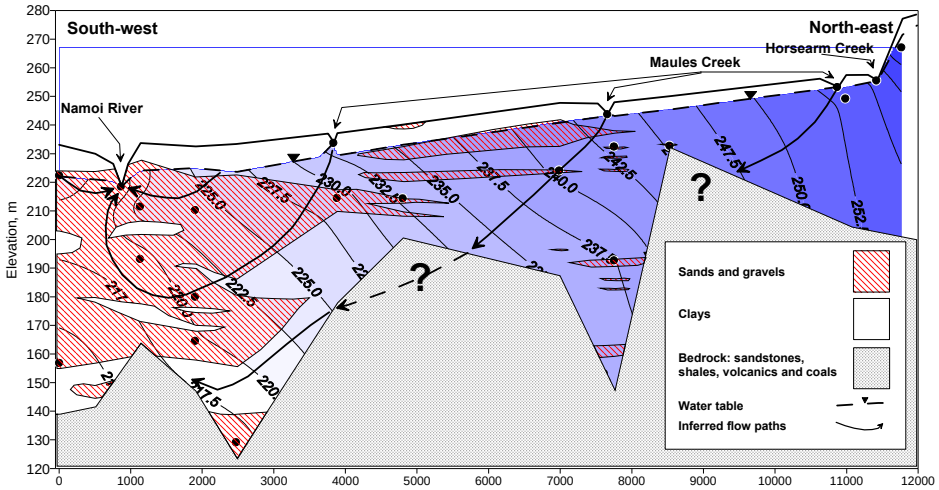

b)

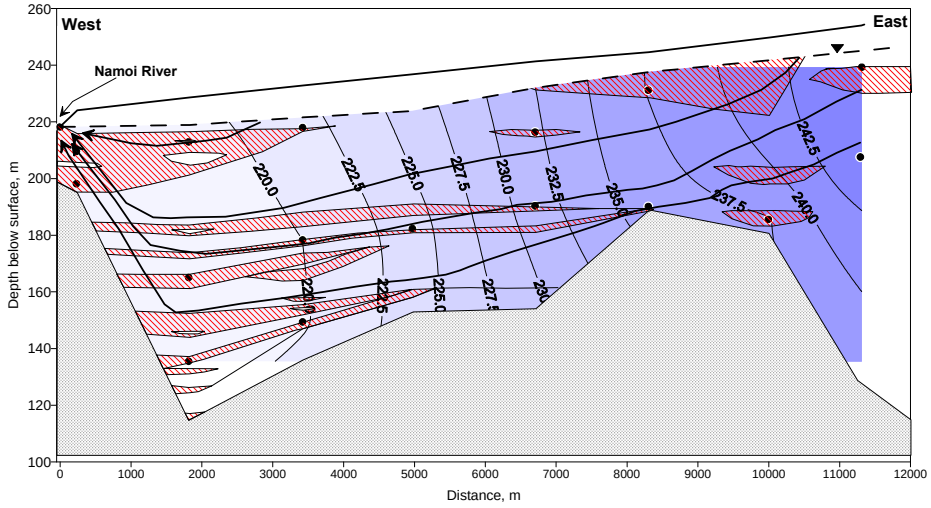

Fig. 12. Cross-sections of point water heads for August 2006. Dots denote the location of piezometer screens. a) Cross-section 1: oriented along Maules Creek b) Cross-section 2: oriented along the Narrabri-Maules Creek road. For Location see Fig. 3.

a)

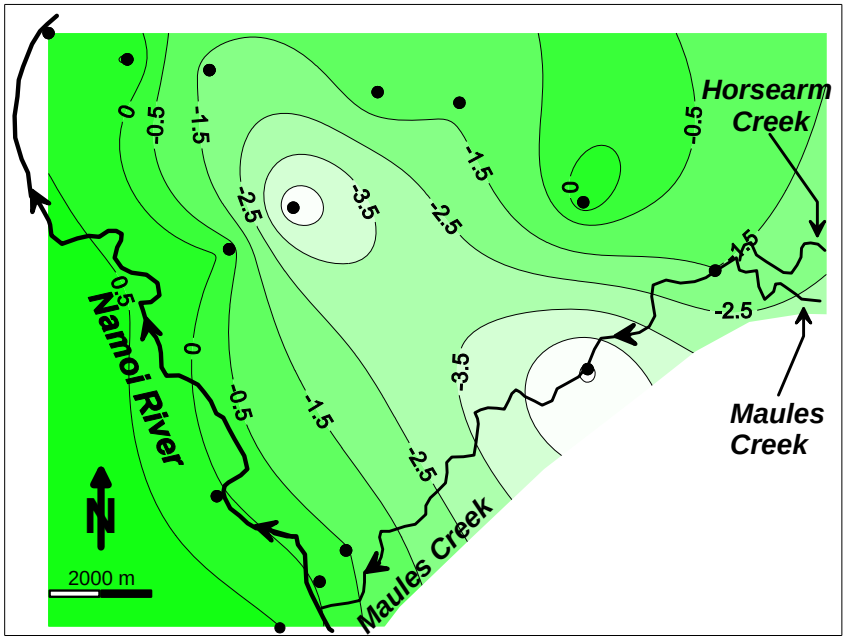

b)

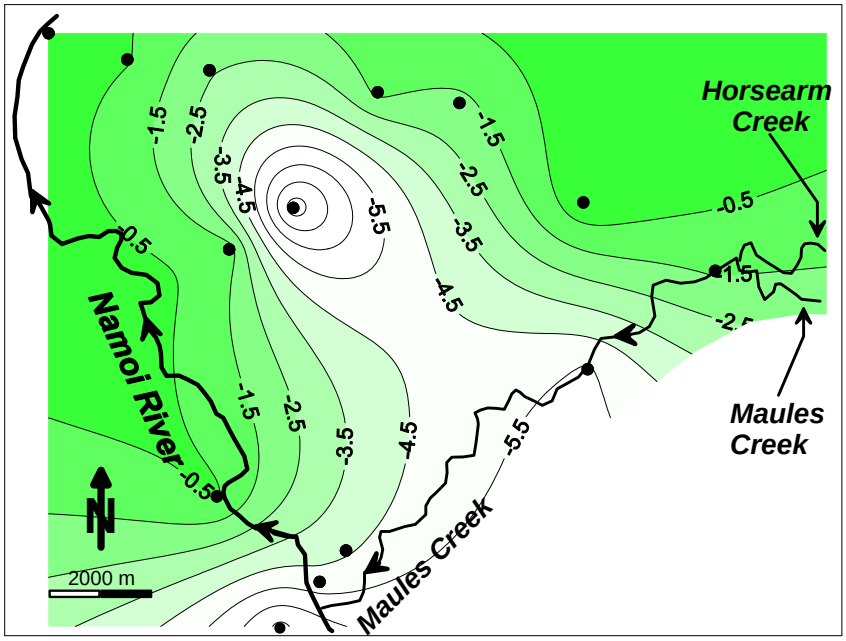

Fig. 13. Head differences (m) between piezometers placed in the upper and lower parts of the system, respectively. a) August 2006 and b) October 2006. Negative values are for downward gradients.

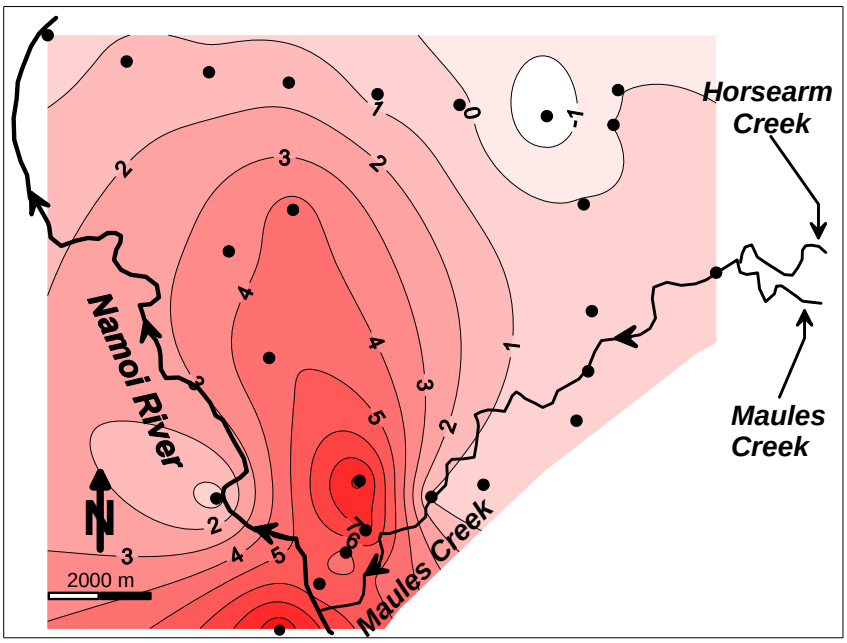

Fig. 14. Change in hydraulic heads (m) between August and October 2006. Positive values indicate drawdowns.

3.4.2 Well Hydrographs and Groundwater Extraction

Some of the monitoring wells of the study area have been monitored by DNR since the early seventies. The resulting hydrographs show long term trends in the general water table, major recharge events and the effects of seasonal groundwater extraction for irrigation. The hydrograph for the piezometers at GW030233 (Fig. 15a for location see Fig. 3) exemplifies all these features: generally a long term decreasing trend in water levels can be observed with a drop of about 5 m since the early seventies. In addition, the hydrographs show the onset of seasonal groundwater extraction around 1985. Furthermore, at locations with several piezometers screened at different depths they may reveal temporal changes in vertical gradients. In Fig. 15a a significant downward gradient between the upper and two lower piezometers is clearly seen. It increases from 1 to 2 m in winter to more than 5 m during the pumping season. Finally, major aquifer recharge events are seen in e.g. 1976, 1977, 1984 and 1998. This is more evident at the piezometers at GW036093 (Fig. 15b for location see Fig. 3). The sharp peaks in the hydrographs at GW036093 appear to indicate that they are closer to the recharge source than the hydrographs at GW030233. GW036093 is closer to Maules Creek and the Namoi River. This could indicate that the source of recharge could be from either or both of the two streams. There is a clear correlation between high stream flow events and peaks in the hydrographs (see Appendix 7). However, it can not be excluded that the recharge source is direct recharge of precipitation through permeable layers.

a)

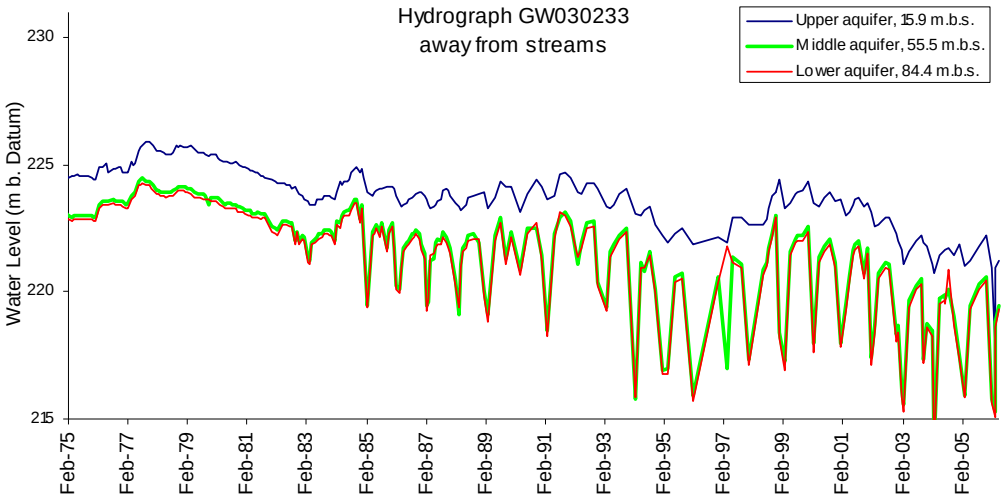

b)

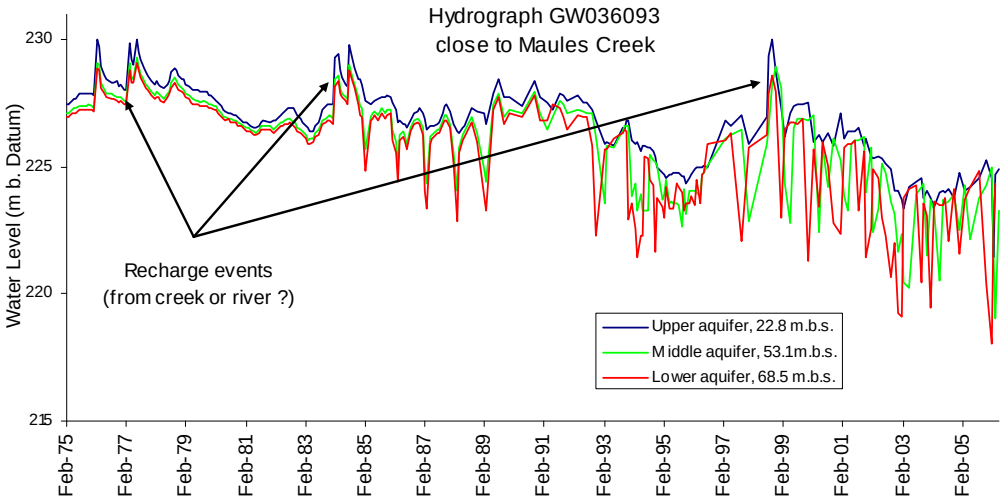

Fig. 15. Example of groundwater hydrographs showing an overall decreasing trend, effects of seasonal pumping and downward gradients. a) GW030233 located distant from streams (3400 m from the Namoi River) and b) GW036093 (460 m from Maule Creek and 620 m from the Namoi River). For locations see Fig. 3. A comparison between GW036093 and stream flow in Maules Creek and the Namoi River is shown in Appendix 7.

The shape of the hydrographs can be used to estimate the spatial extent of certain hydrographical units. This is shown in Fig. 16 where the location of the paleochannel clearly corresponds to the hydrographs showing strong seasonal variations due to groundwater pumping.

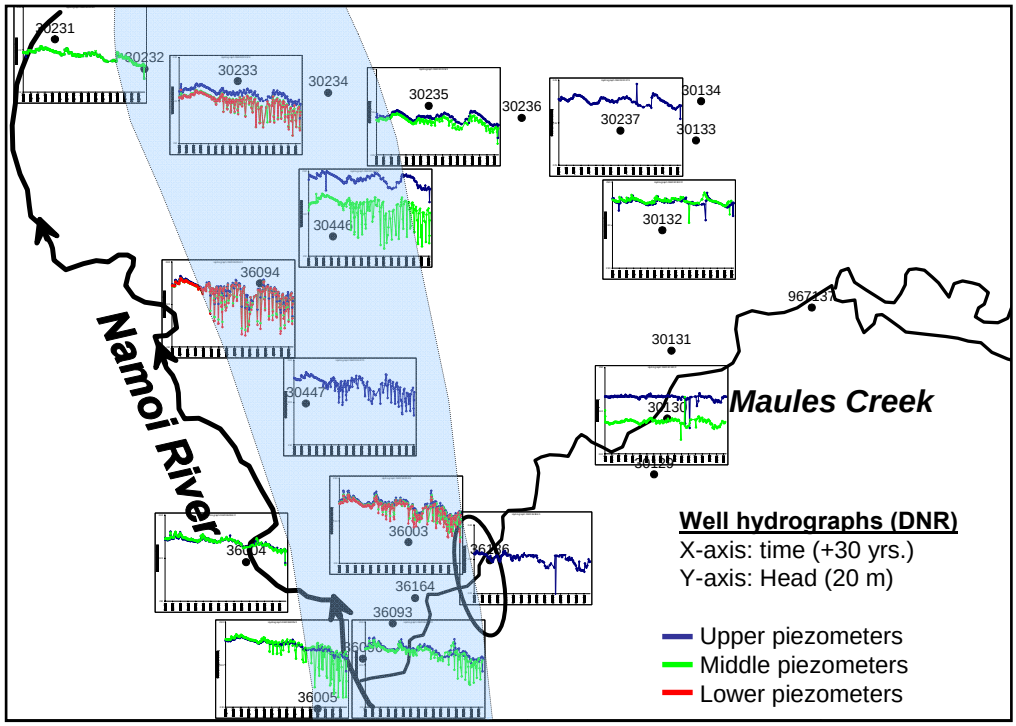

Fig. 16. Distribution of selected type hydrographs in the catchment.

3.5 Water Chemistry

3.5.1 Surface Water Quality

Surface water samples were taken from the 5 different sites along Maules and Horsearm creeks and additionally at 2 sites on the Namoi River. The surface water of Maules Creek is generally clear, well oxygenated and low in nutrients, indicating a natural system with only low levels of pollution (all chemical analyses are tabulated in Appendix 1).

Electrical conductivity, measured in August 2006, shows low EC groundwater (~300 µS/cm) in the Horsearm Creek and much higher EC (~800 µS/cm) in the upper Maules Creek. This probably reflects different sources of groundwater (with different degrees of mineralisation) from the north and south, respectively (Fig. 8d). Generally very fresh water derives from the Horsearm branch in the north and more mineralised water from Maules Creek upstream of the confluence. In addition, there appears to be a general increase in EC in Maules Creek downstream from the confluence. From the confluence of the Horsearm and upper Maules Creek and downstream to where the flow disappears, the EC increases from 330 to 457 µS/cm (Fig. 17a).

The increase in EC is reflected in most cations and anions measured in the surface water samples as seen for Ca (Fig. 17b) and alkalinity (Fig. 17c). Also pH was found to increase

down along the creek (Fig 17d), probably as a result of CO_2 degassing, which is hinted by the decreasing CO_2 partial pressure down along the reach (Fig. 17e). Dissolved silica (Si), as an exception, was found to decrease down the reach (Fig. 17f). See Appendix 8 for plots of additional parameters.

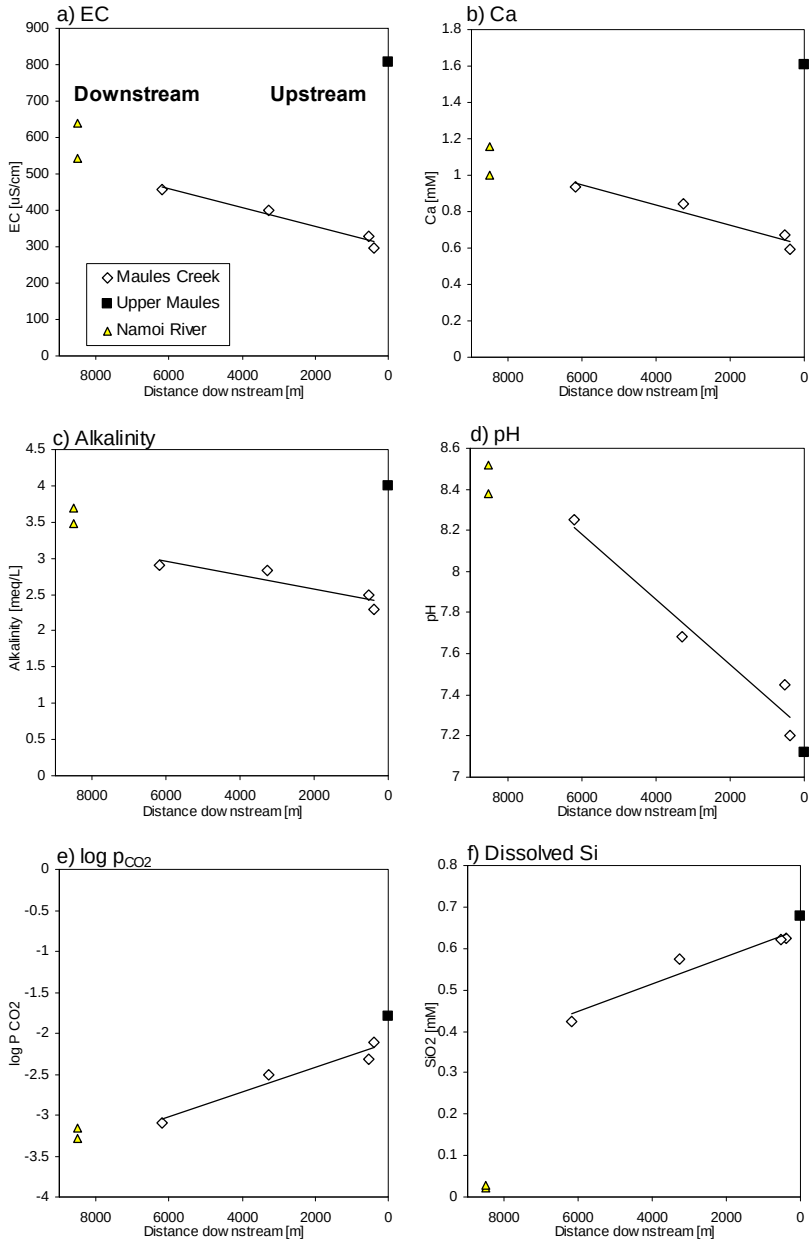

Fig. 17. Selected surface water chemistry parameters down along Maules Creek and the Namoi River. a) EC (uS/cm); b) Ca (mM); c) alkalinity (meq/L); d) pH; e) log(p_{CO2}) and f) Si (mM).

The increase in dissolved ions and EC reflects either mixing with, or an influx of higher conductivity groundwater, as suggested by groundwater EC measurements along the reach (see section 3.5.3 and Fig. 20) or evaporative concentration as water flows down along the reach. The first option is probably most likely considering the low evapotranspiration during winter. Furthermore the ratios of the major cations Na, Ca and Mg (and some minor

trace ions such as Sr) to Cl were found to decrease in the surface water down along Maules Creek (Fig. 18 and Appendix 8).

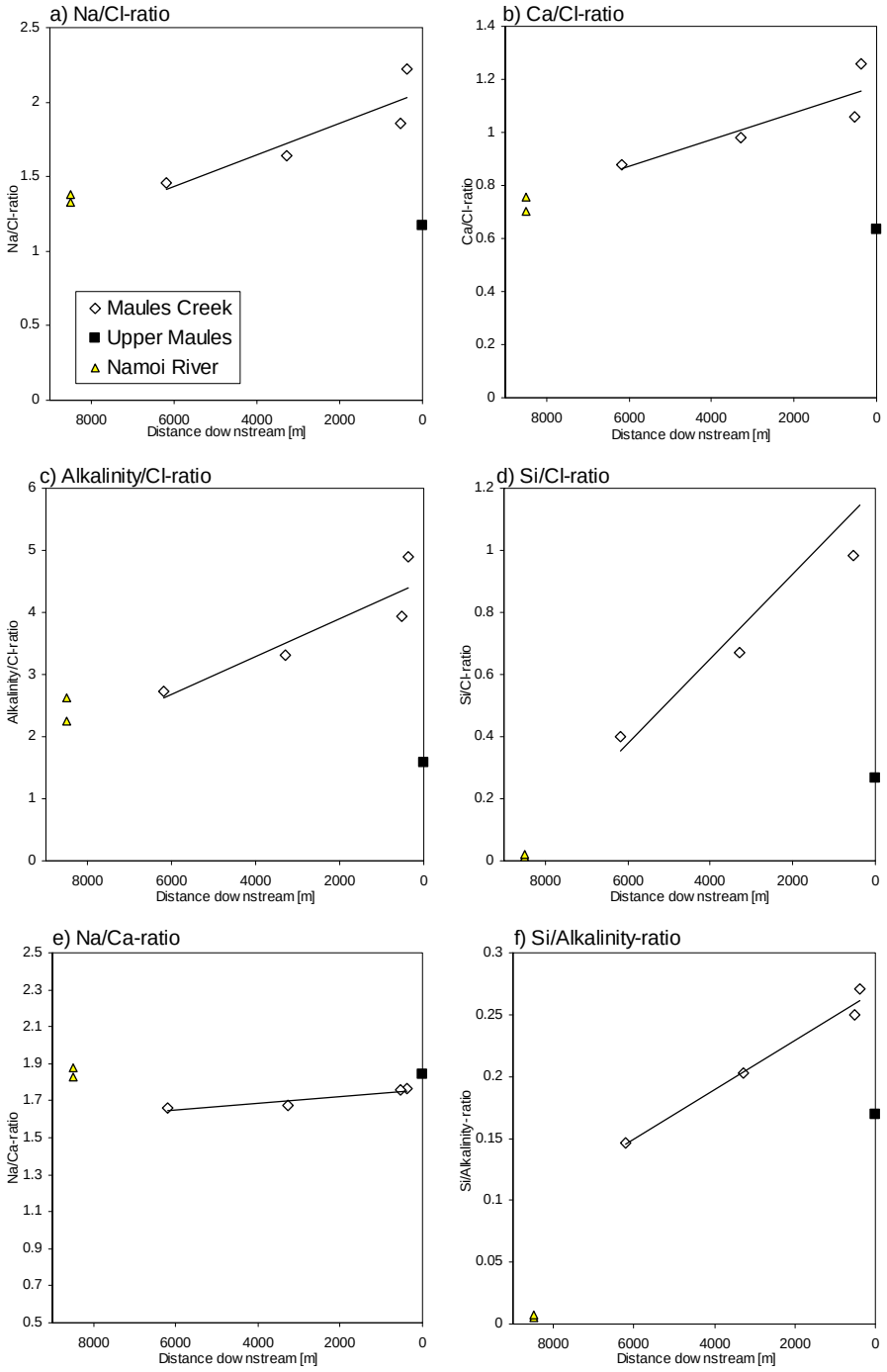

Fig. 18. Selected ion ratios. a) Na/Cl; b) Ca/Cl; c) Alkalinity/Cl; d) Si/Cl; e) Na/Ca; and a) Si/Alkalinity (see Appendix 9 for additional ion ratios).

Due to the consistent decrease for all cation/Cl ratios it seems likely that the increases in concentrations are not caused by evaporative concentration, because that would tend to maintain constant cation/Cl-ratios. Constant cation/Cl-ratios can only be maintained if no major mineral precipitation is occurring during the evaporative up-concentration. Based on

saturation index calculations with the speciation code PHREEQC (see Appendix 2) calcite was found to become supersaturated down along the reach (Fig 19a). Likewise certain silica phases such as quartz and chalcedony (Fig. 19b) were found to be supersaturated. This indicates that minor precipitation of calcite may be occurring and that some solid silica phase (not necessarily Chalcedony) is controlling the concentration of dissolved silica, as also hinted by the decrease in dissolved Si down along the creek (Fig. 17f). However, significant mineral precipitation does not seem to have been taking place, for the data at hand, based on the linear increasing trends in the cation concentrations down along the creek (Appendix 8). It could be speculated that the increase in dissolved ions is caused by re-dissolution of minerals precipitated in the creek bed in evaporating pools from the previous flow/year. An analysis of stable isotope data (O and H) may possibly answer this question. In summary, the increase in dissolved ions along Maules Creek appears to be largely caused by mixing with Cl rich groundwater down along the creek.

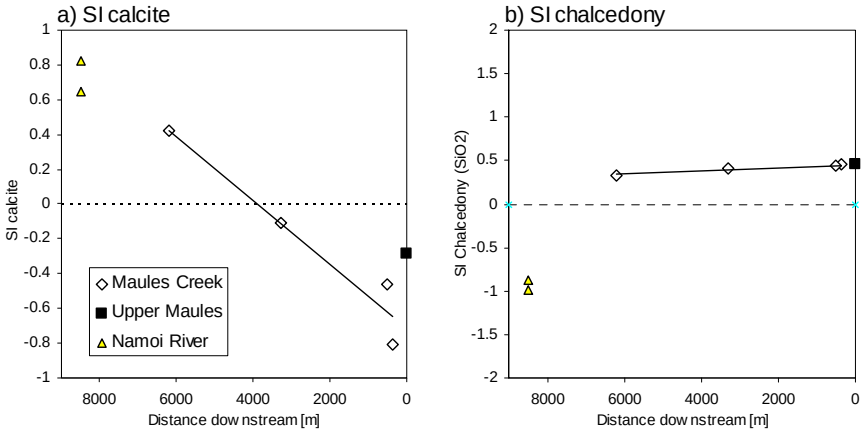

Fig. 19. Saturation indices calculated in PHREEQC for a) calcite and b) chalcedony (SiO_2). See Appendix 2 for saturation indices for additional mineral phases.

The surface water quality of the two samples from the Namoi differs from Maules Creek in several ways. In general the Namoi water appeared more turbid probably due to a higher content of suspended silt and clay particles and possibly also algae. This is also reflected in the concentration of dissolved organic carbon (DOC), which was five times higher in the Namoi with 5 mg C/L vs 1 mg C/L. Algae growth and associated uptake of silica may also explain the low SI for Chalcedony as well as the difference in dissolved silica with Maules Creek having on average 23 times higher silica content than the Namoi with 15.5 mg/L vs 0.65 mg/L (Fig. 16f). In addition major contrasts were found in the surface water concentrations of Mg and K. The Mg concentration was significantly higher in the Namoi, with 25 mg/L vs 11 mg/L in Maules Creek. Likewise for K, the average concentration in the Namoi River was 3.6 mg/L vs 1.6 mg/L in Maules Creek. These marked contrasts may possibly be used to differentiate between aquifer recharge from the two streams.

The surface water EC measurements in October 2006 basically verify the findings of August 2006 with low EC water emanating from the Horsearm branch and much higher EC water coming from the upper Maules Creek branch (Fig. 10b). However, the much more detailed survey of EC down along the flowing reach and the stagnant pools during October 2006 show a more complex picture than revealed by the August data. The EC seems to be fluctuating down along the reach (Fig. 10b). This either indicates exchange with groundwater or hyporheic water of varying freshness or varying degrees of evaporative concentration down along the creek.

3.5.2 Estimating Relative Flow Contributions from Horsearm and the Upper Reach of Maules Creek Using EC

The flow contributions from Horsearm and upper Maules Creek to downstream surface water flow in Maules Creek were estimated using EC measurements (Fig. 17a) from the upper Maules Creek, Horsearm Creek and at Elfin crossing, respectively. The results indicated that about 92 % of the flow is low EC water from the Horsearm tributary and only the remaining 8 % is high EC water from the upper part of Maules. These proportions may well change in response to natural and anthropogenic temporal and spatial hydrologic processes in the upstream parts of the catchment.

3.5.3 Groundwater Chemistry

3.5.3.1 Electrical Conductivity

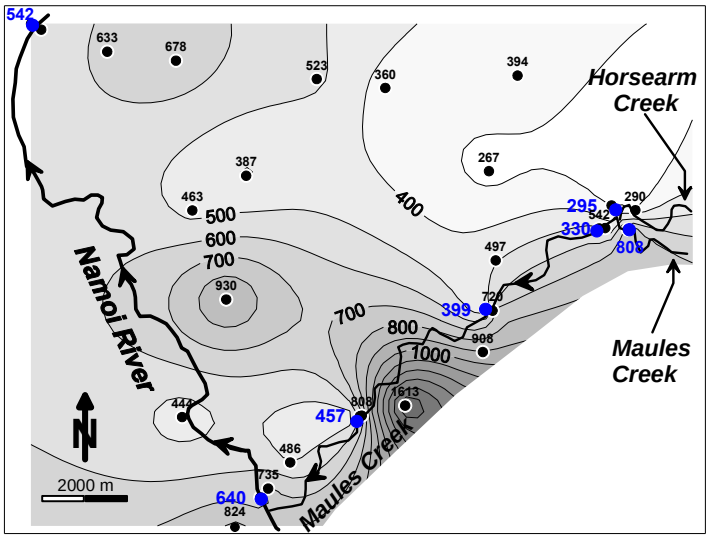

Fig. 20. Distribution of EC (µS/cm) of shallow groundwater (< 30 m) and surface water. Surface water and groundwater sampling sites are indicated by large blue and small black circles, respectively.

Electrical conductivity (EC) was measured in the aquifer in August 2006 (Fig. 20) and was found to vary in a complex pattern in the catchment reflecting different sources of water of varying quality as well as water rock interactions within the aquifer. However, the EC was generally found to increase along the hydraulic gradient from around 260-300 µS/cm in the northeast and east to 440-930 µS/cm in the west and southwest (Fig. 20). Significant deviations from this trend were observed. Generally EC was found to have a minimum at intermediate depths in the aquifer (from 30 to 60 m.b.s.) and increasing both toward the bottom and the surface of the aquifer (Fig. 21a). Fig. 22a show a cross-section of the geology along Maules Creek with the EC distribution superimposed. To the south of Maules Creek high groundwater EC (up to 1613 µS/cm) appears to be related to either the Permian volcanics or Triassic coal-measures located immediately to the south of the study site (Fig. 22a). In contrast to the surface water of Maules Creek, the EC of the groundwater below the creek increases much more rapidly down gradient: up to 1613 µS/cm (Fig. 22a). Downstream from this zone the EC is as low as 406 µS/cm (Fig. 22a), which, interestingly, are EC values comparable with the surface water samples in the lower portion of Maules Creek situated just above. Further westwards near the Namoi River the groundwater EC increases to a maximum of about 824 µS/cm. Low EC values in the western part of the transect seem to correlate with the location of the paleochannel (Fig. 22a). Comparing surface water and groundwater EC indicates low EC groundwater (~300 µS/cm) discharging into the Horsearm Creek and much higher EC groundwater (~800 µS/cm) discharging into the upper Maules Creek reflecting different sources of groundwater from the north and south (Fig. 20).

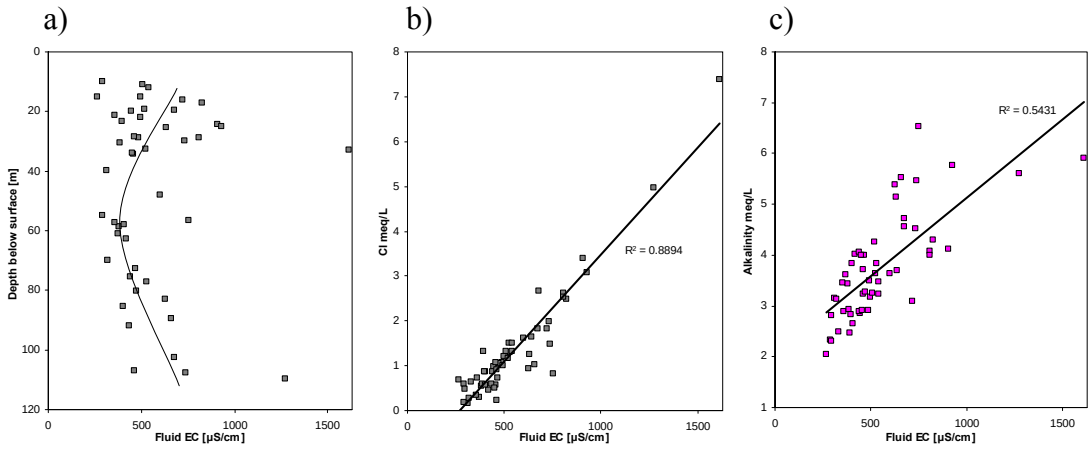

Fig. 21. a) Fluid EC as a function of depth below ground surface; b) Cl (mg/L) vs fluid EC (µS/cm); c) alkalinity (meq/L) vs fluid EC (µS/cm).

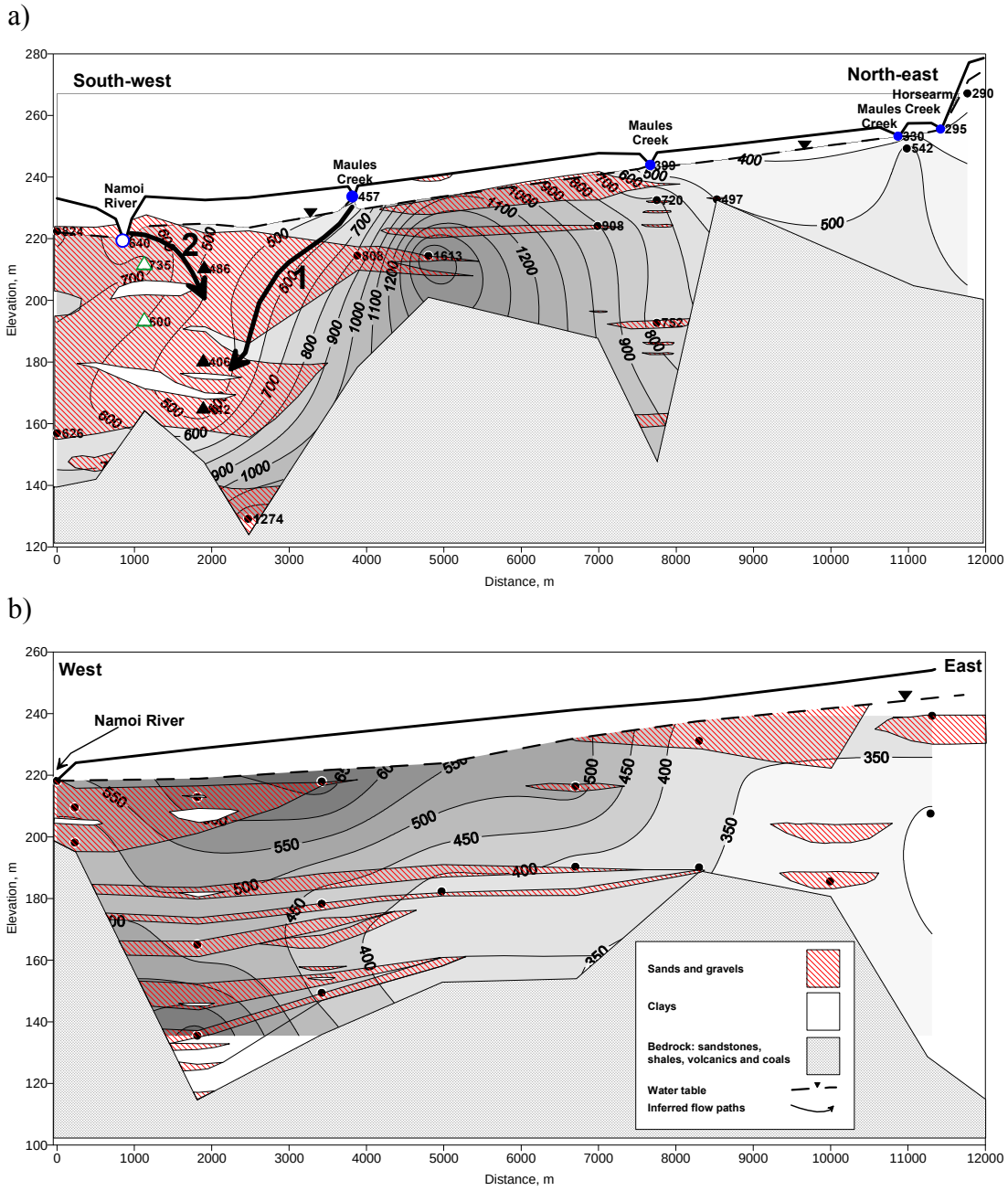

Fig. 22. Cross-sections of the EC distribution (µS/cm). a) Cross-section 1: oriented along Maules Creek b) Cross-section 2: oriented along the Narrabri-Maules Creek road. Notches in the surface indicate where Maules Creek and the Namoi River cuts the cross-sections (for Location see Fig. 3). Varying symbols for individual piezometer screens in a) are referring to the symbols in the Piper diagram (Fig. 28).

3.5.3.2 Major Ion Chemistry

Generally the groundwater has a Ca-HCO_3 or a Na-Cl composition but grades into a Na-HCO_3 composition in the deeper and more down gradient parts of the system and in zones of high EC, as towards the Permian deposits to the south. Fig. 23 summarises the major ion chemistry of all the surface water and groundwater samples collected in the catchment, in a piper diagram. The composition of the surface water samples occupies a narrow region

(light blue ellipse in Fig. 23), were variations are mainly due to variations in Cl content. The groundwater samples show a larger compositional variation. However, when divided into depth-intervals they too occupy distinctly different zones. The upper groundwater samples, < 30 m, (blue ellipse in Fig. 23) have a considerable compositional overlap with the surface water samples. However, the upper groundwater samples tend to have a higher Cl and Na content (and thus higher EC) than the surface water samples. Groundwater samples from the middle of the aquifer 30-60 m (dashed green ellipse in Fig. 23) are generally the freshest and have a major ion composition, similar to the fresher surface water samples. The deep groundwater > 60 m (red ellipse in Fig. 23) shows the largest variability with some samples dominated entirely by a Na-HCO_3^- composition.

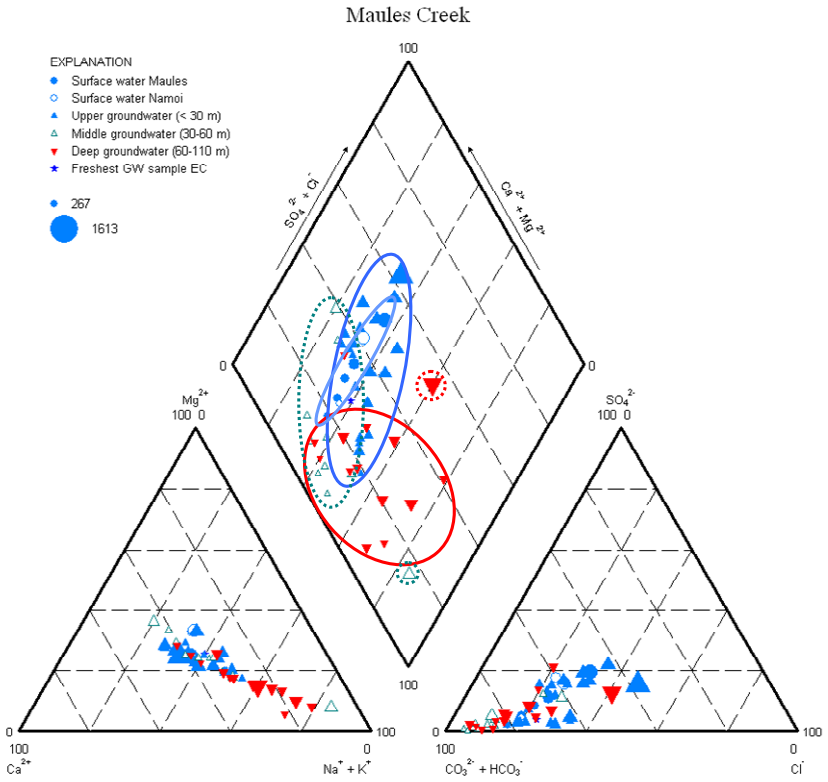

Fig. 23. Piper diagram showing all surface water and groundwater samples. Symbol size is proportional to the electrical conductivity (µS/cm). The ellipses delineate the surface water samples and groundwater samples from 3 different depth-intervals in the aquifer.

Most dissolved major ions generally follow the trend in EC described above (e.g. Fig. 22). For example the concentration of Cl is highly correlated to EC: $r^2 = 0.89$ (Fig. 21b). The increase in Cl is believed to be related to a gradual leaching of salts from the more clayey lithologies (Lavitt, 1999). Major dissolved ions show an increase with Cl, which could well be related to the leaching of salts. In bi-variate plots with Cl, the following correlations coefficients (r^2) were found: Ca = 0.79, Sr = 0.78, SO_4^{2-} = 0.66, Mg = 0.65, Ba = 0.41, Na = 0.35 and alkalinity = 0.27 (n = 54). See Appendix 1 for data and Appendix 10 for selected plots along the cross-section lines of Fig. 3.

The alkalinity also shows a correlation with EC: r^2 = 0.54 (Fig. 21c) indicating that a significant part of the increase in groundwater EC down gradient is related to alkalinity. This increase is probably not related to the leaching of salts, but rather related to water rock interactions in the aquifer such as dissolution of carbonate minerals, silicate weathering or degradation of organic matter (Appelo and Postma 2005). The poorer correlations found between Cl and Na and alkalinity, respectively, was found to be mainly due to a lack of correlation in the deeper parts of the aquifer. The ratios of Na/Cl and Alkalinity/Cl were found to increase with depth (Fig. 24). This increase in e.g. Na could indicate that slow weathering of silicate minerals is contributing significantly to the water composition with higher contact times for the deeper part of the aquifer. Such mineral weathering is probably responsible for part of the general down gradient increase in other dissolved ions. However, the extent to which the increase for individual ions are caused by weathering or leaching of salts are unknown, since the chemical composition of the salt is poorly constrained.

The concentration of dissolved silica (Si) is surprisingly constant throughout the aquifer (averaging 17.8 mg/L) indicating that the precipitation of one or more secondary Si-mineral phases are controlling the concentrations of dissolved Si released from weathering of primary silicate minerals. This is supported by saturation index calculations in PHREEQC (Appendix 2) where both quartz and chalcedony (both SiO_2) were found to be supersaturated for most samples.

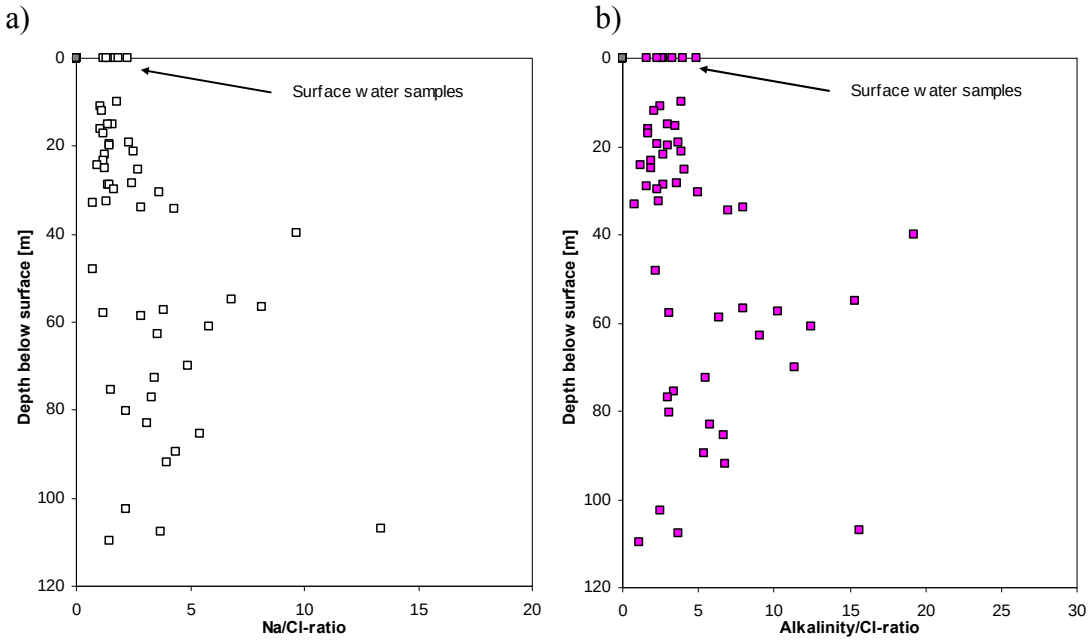

Fig. 24. Ratios of a) Na/Cl and b) alkalinity/Cl as a function of depth.

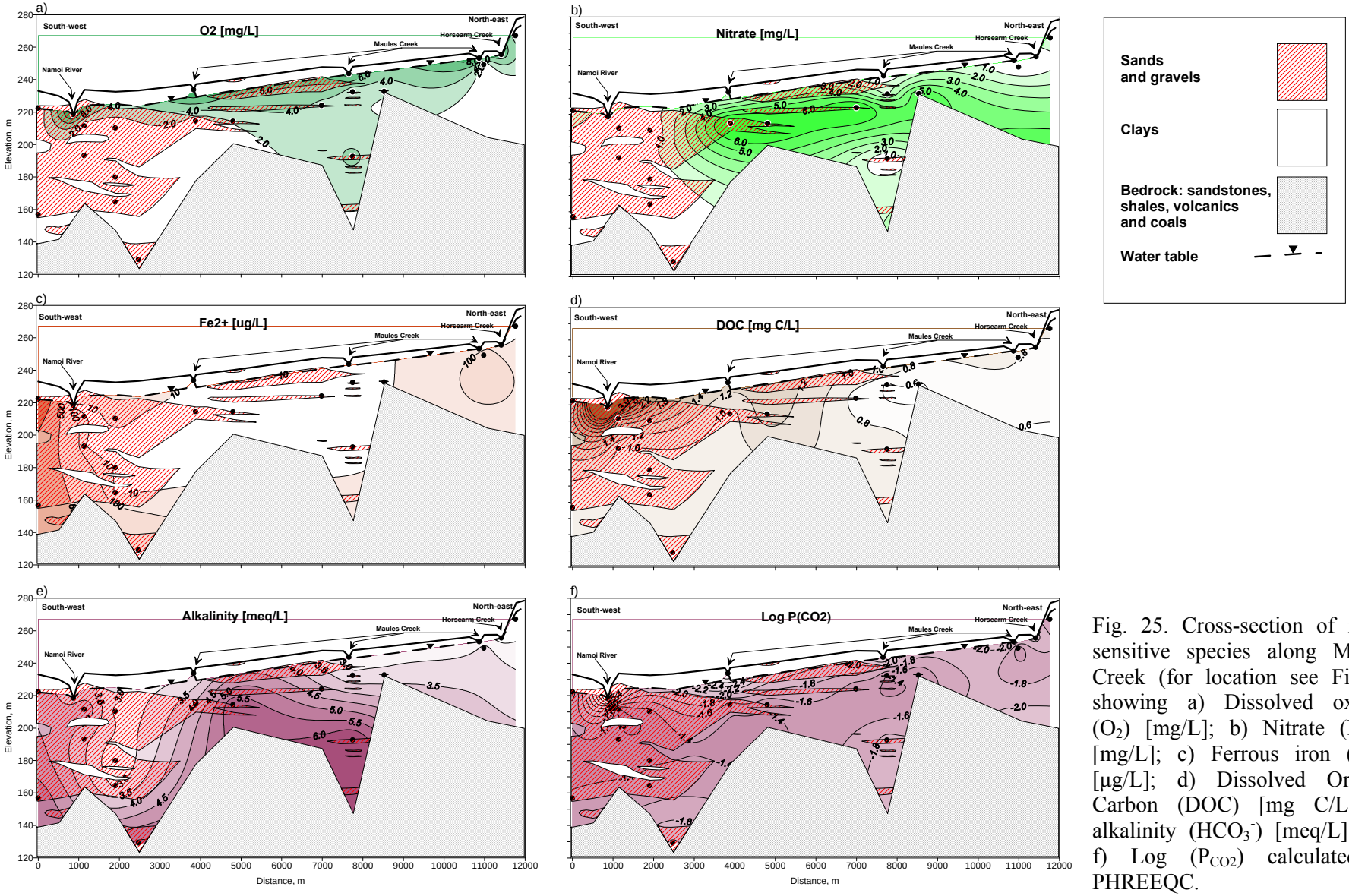

Fig. 25. Cross-section of redox sensitive species along Maules Creek (for location see Fig. 3) showing a) Dissolved oxygen (O_2) [mg/L]; b) Nitrate (NO_3^-) [mg/L]; c) Ferrous iron (Fe^{2+}) [µg/L]; d) Dissolved Organic Carbon (DOC) [mg C/L]; e) alkalinity (HCO_3^-) [meq/L]; and f) Log (P_{CO2}) calculated in PHREEQC.

3.5.3.3 Distribution Redox Species

In general the aquifer displays a classical redox sequence (Appelo and Postma, 2005) changing from oxic to anoxic conditions along the hydraulic gradient. Fig. 25 shows the distribution of some redox-sensitive species along the Maules Creek cross-section (for the cross-section along the Maules Creek-Narrabri road see Appendix 10. Dissolved oxygen (DO) is present in the eastern (up gradient) and upper part of the aquifer (Fig. 25a) in concentrations up to 8 mg/L. In the eastern part DO up to about 5 mg/L is found down to 70 m below ground surface.

Nitrate (NO_3^-) is also present in the aquifer with concentrations up to 16 mg/L. The overall distribution of nitrate (Fig. 25b) is the same as for DO, but tends to have a more shallow distribution than oxygen: the aquifer is, apart from a few outliers, generally free of nitrate below 30 m (Fig. 26a, b). This discrepancy between oxygen and nitrate could indicate that the source of nitrate is recent and possibly related to farming activities in the last decades.

Dissolved ferrous iron (Fe^{2+}) show an inverse correlation to DO and nitrate with increasing concentrations in the western (down gradient) and deeper parts of the aquifer (Fig. 25c). Between 0.1 and 1.5 mg/L of Fe^{2+} were measured in the vicinity of the Namoi River. In this zone reduced manganese (Mn^{2+}) was also detected (1 to 6 µg/L).

Dissolved organic carbon (DOC) concentrations are generally low in the up gradient part of the aquifer ranging from 0.2 to 1.4 mg C/L with an average of 0.9 mg C/L (Fig. 25d). Elevated levels of DOC ranging from 0.8 to 3.7 mg C/L with an average of 1.4 mg C/L were measured in the groundwater in the vicinity of the river (~1-2 km). The levels of DOC in the Namoi River (4.9 mg C/L) were found to be about 5 times higher than in the aquifer in general (see section 3.5.1), possibly reflecting a higher level of pollution with sewage effluent and nutrients in the Namoi River as well as possibly soil erosion with an organic load. In contrast, Maules Creek had DOC levels comparable to the low DOC groundwater.

The levels of CO_2 (plotted as $\log(P_{CO2})$ in Fig. 25f) are quite uniform in the aquifer with $\log(P_{CO2})$ values ranging from -2.0 to -1.3, values comparable to root zone CO_2 pressures (Appelo and Postma, 2005). In the surface water samples the $\log(P_{CO2})$ is much lower ~-1.8 to -3.3 reflecting equilibration with the atmosphere. The uniform CO_2 levels in the aquifer must either reflect that CO_2 produced in the root zone is transported conservatively into the aquifer without significant consumption by buffering processes (such as dissolution of silicate or carbonate minerals) or that CO_2 is being produced intrinsically by degradation

of dissolved or sedimentary organic matter in the aquifer. Some indication of this with a slight down gradient increase in the CO_2 may be seen in Fig. 25f. In addition, the trends in major cations and in redox sensitive species points toward both CO_2 production and consumption occurring simultaneously in the aquifer.

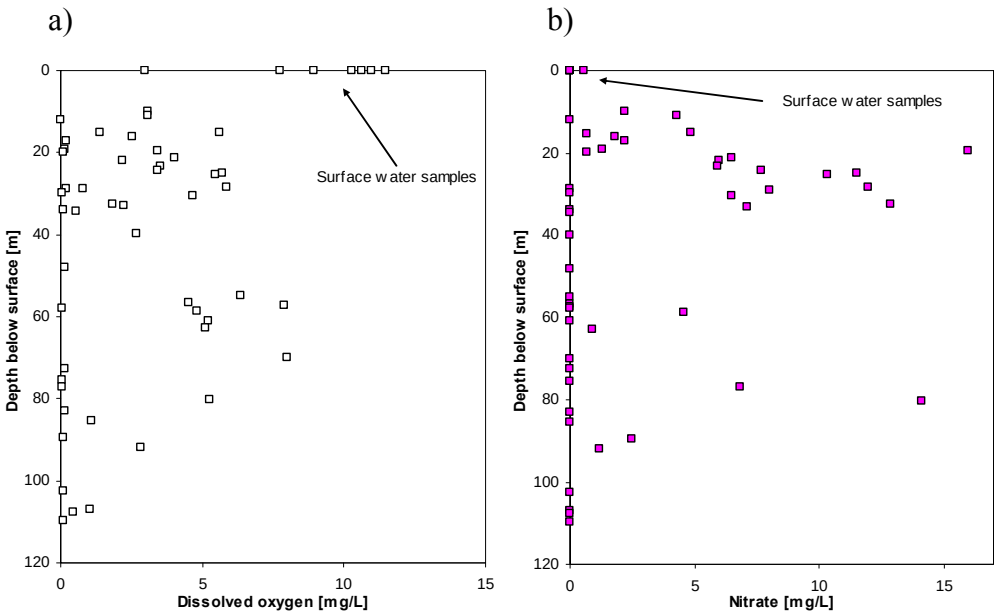

Fig. 26. Concentration of a) dissolved oxygen (O_2 – mg/L) and b) nitrate (NO_3^- – mg/L) as a function of depth.

4. DISCUSSION

The low groundwater EC (down to 406 μS/cm) in the down gradient part of the Maules Creek cross-section (Figs. 20 and 22a) could possibly be explained by infiltration of relatively low EC surface water from Maules Creek into the subsurface (see flow path 1 in Fig. 22a). Significant downward hydraulic gradients were observed for Maules Creek in this zone in August 2006 (Fig. 8b). It is possible that the source of low EC groundwater could be infiltration of surface water from the Namoi River in the west (see flow path 2 in Fig. 22a) at times with either high groundwater extraction from the Namoi paleochannel or high river stage and flow. However, this appears to be less likely based upon the available data as the EC of the Namoi River water was higher (640 μS/cm). Nevertheless lower EC levels are possible during floods, which would also be a hydraulic condition with the highest likelihood of river water recharging the aquifer. Low EC floodwaters have been observed for the Peel River, another tributary to the Namoi River system (Mawhinney, 2005). Time series of river water quality is required to resolve this at the current field site.

Plotting the major ion composition of selected surface water and groundwater samples in a Piper diagram (Fig. 27) gives additional, although not conclusive, clues about the source of the low EC groundwater. In the Piper diagram the surface water samples from Maules Creek plot on a trajectory (circles in Fig. 27) largely indicating an increase in chloride down along the creek. The surface water sample from the Namoi River is situated further along this trend. The three groundwater samples from the low EC zone (solid triangles in Fig. 22a and Fig. 27) plot almost on the line in between the compositions of the Maules Creek and the Namoi River (arrow in Fig. 27). In contrast, the two groundwater samples from the zone between the Namoi River and the zone of low groundwater EC (open triangles in Fig. 22a) are located further away in terms of chemical composition, (however, in opposite directions). It therefore does seem more likely that Maules Creek is the source of the low EC groundwater plume (via flow path 2 in Fig. 22a).

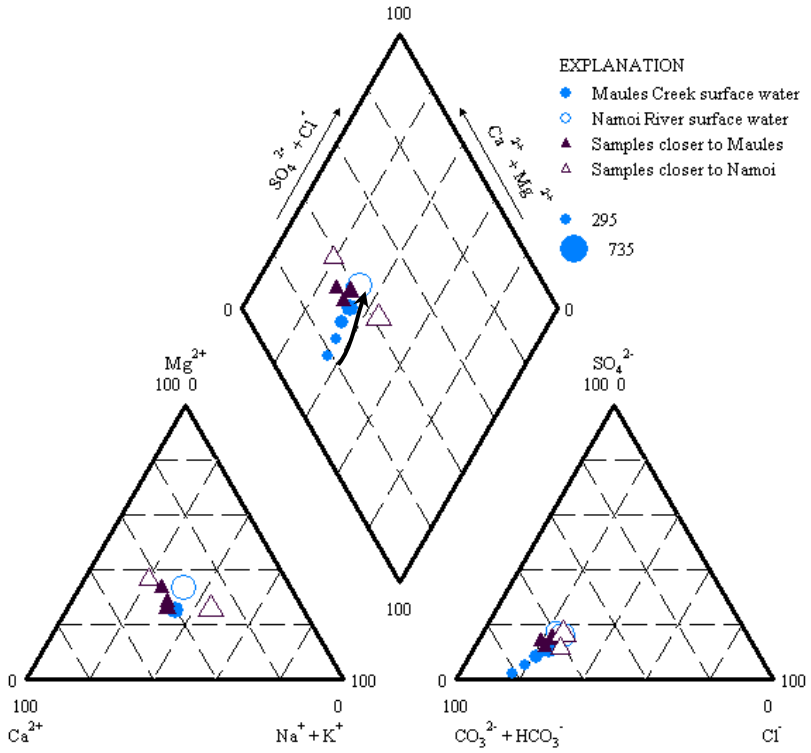

Fig. 27. Piper diagram showing the relative major ion composition of selected surface water and groundwater samples. The arrow indicates change in water composition down along Maules Creek and into the aquifer. For location of samples see symbols in Fig. 22a.

Hydrochemical data from the aquifer along the Namoi River indicate that there may also be interactions between the Namoi River and the aquifer in the proximity of the river. The two surface water samples taken from the Namoi River shows a downstream decrease in EC from 640 to 542 µS/cm over a distance of about 12 km. Other parameters such as Cl also showed a decrease. Such a decrease only seems possible with an influx of lower EC water to dilute the surface water EC. Groundwater of lower EC (~460 µS/cm) is residing in the aquifer near the Namoi River between the two sampling sites.

If groundwater discharge is occurring during winter it is then quite likely that the exchange between surface water and groundwater reverses direction during the groundwater pumping season or depending on river stage and variations in the regional rain fed recharge of the aquifer. Such exchange must be occurring along the Namoi River between Boggabri and Turrawan as suggested by Fig. 7. However, it remains to be determined whether this exchange is occurring in discrete zones or more continuously down along the river.

The DOC distribution and the redox chemistry (Fig. 25) suggest that at times Namoi River water is in fact recharging the aquifer in some locations. Infiltration of river water with a relatively high organic carbon content and subsequent oxidation in the river bed sediments or in the aquifer could be a mechanism explaining such chemically reduced water quality.

Other studies have found elevated groundwater DOC levels believed to be from infiltrating river water (Schwarzenbach *et al.,* 1983; Dahm *et al.,* 1998; Crandall *et al.,* 1999) and lakes (La Baugh, 1986). As a consequence steep redox gradients are often found in aquifers near the surface water interface (Dahm *et al.,* 1998).

The observed redox conditions in the aquifer could thus be explained by a sequence of reaction whereby organic carbon is firstly oxidized by electron acceptors dissolved in the infiltrating water (O_2 and NO_3^-) and subsequently by iron oxides ($Fe(OH)_3$) present in the sediment (Appelo and Postma, 2005). However, at this stage it cannot be ruled out that sedimentary organic matter deposited together with the sands and gravels could be causing the reducing conditions. More detailed studies as well as age dating of the groundwater are necessary to provide more definite answers.

The results of this study show how natural hydrochemical tracers can be used to delineate areas of surface water groundwater exchange. In addition understanding how hydrochemical processes are linked to the infiltration of surface water or discharge of groundwater may give important insight in possible fate of various organic and inorganic pollutants exchanging with the water.

4.3 Further Work

- Re-interpret the water chemistry data in light of the collected stable isotope (^2H and ^{18}O) data.
- Identify clear compositional water source end-members of the catchment to enable the calculation of mixing processes.
- Identify flow paths for reactive transport modelling.
- Setup reactive transport models for conceptualising and quantifying processes.
- Use the above points in conjunction with the hydrogeology to understand processes and to quantify surface water and groundwater interactions in the catchment.
- Establish relationships between river and groundwater.

5. CONCLUSION

Interactions between Maules Creek and the groundwater of the underlying aquifer were studied using a combination of geological data; geophysical methods; hydraulic data; fluid EC; temperature; and water chemistry data. Based on EC and temperature data, zones of groundwater discharge were detected in the upper part of the studied reach. From the initial discharge area the creek appears to be flowing for several kilometres between pools in a relatively thin (2-10 m) layer of sand and coarse gravel on top of more massive clayey layers as indicated by the resistivity imaging. However, the resistivity images also suggest that the clay is not laterally continuous with possible hydraulic connections to the aquifer below. Variations in the surface water fluid EC downstream seems to indicate a possible influx of or mixing with groundwater with varying EC. It cannot be discounted that evapotranspirative concentration down the reach may also have some influence on this trend in EC. This should be quantified so that EC data can be used to derive quantitative estimates of the exchange of water between the stream and aquifer. Further downstream, the stream is potentially recharging the regional aquifer as were inferred by downward hydraulic gradients, by inspecting the geological data, and by the existence of a plume of fresh groundwater below the creek with a chemical composition similar to surface water within Maules Creek above.

Along the Namoi River EC data and redox chemistry suggests both groundwater discharge into the river and surface water infiltration into the aquifer. Relatively high levels of dissolved organic carbon (DOC) in the river water appear to lead to elevated DOC levels; anoxic conditions; and elevated dissolved Fe^{2+} in the aquifer in the vicinity of the river.

It is possible that stream fed recharge from Maules Creek (and possibly also the Namoi) is enhanced by drawdowns in the regional aquifer caused by extraction of groundwater. The initial results of this study are qualitative and actual fluxes needs to be established. In addition the relative proportions of direct recharge; recharge via Maules Creek and via dam releases and flooding in the Namoi River are largely unknown. Furthermore the results are obtained during low flow conditions and the dynamics of surface water groundwater interactions in relation to major precipitation and flooding events needs to be studied in greater detail.

In summary, this study shows how hydrochemical analysis of surface water and groundwater samples in conjunction with hydrogeological investigations may provide important information about surface water groundwater interactions by revealing connectivity and delineating flow paths.

REFERENCES

Appelo, C.A.J., Postma, D., (2005), *Geochemistry, Groundwater, and Pollution*. 2nd ed. A.A. Balkema, Rotterdam. 649 pp.

Cline, J.D., (1967), Spectrophotometric determination of hydrogen sulfide in natural waters. *Limnol. Oceanogr*. 14, 454-458.

Crandall C.A., Katz B.G., Hirten J.J., (1999), Hydrochemical evidence for mixing of river water and groundwater during high-flow conditions, lower Suwannee River basin, Florida, USA. *Hydrogeology Journal* 7: 454-467.

Dahm C.N., Grimm N.B., Marmonier P., Valett H.M., Vervier P., (1998), Nutrient dynamics at the interface between surface waters and groundwaters. *Freshwater Biology* 40: 427-451.

DMR, (1998), Gunnedah coalfield (north) regional geology (1:100 000 map). Geological Survey of NSW, Department of Mineral Resources.

DMR, (2002), Geology – Integration and upgrade, NSW Western regional assessments

Brigalow Belt South Bioregion (Stage 2). Geological Survey of NSW, Department of Mineral Resources.

DNR, (2006), Bore log data base. Department of Natural Resources, NSW, Australia.

La Baugh J.W., (1986), Limnological characteristics of selected lakes in the Nebraska sandhills, U.S.A., and their relation to chemical characteristics of adjacent ground water. *J. of Hydrol.* 86, 279-298.

Lavitt, N., (1999), Integrated Approach to Geology, Hydrogeology and Hydrochemistry in the Lower Mooki River Catchment. PhD thesis, University of New South Wales. 388 pp.

Mawhinney W., (2005), Water Quality in the Namoi Catchment 2003/2004. Department of Natural Resources, NSW, Australia. ISBN 0-7347-5619- 4.

Parkhurst D.L., Appelo C.A.J., (1999), User's guide to PHREEQC (Version 2). U.S. Geol. Surv. Water Resour. Inv. Rep., 99–4259.

Schwarzenbach R.P., Giger W., Hoehn E., Schneider J.K., (1983), Behaviour of organic compounds during infiltration of river water to groundwater. Field studies. *Environ. Sci. Technol.* 17: 472-479.

Sinclair P., Barret C., Wiliams R.M., (2005), Impact of groundwater extraction on Maules Creek – Upper Namoi Valley, NSW, Australia. Proceedings of the NZHS-IAH-NZSSS 2005 Conference, Auckland, 29 November – 1 December 2005.

Stookey, L.L., (1970), Ferrozine – A new spectrophotometric reagent for iron. *Anal. Chem.* 42, 7, 779-781.

Stumm, W. and Morgan, J.J., (1981), *Aquatic chemistry*. 2nd ed. Wiley & Sons, New York, 780 pp.

APPENDICES

Appendix 1. Hydrochemical data
Appendix 2. Saturation index (SI) calculations using PHREEQC
Appendix 3. Geophysical well logs
Appendix 4. Resistivity images near the Namoi River on the Property of Darren Eather
Appendix 5. Head distributions in the upper, middle and lower aquifer in August 2006
Appendix 6. Head distributions in the upper, middle and lower aquifer in October 2006
Appendix 7. Comparison of Groundwater hydrograph GW036093 and stream flow in Maules Creek and the Namoi River
Appendix 8. Plots of surface water chemistry
Appendix 9. Surface water ion ratios
Appendix 10. Cross-section plots of redox-chemistry along the Narrabri-Maules Creek Rd

Appendix 1. Hydrochemical Data

Well name	UTM East	UTM North	Elevation mid screen	Surface elevation	Water level elevation	Water level elevation	EC	Eh	pH	Temp.	O2	Alkalinity	Fe2+	Sulfide	Ba	Ca	Fe-tot	K
Groundwater	**zone 56**		**m**		**August**	**October**	**uS/cm**	**mV**	**Field**	**C**	**Field**	**meq/L**	**Field**	**Field**	**Lab**	**Lab**	**Lab**	**Lab**
30129	217158	6619595	224.1	247.7	240.7	240.6	908	120	6.82	20.9	3.45	4.11	> 5.0	> 5.0	0.066	72.37	-0.005	1.42
30130-1	217382	6620550	232.5	247.9	243.2	243.0	720	68	6.61	19.9	2.53	3.09	> 5.0	> 5.0	0.056	63.66	0.003	1.67
30130-2	217382	6620550	192.7	247.9	237.6	237.4	752	50	7.44	20.6	4.52	6.54	> 5.0	> 5.0	0.018	11.87	-0.004	2.32
30131	217455	6621713	232.8	250.0	245.4	245.2	497	-16	6.68	20.9	2.18	3.18	> 5.0	> 5.0	0.022	44.56	-0.005	1.17
30132-1	217299	6623776	242.5	250.8	245.2	245.2	267	120	6.45	21.2	5.59	2.05	57.6	> 5.0	0.010	18.77	-0.004	0.46
30132-2	217299	6623776	218.0	250.8	245.5	245.4	313	105	6.82	21.6	2.68	3.14	7.3	> 5.0	0.022	21.68	-0.004	1.60
30133	217872	6625313	207.6	254.0	244.9	244.9	293	90	6.68	21.2	6.35	2.82	14.6	> 5.0	0.028	20.92	0.013	1.85
30134	217960	6625985	239.3	254.7	245.0	245.0	394	40	6.41	20.6	3.53	2.46	> 5.0	> 5.0	0.039	27.68	-0.001	1.06
30231-1	206951	6627046	209.6	224.2	218.3	218.2	518	-37	6.91	20.1	0.15	4.27	> 5.0	> 5.0	0.038	33.06	0.054	2.27
30231-2	206951	6627046	198.2	224.2	218.3	218.2	455	-1	6.91	20.6	0.55	3.99	> 5.0	> 5.0	0.037	29.10	0.005	2.04
30232-1	208476	6626537	212.9	228.7	219.0	218.5	633	57	6.87	21.9	5.44	5.15	> 5.0	> 5.0	0.024	39.95	-0.005	1.25
30232-2	208476	6626537	165.1	228.7	219.1	218.4	467	-50	6.9	22.3	0.13	3.99	371.5	> 5.0	0.056	30.09	0.347	2.13
30232-3	208476	6626537	135.5	228.7	219.5	218.1	675	-152	7.23	22.3	0.11	4.55	690.7	> 5.0	0.141	35.92	0.704	2.73
30233-1	210065	6626330	218.0	232.9	221.6	221.0	678	120	6.69	20.6	3.41	4.72	> 5.0	> 5.0	0.054	44.22	-0.003	2.31
30233-2	210065	6626330	178.3	232.9	220.0	218.8	420	74	6.89	22.1	5.13	4.02	> 5.0	> 5.0	0.061	35.29	-0.003	2.59
30233-3	210065	6626330	149.4	232.9	219.8	218.6	437	80	6.98	22.4	2.82	4.06	> 5.0	> 5.0	0.039	29.88	-0.005	2.33
30234	211605	6626129	182.3	236.9	223.8	222.2	372	133	6.84	21.5	5.21	3.62	> 5.0	> 5.0	0.053	26.73	-0.005	2.15
30235-1	213319	6625906	216.4	241.3	232.1	231.9	523	112	6.5	21.1	1.86	3.63	5.2	> 5.0	0.045	41.94	-0.004	2.19
30235-2	213319	6625906	190.3	241.3	231.4	230.7	382	100	6.64	21.8	4.8	3.44	> 5.0	> 5.0	0.046	30.35	0.001	2.18
30236-1	214902	6625699	231.2	244.7	237.6	237.7	360	150	6.89	21.7	4.04	2.89	> 5.0	> 5.0	0.012	23.49	-0.003	0.92
30236-2	214902	6625699	190.1	244.7	236.2	235.9	356	128	6.73	21.9	7.91	3.44	> 5.0	> 5.0	0.050	31.24	-0.002	2.39
30237	216585	6625481	185.6	249.7	237.4	239.3	321	136	6.67	21.9	7.99	3.13	> 5.0	> 5.0	0.033	25.99	-0.002	2.25
30446-1	211687	6623670	213.3	235.1	227.9	227.4	387	68	6.84	21.6	4.67	2.93	> 5.0	> 5.0	0.019	22.76	-0.005	1.41
30446-2	211687	6623670	152.1	235.1	222.7	218.3	402	20	7.8	21.8	1.07	3.84	> 5.0	> 5.0	0.003	19.23	-0.005	1.64
30447	211226	6620808	216.2	232.5	222.8	217.9	930	55	6.95	20.4	5.7	5.77	> 5.0	> 5.0	0.055	73.60	-0.003	2.03
36003	212973	6618434	135.4	233.5	223.9	215.6	463	57	7	21	1.02	3.72	> 5.0	> 5.0	0.011	17.56	-0.001	1.52
36004-1	210207	6618092	219.9	231.4	221.8	221.8	444	-68	6.96	21.4	0.09	2.86	153.7	> 5.0	0.081	33.33	0.161	1.81
36004-2	210207	6618092	205.1	231.4	221.9	221.4	449	5	6.79	20.4	0.09	3.99	43	> 5.0	0.024	39.78	0.040	1.52
36005-1	211426	6615579	222.4	232.0	222.0	221.5	824	-84	6.64	21.9	0.21	4.30	1575.733	> 5.0	0.046	57.54	1.602	1.07
36005-2	211426	6615579	156.9	232.0	222.5	213.7	626	-87	6.91	21.7	0.16	5.39	931.8	> 5.0	0.038	42.44	0.948	1.87
36093-1	212705	6617043	210.3	232.5	224.9	224.0	486	67	6.54	18.6	0.2	2.91	50.3	> 5.0	0.047	41.15	0.048	1.46
36093-2	212707	6617044	180.0	232.5	224.6	220.8	406	108	6.56	20	0.06	2.64	> 5.0	> 5.0	0.013	32.92	-0.004	1.26
36093-3	212709	6617046	164.6	232.1	224.5	219.7	442	100	6.67	20.3	0.05	2.90	> 5.0	> 5.0	0.015	35.40	-0.001	1.31
36094-1	210444	6622868	210.0	231.2	222.0	219.5	463	98	6.76	21.5	5.85	3.24	> 5.0	> 5.0	0.021	30.44	-0.005	1.25
36094-2	210446	6622867	159.7	231.2	221.9	218.7	472	73	6.74	21.9	5.26	3.26	> 5.0	> 5.0	0.018	31.30	-0.004	1.46
36094-3	210448	6622867	132.3	231.2	221.9	218.5	738	35	7.3	21.7	0.43	5.47	> 5.0	> 5.0	0.007	24.65	-0.004	1.65
36096-1	212196	6616438	211.5	233.7		223.8	735	108	6.56	20.8	0.05	4.52	20.3	> 5.0	0.086	43.18	0.012	2.28
36096-2	212198	6616441	193.2	233.3	224.1	218.8	600	132	6.57	19.7	0.16	3.64	19.8	> 5.0	0.006	52.43	0.016	1.73
36164	213088	6617477	129.2	233.3	223.8	216.4	1274	-157	7.51	19.9	0.11	5.62	326.6	> 5.0	0.089	60.79	0.330	1.69
36186	214359	6618123	214.5	237.2	229.4	228.6	808	95	6.85	20	0.77	4.07	> 5.0	> 5.0	0.052	58.58	-0.004	1.36
36187	215362	6618356	214.4	240.1	233.1	232.9	1613	100	6.93	20.7	2.24	5.90	> 5.0	> 5.0	0.155	137.27	-0.001	1.89
41025	226991	6622430	214.0	287.0	277.9	280.1	659	-192	7.25	21.6	0.1	5.52	144.9	> 5.0	0.067	29.64	0.151	2.22
41027	232731	6620522	307.2	317.5	309.8	309.2	494	-140	6.7	20.8	1.38	3.50	11.2	11.67	0.007	46.86	0.002	1.03
967137-1	219846	6622452	249.3	257.4	253.2	252.9	542	-130	6.69	20.8	0.02	3.23	231.6	> 5.0	0.023	47.35	0.232	1.24
967137-2	219854	6622456	189.2	257.4	251.6	251.5	531	-285	7.76	20.9	0.07	3.84	24	41.97	0.021	14.39	0.022	2.58
967138	227001	6622422	280.1	287.5	282.4	281.8	508	90	6.7	21.3	3.08	3.26	> 5.0	> 5.0	0.008	47.25	-0.002	1.01
Fassifern	220683	6622873	267.1	277.1	271.5	262.1	290	70	6.69	20.6	3.07	2.32	> 5.0	> 5.0	0.011	22.75	-0.002	1.49
Surface water samples																		
Maules crk Harparary	214320	6618115	233.8	233.8	233.8	233.8	457	190	8.25	11.5	10.62	2.91	> 5.0	> 5.0	0.022	37.39	-0.004	2.01
Maules crk surface sample 1	217226	6620585	243.8	243.8	243.8	243.8	399	147	7.68	16.4	8.96	2.84	> 5.0	> 5.0	0.015	33.70	0.029	1.50
Upper Maules crk	220511	6622426	253.9	253.9	253.9	253.9	808	50	7.12	18.1	3	4.00	> 5.0	> 5.0	0.025	64.51	0.004	1.59
Upper Horsearm	220132	6622983	255.6	255.6	255.6	255.6	295	76	7.2	16	7.77	2.30	> 5.0	> 5.0	0.014	23.77	0.014	1.42
Elfin crossing 50 m downstream	219988	6622462	253.3	253.3	253.3	253.3	330	105	7.45	17.4	11.49	2.49	> 5.0	> 5.0	0.014	26.77	0.020	1.46
Namoi-1	206716	6627182	218.2	218.2	218.2	218.2	542	30	8.38	13.4	10.26	3.48	> 5.0	> 5.0	0.039	40.18	-0.004	3.59
Namoi-2	212016	6616234	218.5	218.5	218.5	218.2	640	85	8.52	11.5	10.98	3.69	> 5.0	> 5.0	0.043	46.40	-0.001	3.85
Blind samples																		
36000															-0.006	0.11	-0.005	0.32
36001												0.02			-0.005	0.11	-0.005	0.31
36002												0.04			-0.003	0.09	-0.004	0.29

Well name	Li Lab	Mg Lab	Mn Lab	Na Lab	Si Lab	Sr Lab	Cl Lab	NO2 Lab	Br Lab	NO3 Lab	PO4 Lab	SO4 Lab	DOC corrected for blind	EC/100	sum cations	sum anions	Ion balance
Groundwater	mg/L	mg/L	mg/L	mg/L	mg/L	mg/L	mg/L	mg/L	mg/L	mg/L	mg/L	mg/L	mg C/L		meq/L	meq/L	%
30129	0.005	28.23	-0.001	73.63	20.96	0.68	120.0	<0.3	<0.3	7.66	<0.3	100.00	0.72	9.08	9.19	9.70	-2.70
30130-1	0.005	24.65	0.014	43.83	20.03	0.57	65.0	<0.3	<0.3	1.8	<0.3	44.00	0.57	7.2	7.17	5.87	9.97
30130-2	0.009	7.51	0.000	154.36	17.20	0.28	29.2	<0.3	<0.3	<0.3	<0.3	18.50	0.99	7.52	7.99	7.75	1.55
30131	0.004	16.11	-0.001	35.50	21.62	0.41	42.6	<0.3	<0.3	5.96	<0.3	26.60	0.57	4.97	5.13	5.03	0.99
30132-1	0.004	8.28	-0.001	24.63	26.42	0.18	24.1	<0.3	<0.3	4.86	<0.3	4.81	0.24	2.67	2.71	2.91	-3.52
30132-2	0.000	7.94	-0.001	36.28	21.27	0.24	5.8	<0.3	<0.3	<0.3	<0.3	1.10	0.29	3.13	3.36	3.33	0.46
30133	0.003	8.81	0.013	28.63	22.18	0.24	6.5	<0.3	<0.3	<0.3	<0.3	<0.3	0.65	2.93	3.07	3.00	1.08
30134	0.003	11.70	-0.001	35.63	24.29	0.36	47.0	<0.3	<0.3	5.94	<0.3	5.60	0.83	3.94	3.93	4.00	-0.88
30231-1	0.002	12.61	0.678	61.12	18.28	0.41	41.0	<0.3	<0.3	1.32	<0.3	19.40	1.03	5.18	5.44	5.85	-3.61
30231-2	0.002	10.40	0.065	56.13	18.13	0.37	20.2	<0.3	<0.3	<0.3	<0.3	8.00	0.93	4.55	4.81	4.73	0.88
30232-1	0.001	16.60	-0.002	77.32	22.60	0.41	44.4	<0.3	<0.3	10.36	<0.3	8.44	1.47	6.33	6.76	6.74	0.18
30232-2	0.001	10.34	0.283	58.11	18.76	0.39	26.0	<0.3	<0.3	<0.3	<0.3	7.90	1.09	4.67	4.97	4.89	0.78
30232-3	0.004	12.67	0.151	92.22	15.21	0.49	64.9	<0.3	<0.3	<0.3	<0.3	21.60	0.99	6.75	6.96	6.83	0.94
30233-1	0.004	20.18	0.000	70.64	21.73	0.59	73.9	<0.3	<0.3	15.98	<0.3	7.12	1.14	6.78	7.01	8.63	-10.32
30233-2	0.002	13.78	0.007	36.51	20.60	0.42	15.8	<0.3	<0.3	0.9	<0.3	1.34	1.06	4.2	4.56	4.51	0.55
30233-3	0.001	10.20	-0.001	54.39	19.54	0.40	21.2	<0.3	<0.3	1.2	<0.3	7.72	1.07	4.37	4.77	4.84	-0.79
30234	0.003	11.60	-0.002	38.83	20.55	0.39	10.3	<0.3	<0.3	<0.3	<0.3	3.92	1.26	3.72	4.04	4.00	0.58
30235-1	0.002	14.37	-0.001	46.28	22.44	0.50	53.0	<0.3	<0.3	12.9	<0.3	6.40	1.10	5.23	5.36	5.46	-0.98
30235-2	0.000	11.77	0.000	35.25	21.51	0.39	19.0	<0.3	<0.3	4.6	<0.3	2.70	1.07	3.82	4.08	4.10	-0.27
30236-1	0.002	8.98	-0.001	42.01	25.11	0.23	26.0	<0.3	<0.3	6.5	<0.3	5.50	0.66	3.6	3.77	3.84	-0.94
30236-2	0.002	11.54	-0.001	29.59	21.38	0.36	11.9	<0.3	<0.3	<0.3	<0.3	0.90	0.67	3.56	3.87	3.80	0.88
30237	0.002	9.46	-0.001	31.08	21.24	0.30	9.8	<0.3	<0.3	<0.3	<0.3	2.53	0.75	3.21	3.49	3.46	0.49
30446-1	0.003	8.33	-0.002	49.81	24.23	0.25	21.0	<0.3	<0.3	6.5	<0.3	3.00	0.53	3.87	4.03	3.69	4.42
30446-2	0.003	2.86	0.005	71.96	13.25	0.26	20.5	<0.3	<0.3	<0.3	<0.3	1.64	0.49	4.02	4.37	4.45	-0.89
30447	0.004	24.48	-0.001	87.26	18.88	0.77	109.0	<0.3	<0.3	11.5	<0.3	18.90	2.03	9.3	9.55	9.42	0.70
36003	0.002	7.58	0.004	73.05	19.05	0.27	8.4	<0.3	<0.3	<0.3	<0.3	4.00	0.71	4.63	4.72	4.04	7.81
36004-1	0.004	15.39	6.224	31.77	10.60	0.36	34.4	<0.3	<0.3	0.66	<0.3	28.00	3.65	4.44	4.60	4.42	2.00
36004-2	0.003	17.25	0.096	32.69	19.03	0.44	17.7	<0.3	<0.3	<0.3	<0.3	4.08	0.77	4.49	4.88	4.58	3.24
36005-1	0.004	34.68	0.972	66.44	20.09	0.60	88.0	<0.3	<0.3	2.2	<0.3	76.00	1.52	8.24	8.75	8.40	2.03
36005-2	0.002	20.77	0.452	67.07	17.37	0.54	33.0	<0.3	<0.3	<0.3	<0.3	18.10	0.86	6.26	6.86	6.69	1.20
36093-1	0.000	15.41	0.650	34.09	15.27	0.38	37.7	<0.3	<0.3	<0.3	<0.3	33.26	1.48	4.86	4.88	4.66	2.25
36093-2	0.003	16.28	0.006	23.46	18.58	0.38	30.8	<0.3	<0.3	<0.3	<0.3	22.56	0.89	4.06	4.04	3.98	0.77
36093-3	0.003	14.77	0.228	29.46	16.90	0.36	30.4	<0.3	<0.3	<0.3	<0.3	28.70	0.92	4.42	4.31	4.35	-0.42
36094-1	0.002	11.11	-0.002	51.91	24.17	0.32	32.3	<0.3	<0.3	12	<0.3	5.76	0.45	4.63	4.73	4.47	2.87
36094-2	0.001	11.25	-0.001	53.04	24.10	0.34	37.4	<0.3	<0.3	14.1	<0.3	9.60	0.51	4.72	4.84	4.75	0.99
36094-3	0.003	9.03	-0.001	126.46	14.78	0.30	52.4	<0.3	<0.3	**	<0.3	30.20	1.57	7.38	7.52	7.58	-0.36
36096-1	0.004	22.97	1.883	74.71	15.25	0.47	70.0	<0.3	<0.3	<0.3	<0.3	61.20	1.84	7.35	7.44	7.77	-2.20
36096-2	0.003	26.49	0.039	26.85	19.45	0.58	57.6	<0.3	<0.3	**	<0.3	31.40	0.99	6	6.02	5.92	0.86
36164	0.001	21.44	0.608	167.47	13.23	0.67	176.0	<0.3	<0.3	**	<0.3	72.30	0.88	12.74	12.18	12.08	0.38
36186	0.002	22.15	0.000	86.65	20.56	0.54	93.2	<0.3	<0.3	8	<0.3	63.70	0.92	8.08	8.56	8.16	2.43
36187	0.005	49.09	-0.002	123.85	23.50	1.29	262.0	<0.3	<0.3	7.1	<0.3	114.00	1.32	16.13	16.36	15.78	1.80
41025	-0.001	11.59	0.369	102.99	17.35	0.47	36.6	<0.3	<0.3	2.5	<0.3	16.60	0.96	6.59	7.00	6.94	0.41
41027	0.004	17.49	0.006	32.64	16.83	0.32	35.6	<0.3	<0.3	0.66	<0.3	38.60	1.41	4.94	5.23	5.32	-0.79
967137-1	0.004	18.14	0.155	38.06	18.88	0.40	53.6	<0.3	<0.3	<0.3	<0.3	40.90	0.81	5.42	5.57	5.59	-0.21
967137-2	0.003	5.44	0.038	99.22	9.44	0.21	46.3	<0.3	<0.3	6.84	<0.3	65.60	0.56	5.31	5.56	6.62	-8.76
967138	0.004	17.69	0.000	32.08	16.69	0.34	46.5	<0.3	<0.3	4.32	<0.3	28.90	1.09	5.08	5.24	5.24	0.00
Fassifern	0.003	8.95	-0.002	24.35	17.73	0.23	20.9	<0.3	<0.3	2.2	<0.3	6.30	0.86	2.9	2.97	3.07	-1.64
Surface water samples																	
Maules crk Harparary	0.002	14.01	-0.001	35.64	11.92	0.32	37.7	<0.3	<0.3	<0.3	<0.3	23.00	1.31	4.57	4.63	4.45	1.96
Maules crk surface sample 1	0.004	12.93	0.017	32.33	16.14	0.29	30.4	<0.3	<0.3	<0.3	<0.3	15.94	1.11	3.99	4.20	4.03	2.06
Upper Maules crk	0.003	24.81	0.014	68.20	19.05	0.51	90.0	<0.3	<0.3	<0.3	<0.3	74.00	1.05	8.08	8.28	8.08	1.23
Upper Horsearm	0.001	9.24	0.019	24.08	17.51	0.23	16.7	<0.3	<0.3	<0.3	<0.3	2.56	0.74	2.95	3.04	2.83	3.59
Elfin crossing 50 m downstream	0.002	10.42	0.051	26.97	17.48	0.25	22.4	<0.3	<0.3	<0.3	<0.3	7.74	0.93	3.3	3.41	3.29	1.87
Namoi-1	0.001	23.42	0.003	42.10	0.76	0.39	47.0	<0.3	<0.3	0.58	<0.3	48.50	4.94	5.42	5.86	5.83	0.33
Namoi-2	0.002	27.59	0.015	50.06	0.58	0.46	58.3	<0.3	<0.3	<0.3	<0.3	47.70	4.83	6.4	6.87	6.33	4.11
Blind samples																	
36000	0.000	0.00	-0.002	1.93	0.11	0.00	2.3	<0.3	<0.3	0.16	<0.3	<0.3	-0.17		0.10	0.07	18.25
36001	0.001	-0.01	-0.002	1.84	0.13	0.00	5.5	<0.3	<0.3	0.97	<0.3	1.52	0.40		0.09	0.23	-41.54
36002	0.000	-0.02	-0.002	1.83	0.11	0.00	3.8	<0.3	<0.3	0.56	<0.3	<0.3	0.04		0.09	0.16	-26.01

Appendix 2. Saturation Index (SI) Calculations Using PHREEQC

Groundwater	Anhydrite $CaSO_4$	Aragonite $CaCO_3$	Barite $BaSO_4$	Calcite $CaCO_3$	Celestite $SrSO_4$	Chalcedony SiO_2	Chrysotile $Mg_3Si_2O_5(OH)_4$	CO2(g) $logP_{CO2}$	Dolomite $CaMg(CO_3)_2$	Gypsum $CaSO_4{*}2H_2O$	H2(g) $logP_{H2}$	Halite NaCl
30129	-1.89	-0.65	0.18	-0.51	-1.98	0.47	-7.54	-1.47	-1.12	-1.66	-41.70	-6.64
30130-1	-2.24	-1.01	-0.14	-0.86	-2.35	0.47	-9.02	-1.38	-1.85	-2.00	-41.80	-7.11
30130-2	-3.29	-0.57	-0.95	-0.42	-2.97	0.39	-5.64	-1.88	-0.75	-3.05	-41.81	-6.91
30131	-2.55	-1.04	-0.71	-0.89	-2.65	0.49	-8.90	-1.43	-1.93	-2.32	-41.60	-7.38
30132-1	-3.56	-1.77	-1.66	-1.62	-3.63	0.57	-10.79	-1.37	-3.30	-3.32	-41.75	-7.77
30132-2	-4.15	-1.16	-2.00	-1.01	-4.18	0.47	-8.79	-1.56	-2.15	-3.92	-41.52	-8.22
30133		-1.36		-1.21		0.49	-9.50	-1.47	-2.50		-41.78	-8.27
30134	-3.37	-1.60	-1.06	-1.45	-3.33	0.54	-10.79	-1.26	-2.98	-3.14	-41.75	-7.33
30231-1	-2.81	-0.82	-0.59	-0.68	-2.78	0.42	-8.09	-1.53	-1.49	-2.57	-41.15	-7.16
30231-2	-3.22	-0.88	-0.95	-0.74	-3.17	0.41	-8.24	-1.56	-1.63	-2.98	-41.35	-7.50
30232-1	-3.12	-0.69	-1.21	-0.54	-3.17	0.49	-7.59	-1.40	-1.15	-2.89	-41.63	-7.03
30232-2	-3.21	-0.86	-0.81	-0.71	-3.17	0.41	-8.07	-1.54	-1.57	-2.98	-40.75	-7.38
30232-3	-2.75	-0.43	-0.04	-0.28	-2.68	0.32	-6.09	-1.82	-0.70	-2.52	-40.71	-6.79
30233-1	-3.16	-0.88	-0.92	-0.74	-3.10	0.49	-8.62	-1.27	-1.52	-2.93	-41.75	-6.85
30233-2	-3.92	-0.79	-1.54	-0.65	-3.90	0.45	-7.68	-1.52	-1.39	-3.69	-41.58	-7.80
30233-3	-3.22	-0.77	-0.98	-0.62	-3.16	0.42	-7.56	-1.61	-1.39	-2.99	-41.40	-7.50
30234	-3.54	-1.00	-1.10	-0.86	-3.44	0.46	-8.26	-1.52	-1.77	-3.31	-41.69	-7.95
30235-1	-3.19	-1.18	-1.00	-1.03	-3.17	0.50	-10.05	-1.19	-2.23	-2.96	-41.53	-7.17
30235-2	-3.66	-1.17	-1.33	-1.02	-3.61	0.47	-9.37	-1.34	-2.15	-3.42	-41.62	-7.73
30236-1	-3.44	-1.10	-1.57	-0.95	-3.51	0.54	-8.08	-1.67	-2.02	-3.20	-41.60	-7.51
30236-2	-4.12	-1.06	-1.78	-0.91	-4.12	0.47	-8.83	-1.43	-1.95	-3.88	-41.71	-8.01
30237	-3.73	-1.23	-1.49	-1.09	-3.73	0.47	-9.44	-1.41	-2.30	-3.49	-41.71	-8.07
30446-1	-3.71	-1.16	-1.64	-1.01	-3.73	0.53	-8.52	-1.61	-2.15	-3.48	-41.65	-7.53
30446-2	-4.04	-0.16	-2.68	-0.02	-3.97	0.26	-4.68	-2.46	-0.55	-3.81	-41.29	-7.38
30447	-2.59	-0.36	-0.56	-0.21	-2.63	0.43	-7.04	-1.45	-0.61	-2.35	-41.89	-6.60
36003	-3.70	-1.02	-1.74	-0.88	-3.59	0.43	-7.99	-1.67	-1.82	-3.47	-41.42	-7.76
36004-1	-2.63	-0.92	-0.12	-0.77	-2.66	0.17	-7.81	-1.75	-1.58	-2.40	-40.82	-7.52
36004-2	-3.40	-0.88	-1.45	-0.73	-3.42	0.44	-8.29	-1.44	-1.53	-3.16	-40.99	-7.79
36005-1	-2.09	-0.88	-0.08	-0.74	-2.14	0.44	-8.23	-1.26	-1.39	-1.86	-40.92	-6.82
36005-2	-2.78	-0.61	-0.68	-0.47	-2.73	0.38	-7.33	-1.43	-0.94	-2.54	-40.90	-7.23
36093-1	-2.48	-1.28	-0.24	-1.14	-2.58	0.36	-10.38	-1.34	-2.43	-2.24	-41.47	-7.44
36093-2	-2.72	-1.36	-0.96	-1.22	-2.72	0.43	-9.80	-1.39	-2.45	-2.48	-40.97	-7.69
36093-3	-2.59	-1.19	-0.80	-1.04	-2.65	0.39	-9.33	-1.46	-2.17	-2.36	-40.88	-7.60
36094-1	-3.34	-1.08	-1.35	-0.94	-3.37	0.53	-8.68	-1.49	-2.01	-3.10	-41.71	-7.33
36094-2	-3.11	-1.09	-1.22	-0.94	-3.14	0.52	-8.74	-1.47	-2.02	-2.88	-41.62	-7.26
36094-3	-2.77	-0.46	-1.21	-0.31	-2.74	0.31	-6.23	-1.81	-0.75	-2.53	-41.11	-6.75
36096-1	-2.27	-1.07	-0.92	-0.92	-2.29	0.34	-9.58	-1.16	-1.82	-2.03	-40.80	-6.85
36096-2	-2.45	-1.06	-1.26	-0.91	-2.47	0.46	-9.19	-1.27	-1.83	-2.22	-41.23	-7.37
36164	-2.12	0.07	0.20	0.21	-2.14	0.28	-4.31	-2.04	0.26	-1.88	-41.12	-6.12
36186	-2.14	-0.71	-0.04	-0.56	-2.23	0.48	-7.75	-1.50	-1.26	-1.90	-41.52	-6.67
36187	-1.69	-0.17	0.49	-0.03	-1.78	0.53	-6.21	-1.44	-0.20	-1.45	-41.64	-6.10
41025	-2.94	-0.41	-0.45	-0.27	-2.80	0.38	-6.06	-1.76	-0.64	-2.71	-40.81	-6.99
41027	-2.38	-0.97	-1.06	-0.82	-2.61	0.38	-8.93	-1.41	-1.77	-2.15	-41.52	-7.50
967137-1	-2.36	-1.01	-0.53	-0.86	-2.49	0.43	-8.85	-1.43	-1.85	-2.12	-40.60	-7.25
967137-2	-2.63	-0.39	-0.35	-0.25	-2.54	0.12	-4.63	-2.43	-0.62	-2.40	-40.85	-6.90
967138	-2.50	-0.98	-1.12	-0.83	-2.71	0.37	-8.84	-1.43	-1.79	-2.27	-41.61	-7.39
Fassifern	-3.37	-1.41	-1.52	-1.26	-3.43	0.40	-9.69	-1.57	-2.64	-3.14	-41.72	-7.84
Surface water												
Maules crk Harparary	-2.67	0.26	-0.57	0.42	-2.77	0.34	-1.40	-3.10	0.56	-2.42	-43.58	-7.40
Maules crk surface sample 1	-2.86	-0.26	-0.98	-0.11	-2.97	0.41	-3.97	-2.50	-0.41	-2.61	-42.68	-7.55
Upper Maules crk	-2.04	-0.44	-0.27	-0.29	-2.20	0.47	-6.30	-1.79	-0.73	-1.80	-42.14	-6.78
Upper Horsearm	-3.75	-0.95	-1.73	-0.80	-3.81	0.45	-7.19	-2.11	-1.79	-3.50	-42.71	-7.93
Elfin crossing 50 m downstream	-3.23	-0.61	-1.30	-0.46	-3.31	0.44	-5.38	-2.92	-1.08	-2.99	-42.56	-7.76
Namoi-1	-2.37	0.49	-0.09	0.65	-2.42	-0.88	-2.17	-3.15	1.24	-2.12	-43.23	-7.25
Namoi-2	-2.34	0.67	-0.04	0.83	-2.38	-0.98	-1.64	-3.29	1.58	-2.08	-43.59	-7.08

Groundwater	Hausmannite Mn_3O_4	Manganite MnOOH	Melanterite $FeSO_4*7H_2O$	O2(g) $logP_{O2}$	Pyrochroite $Mn(OH)_2$	Pyrolusite MnO_2*H_2O	Quartz SiO_2	Rhodochrosite $MnCO_3$	Sepiolite $Mg_2Si_3O_{7.5}OH*3H_2O$	Siderite $FeCO_3$	Amorph Silica $SiO_2(a)$	Strontianite $SrCO_3$	Talc $Mg_3Si_4O_{10}(OH)_2$	Witherite $BaCO_3$
30129			-8.95	-1.10			0.90		-4.30	-3.07	-0.38	-2.06	-2.95	-4.01
30130-1	-21.99	-8.36	-8.77	-1.25	-8.83	-14.62	0.89	-2.07	-5.26	-2.92	-0.39	-2.43	-4.46	-4.35
30130-2			-10.27	-0.99			0.81		-3.16	-2.92	-0.46	-1.58	-1.22	-3.66
30131			-9.00	-1.30			0.91		-5.18	-2.85	-0.37	-2.46	-4.28	-4.62
30132-1			-8.36	-0.89			0.99		-6.31	-1.93	-0.28	-3.16	-6.00	-5.31
30132-2			-9.95	-1.21			0.89		-5.16	-2.31	-0.38	-2.51	-4.20	-4.43
30133	-21.00	-8.12		-0.84	-8.66	-14.09	0.91	-1.97	-5.58	-2.18	-0.36	-2.68	-4.86	-4.52
30134			-9.85	-1.10			0.96		-6.34	-3.44	-0.31	-2.87	-6.07	-4.72
30231-1	-14.55	-5.80	-9.70	-2.47	-6.57	-11.73	0.85	0.05	-4.72	-3.08	-0.43	-2.11	-3.61	-4.04
30231-2	-17.43	-6.80	-9.71	-1.90	-7.57	-12.65	0.84	-0.97	-4.85	-2.74	-0.44	-2.16	-3.77	-4.05
30232-1			-10.31	-0.90			0.91		-4.33	-3.22	-0.36	-2.07	-2.94	-4.20
30232-2	-15.16	-6.19	-7.47	-2.52	-6.95	-11.77	0.82	-0.32	-4.81	-0.45	-0.44	-2.14	-3.59	-3.87
30232-3	-13.52	-5.54	-6.83	-2.59	-6.63	-10.78	0.73	-0.28	-3.64	0.15	-0.53	-1.68	-1.79	-3.13
30233-1			-9.94	-1.11			0.92		-4.97	-3.02	-0.36	-2.14	-3.99	-4.07
30233-2	-20.16	-7.85	-11.34	-0.92	-8.60	-13.46	0.87	-1.96	-4.47	-3.55	-0.40	-2.10	-3.12	-3.83
30233-3			-9.82	-1.18			0.84		-4.44	-2.71	-0.42	-2.04	-3.04	-3.95
30234			-10.07	-0.92			0.88		-4.83	-2.88	-0.39	-2.22	-3.70	-3.98
30235-1			-9.42	-1.37			0.92		-5.93	-2.76	-0.35	-2.48	-5.40	-4.42
30235-2			-9.94	-0.95			0.89		-5.55	-2.80	-0.38	-2.45	-4.76	-4.27
30236-1			-9.95	-1.03			0.96		-4.57	-2.96	-0.31	-2.49	-3.34	-4.66
30236-2			-11.64	-0.74			0.89		-5.20	-3.93	-0.38	-2.39	-4.24	-4.14
30237			-10.43	-0.73			0.88		-5.61	-3.28	-0.38	-2.57	-4.85	-4.41
30446-1			-10.35	-0.97			0.95		-4.88	-3.14	-0.32	-2.50	-3.81	-4.51
30446-2	-13.64	-5.34	-10.82	-1.61	-7.00	-10.10	0.68	-1.30	-2.78	-2.28	-0.59	-1.41	-0.50	-4.22
30447			-9.63	-0.89			0.86		-4.01	-2.76	-0.42	-1.71	-2.53	-3.76
36003	-20.20	-7.73	-9.40	-1.63	-8.59	-13.42	0.85	-2.11	-4.67	-2.08	-0.42	-2.23	-3.48	-4.49
36004-1	-10.81	-4.65	-7.28	-2.68	-5.47	-10.31	0.59	0.94	-5.00	-0.92	-0.68	-2.27	-3.82	-3.83
36004-2	-17.92	-6.99	-8.69	-2.69	-7.64	-12.98	0.86	-0.93	-4.84	-1.53	-0.42	-2.21	-3.78	-4.36
36005-1	-15.86	-6.48	-5.99	-2.31	-6.98	-12.38	0.86	-0.08	-4.84	-0.12	-0.41	-2.26	-3.68	-4.30
36005-2	-14.78	-6.01	-6.80	-2.43	-6.78	-11.68	0.80	-0.05	-4.34	0.02	-0.47	-1.90	-2.91	-3.94
36093-1	-17.80	-6.88	-7.66	-2.36	-7.28	-13.43	0.79	-0.48	-6.29	-1.86	-0.50	-2.69	-6.05	-4.50
36093-2	-23.26	-8.81	-8.93	-2.87	-9.23	-15.10	0.86	-2.47	-5.84	-2.95	-0.43	-2.68	-5.31	-5.04
36093-3	-17.69	-6.94	-9.02	-2.95	-7.47	-13.08	0.81	-0.78	-5.61	-2.98	-0.47	-2.56	-4.92	-4.83
36094-1			-10.30	-0.87			0.95		-4.98	-3.40	-0.32	-2.45	-3.97	-4.52
36094-2				-0.91			0.94		-5.06		-0.33	-2.44	-4.04	-4.62
36094-3				-2.00			0.73		-3.73		-0.54	-1.76	-1.96	-4.32
36096-1	-15.89	-6.42	-7.92	-2.94	-6.84	-12.58	0.76	0.15	-5.88	-2.08	-0.52	-2.41	-5.27	-4.07
36096-2	-21.05	-8.04	-8.17	-2.45	-8.47	-14.38	0.88	-1.60	-5.38	-2.15	-0.40	-2.39	-4.66	-5.30
36164	-10.38	-4.19	-6.74	-2.61	-5.56	-9.55	0.71	0.55	-2.42	0.07	-0.57	-1.27	-0.11	-3.06
36186	-24.56	-9.15	-9.01	-1.76	-9.86	-15.15	0.90	-3.21	-4.40	-2.95	-0.38	-2.12	-3.16	-4.05
36187			-8.86	-1.29			0.95		-3.31	-2.71	-0.33	-1.58	-1.51	-3.43
41025	-12.45	-5.11	-7.63	-2.64	-6.22	-10.45	0.80	0.18	-3.49	-0.45	-0.47	-1.60	-1.64	-3.34
41027	-22.20	-8.48	-8.31	-1.50	-9.04	-14.50	0.80	-2.29	-5.37	-2.26	-0.47	-2.51	-4.52	-5.08
967137-1	-17.98	-7.07	-6.97	-3.34	-7.62	-13.11	0.85	-0.90	-5.24	-0.99	-0.42	-2.46	-4.34	-4.61
967137-2	-11.64	-4.61	-7.77	-2.80	-6.23	-9.56	0.55	-0.51	-2.94	-0.89	-0.73	-1.62	-0.74	-3.54
967138			-8.84	-1.15			0.79		-5.35	-2.68	-0.48	-2.51	-4.45	-5.02
Fassifern			-9.87	-1.16			0.83		-5.83	-3.28	-0.45	-2.79	-5.24	-4.99
Surface water														
Maules crk Harparary				-0.70			0.80		-0.06		-0.55	-1.11	2.79	-3.16
Maules crk surface sample 1	-14.19	-5.10	-9.95	-0.73	-6.64	-10.88	0.85	-1.03	-1.84	-2.78	-0.46	-1.67	0.44	-3.86
Upper Maules crk	-18.54	-6.89	-8.59	-1.19	-7.87	-12.94	0.90	-1.53	-3.37	-2.38	-0.40	-1.90	-1.76	-4.13
Upper Horsearm	-17.76	-6.42	-9.82	-0.79	-7.48	-12.74	0.90	-1.47	-3.90	-2.46	-0.42	-2.31	-2.70	-4.42
Elfin crossing 50 m downstream	-14.19	-5.27	-9.96	-0.61	-6.58	-11.10	0.87	-0.77	-2.79	-2.76	-0.43	-1.99	-0.91	-4.15
Namoi-1	-12.45	-4.02	-9.59	-0.70	-6.26	-9.62	-0.43	-1.32	-2.68	-2.21	-1.76	-0.84	-0.39	-2.73
Namoi-2	-10.06	-3.01	-9.43	-0.68	-5.39	-8.79	-0.52	-0.61	-2.42	-1.93	-1.87	-0.64	-0.09	-2.55

Appendix 3. Geophysical Well Logs

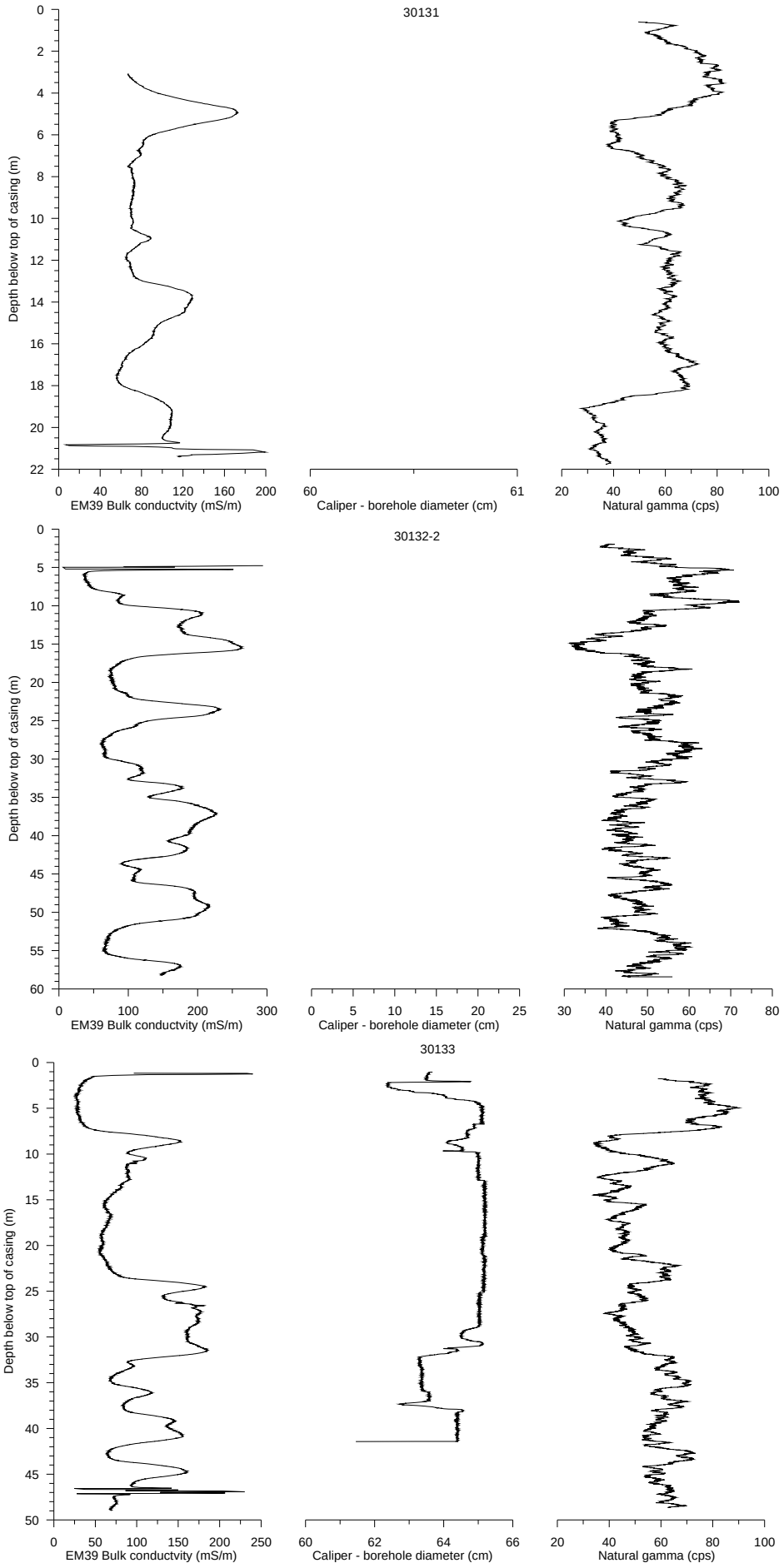

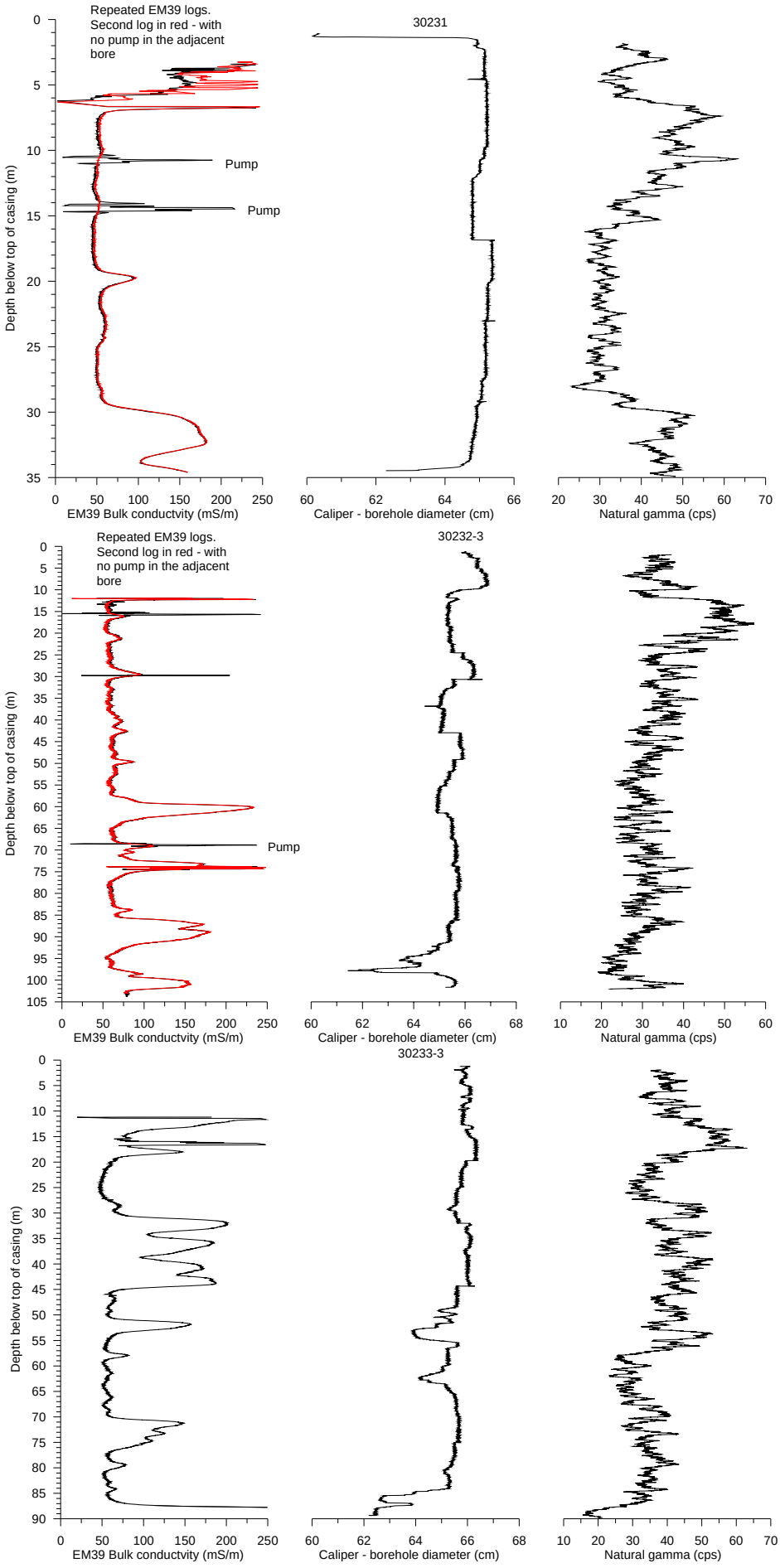
Repeated EM39 logs.
Second log in red - with no pump in the adjacent bore
Pump
Pump
Depth below top of casing (m)
EM39 Bulk conductvity (mS/m)
30231
Caliper - borehole diameter (cm)
Natural gamma (cps)
Repeated EM39 logs.
Second log in red - with no pump in the adjacent bore
Pump
Depth below top of casing (m)
EM39 Bulk conductvity (mS/m)
30232-3
Caliper - borehole diameter (cm)
Natural gamma (cps)
30233-3
Depth below top of casing (m)
EM39 Bulk conductvity (mS/m)
Caliper - borehole diameter (cm)
Natural gamma (cps)

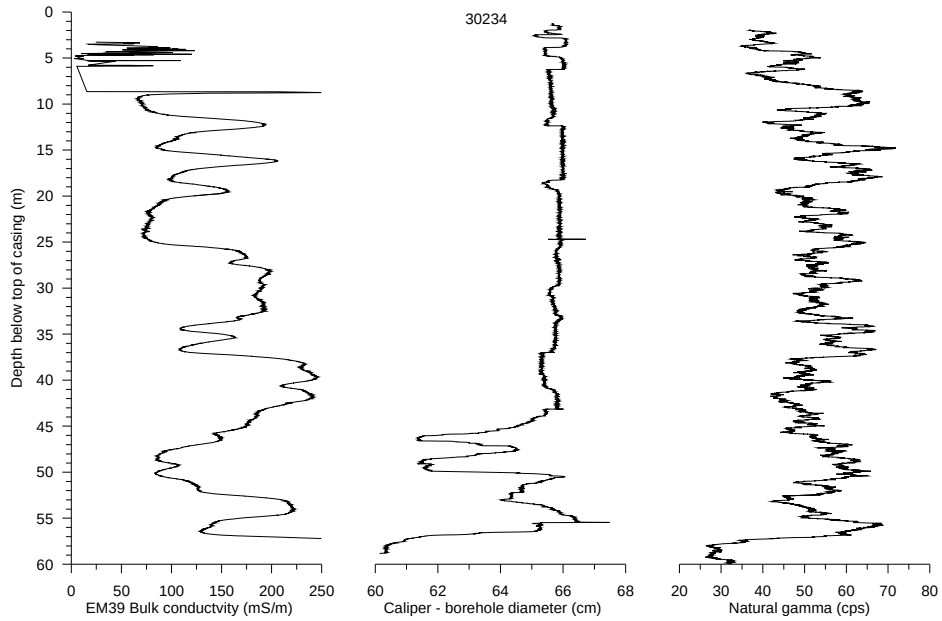
30234
Depth below top of casing (m)
EM39 Bulk conductvity (mS/m)
Caliper - borehole diameter (cm)
Natural gamma (cps)

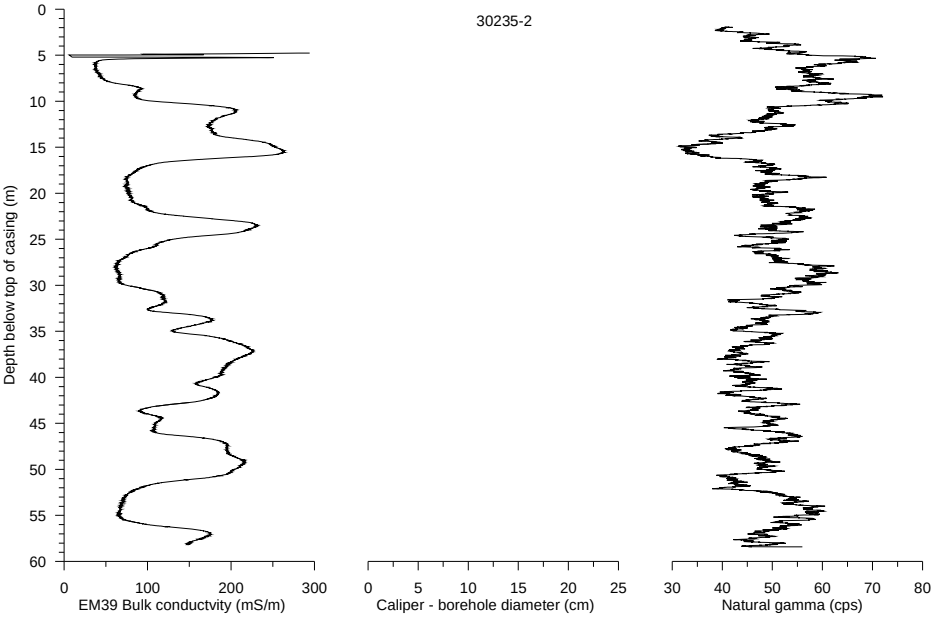
30235-2
Depth below top of casing (m)
EM39 Bulk conductvity (mS/m)
Caliper - borehole diameter (cm)
Natural gamma (cps)

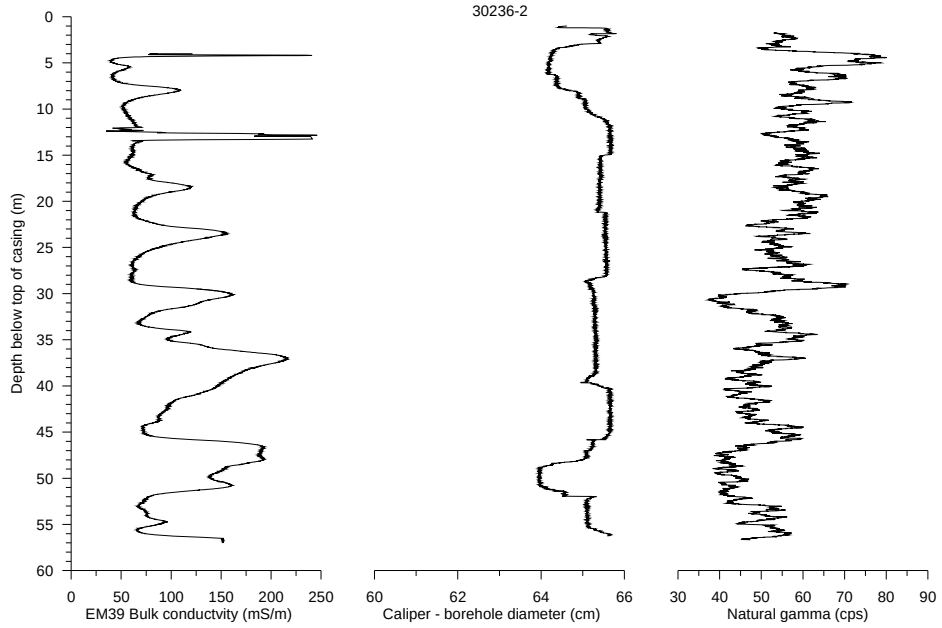
30236-2
Depth below top of casing (m)
EM39 Bulk conductvity (mS/m)
Caliper - borehole diameter (cm)
Natural gamma (cps)

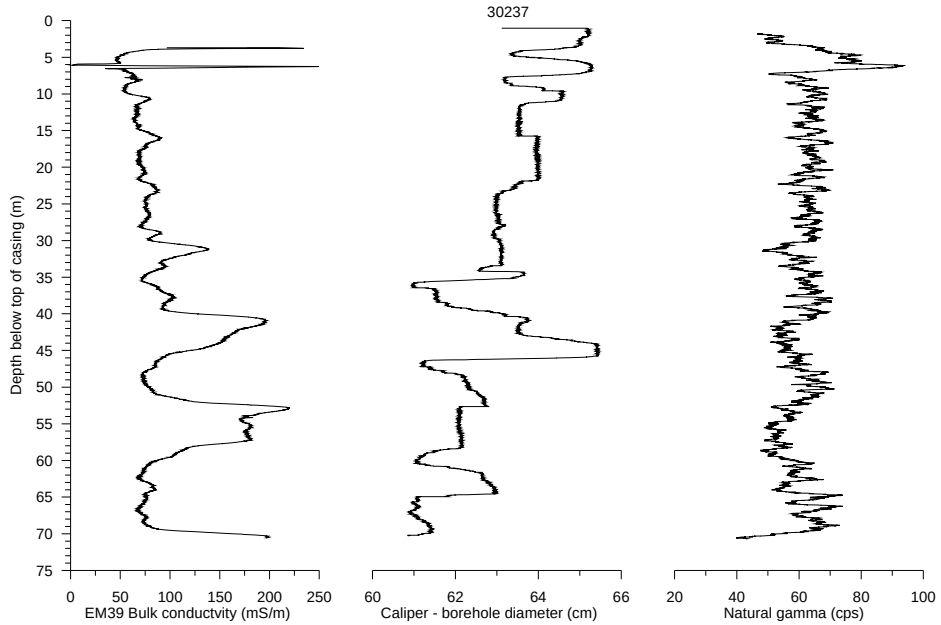
30237
Depth below top of casing (m)
EM39 Bulk conductvity (mS/m)
Caliper - borehole diameter (cm)
Natural gamma (cps)

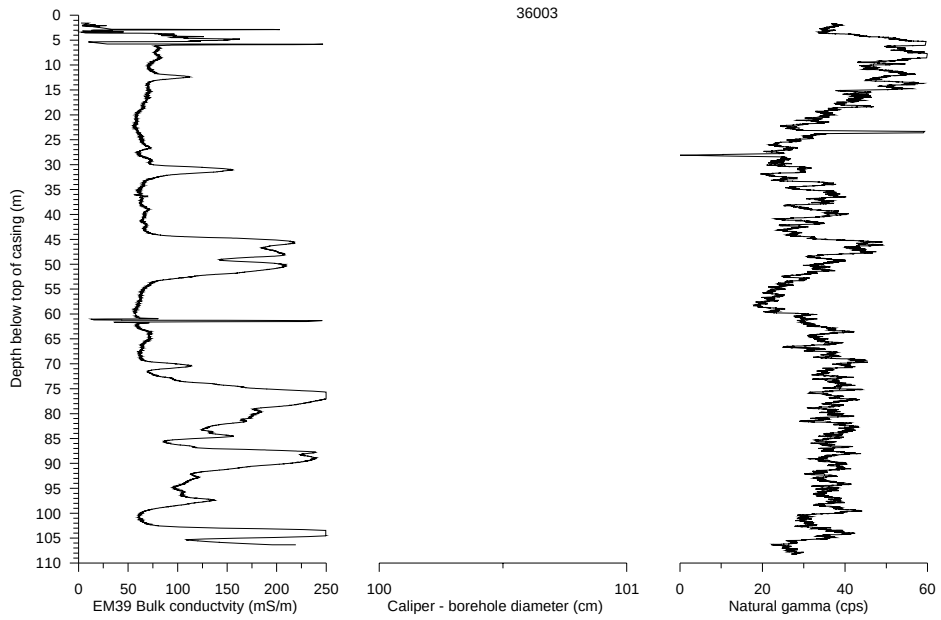
36003
Depth below top of casing (m)
EM39 Bulk conductvity (mS/m)
Caliper - borehole diameter (cm)
Natural gamma (cps)

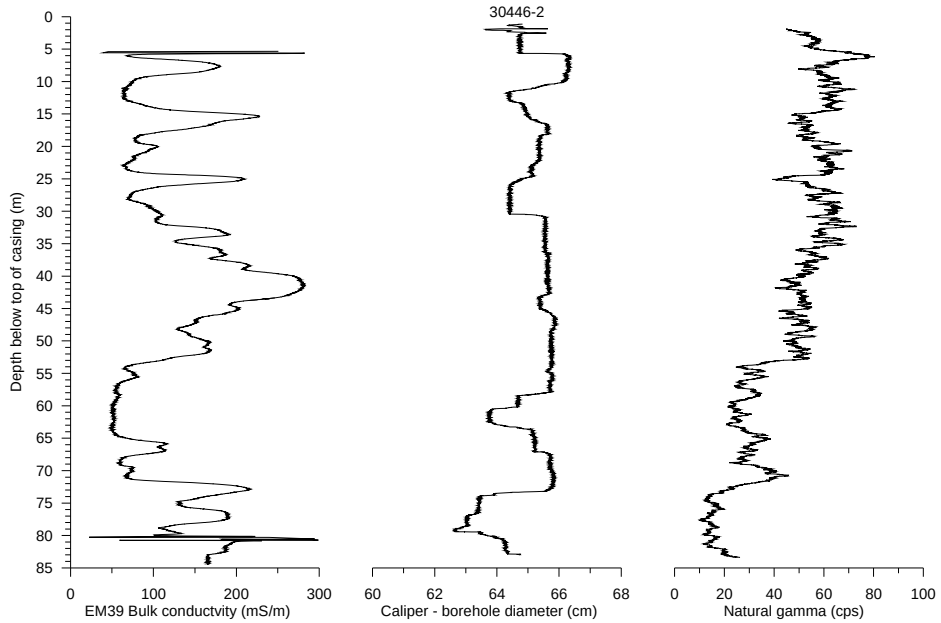
30446-2
Depth below top of casing (m)
EM39 Bulk conductvity (mS/m)
Caliper - borehole diameter (cm)
Natural gamma (cps)

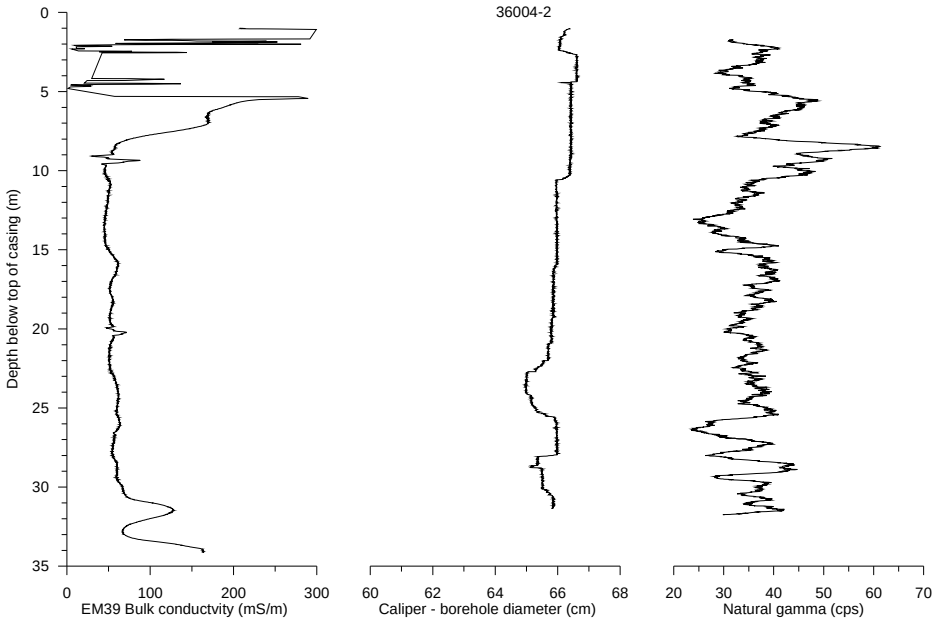
36004-2
Depth below top of casing (m)
EM39 Bulk conductvity (mS/m)
Caliper - borehole diameter (cm)
Natural gamma (cps)

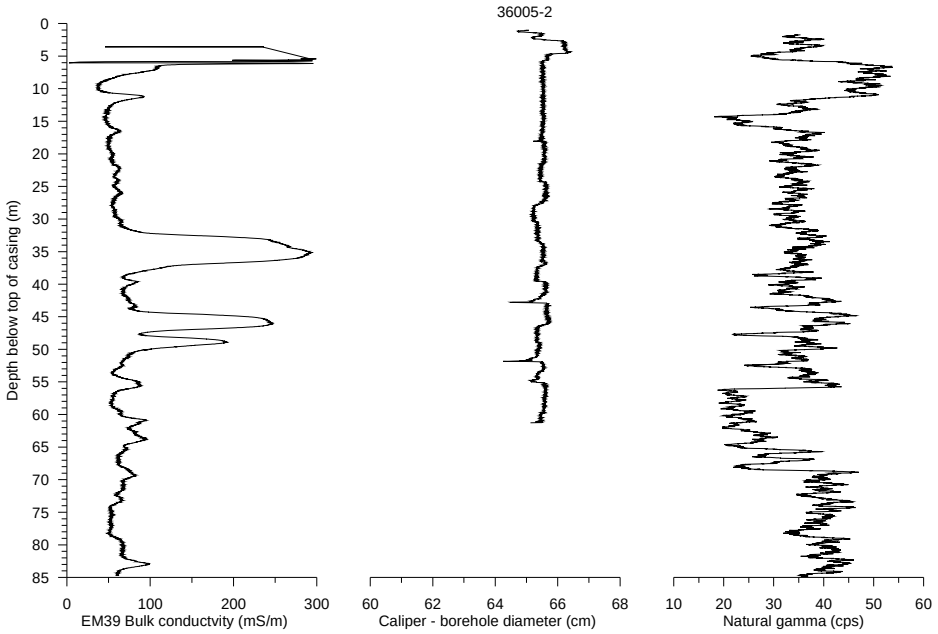
36005-2
Depth below top of casing (m)
EM39 Bulk conductvity (mS/m)
Caliper - borehole diameter (cm)
Natural gamma (cps)

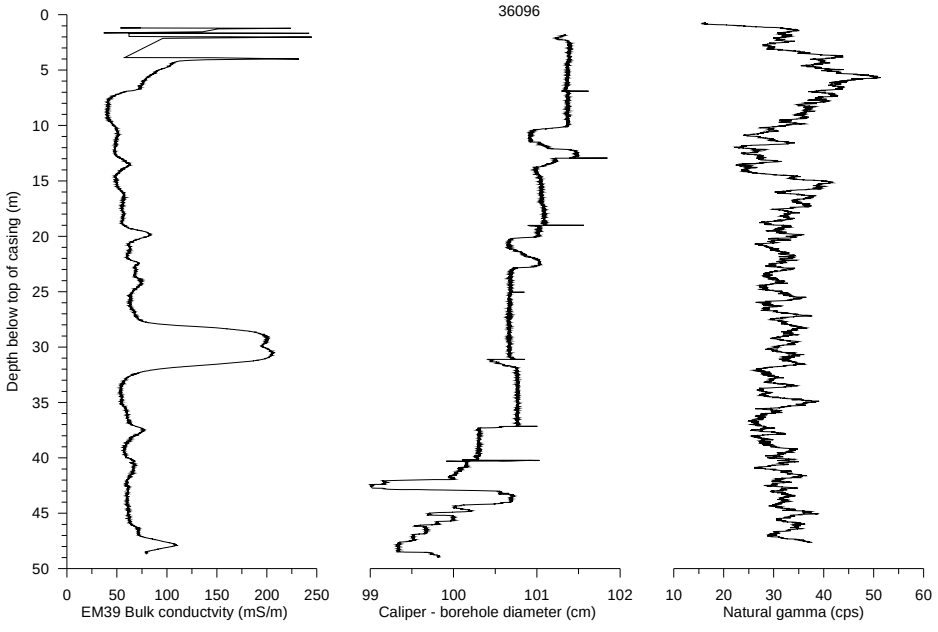
36096
Depth below top of casing (m)
EM39 Bulk conductvity (mS/m)
Caliper - borehole diameter (cm)
Natural gamma (cps)

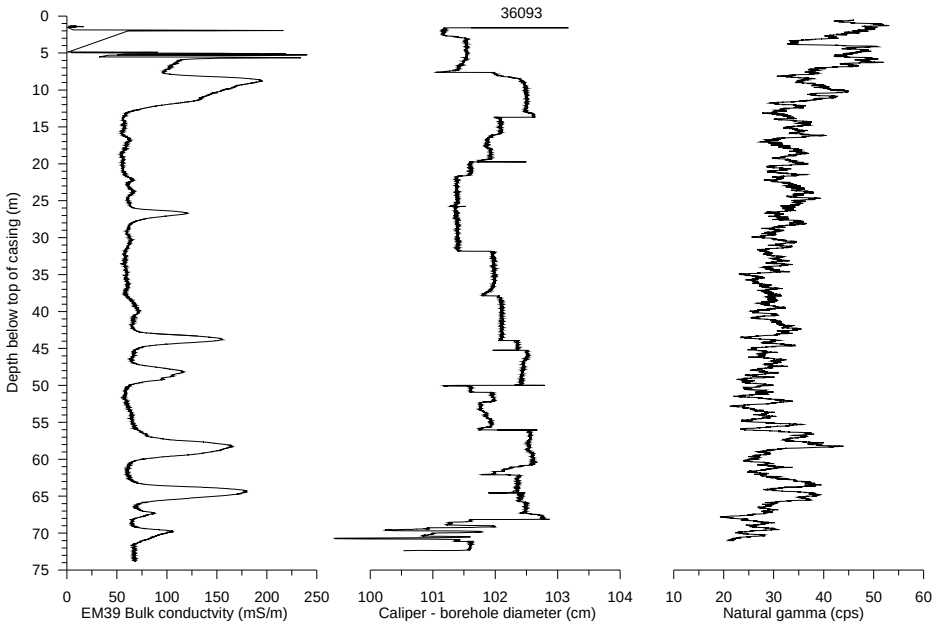
36093
Depth below top of casing (m)
EM39 Bulk conductvity (mS/m)
Caliper - borehole diameter (cm)
Natural gamma (cps)

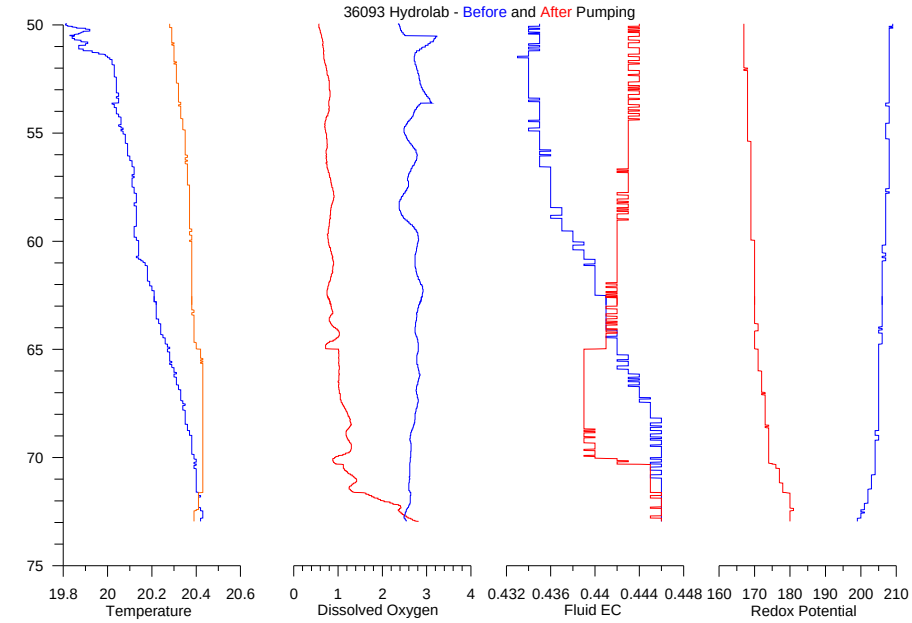
36093 Hydrolab - Before and After Pumping
Temperature
Dissolved Oxygen
Fluid EC
Redox Potential

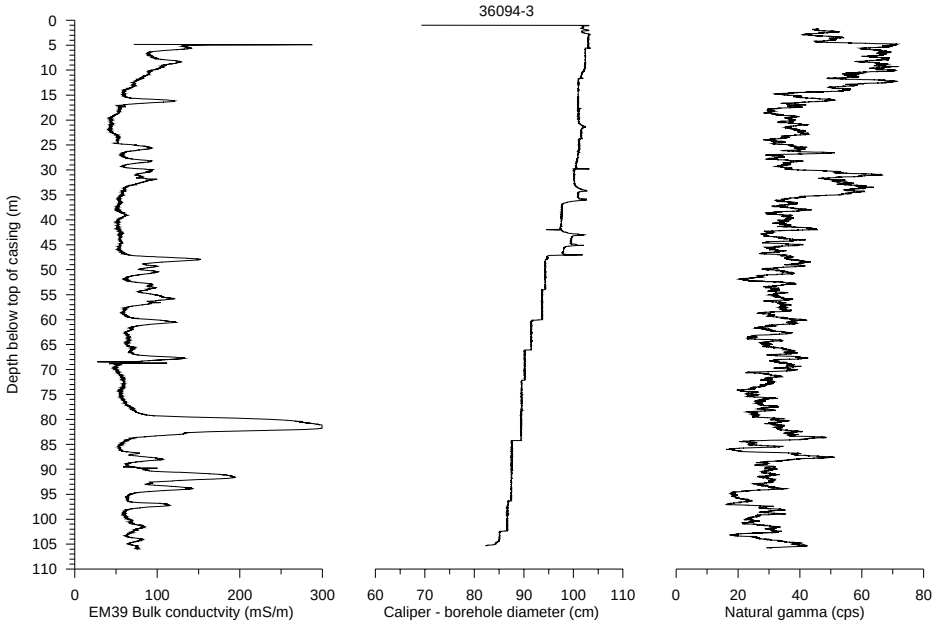
36094-3
Depth below top of casing (m)
EM39 Bulk conductvity (mS/m)
Caliper - borehole diameter (cm)
Natural gamma (cps)

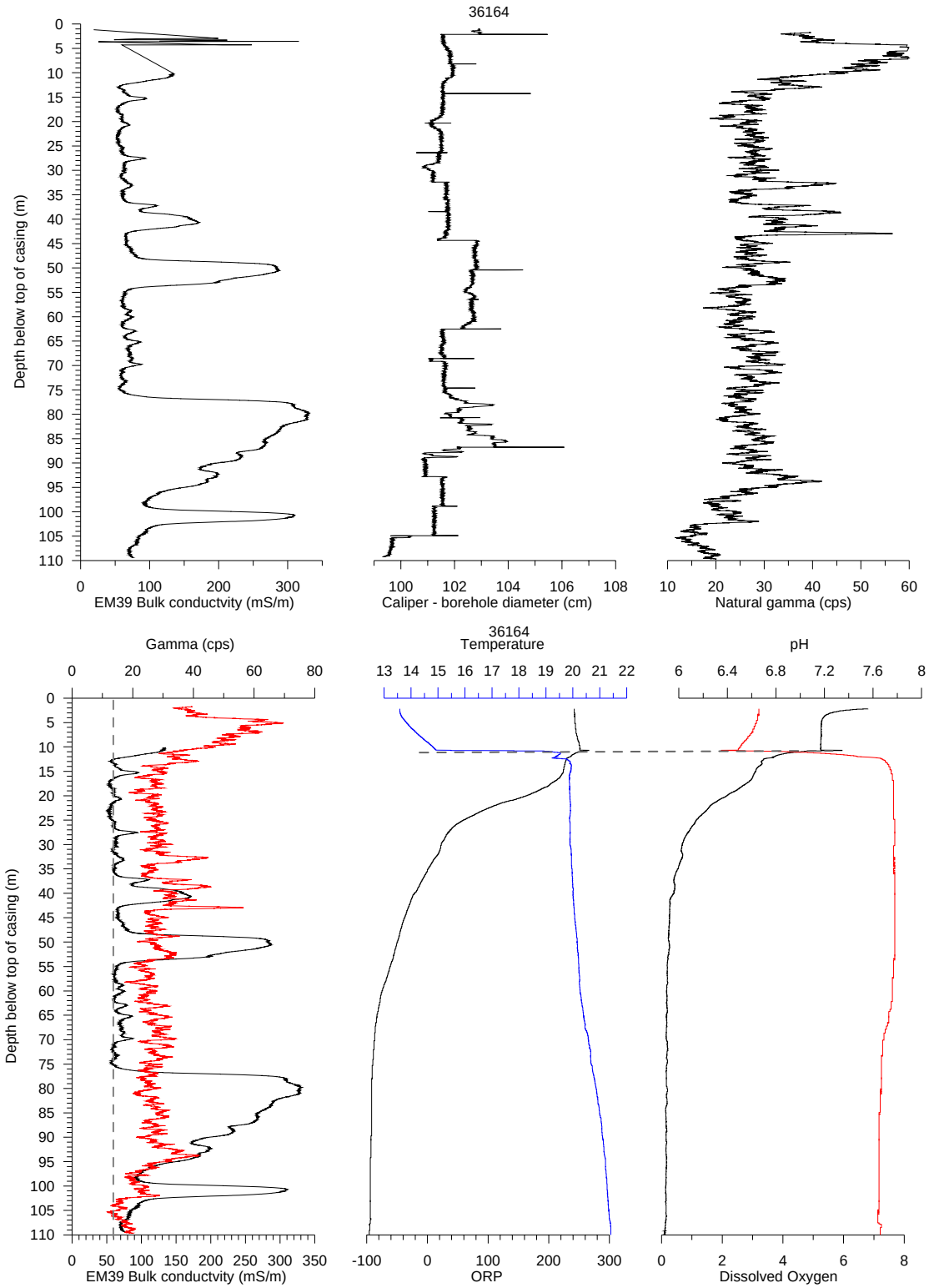
36164
Depth below top of casing (m)
EM39 Bulk conductvity (mS/m)
Caliper - borehole diameter (cm)
Natural gamma (cps)
Gamma (cps)
36164
Temperature
pH
Depth below top of casing (m)
EM39 Bulk conductvity (mS/m)
ORP
Dissolved Oxygen

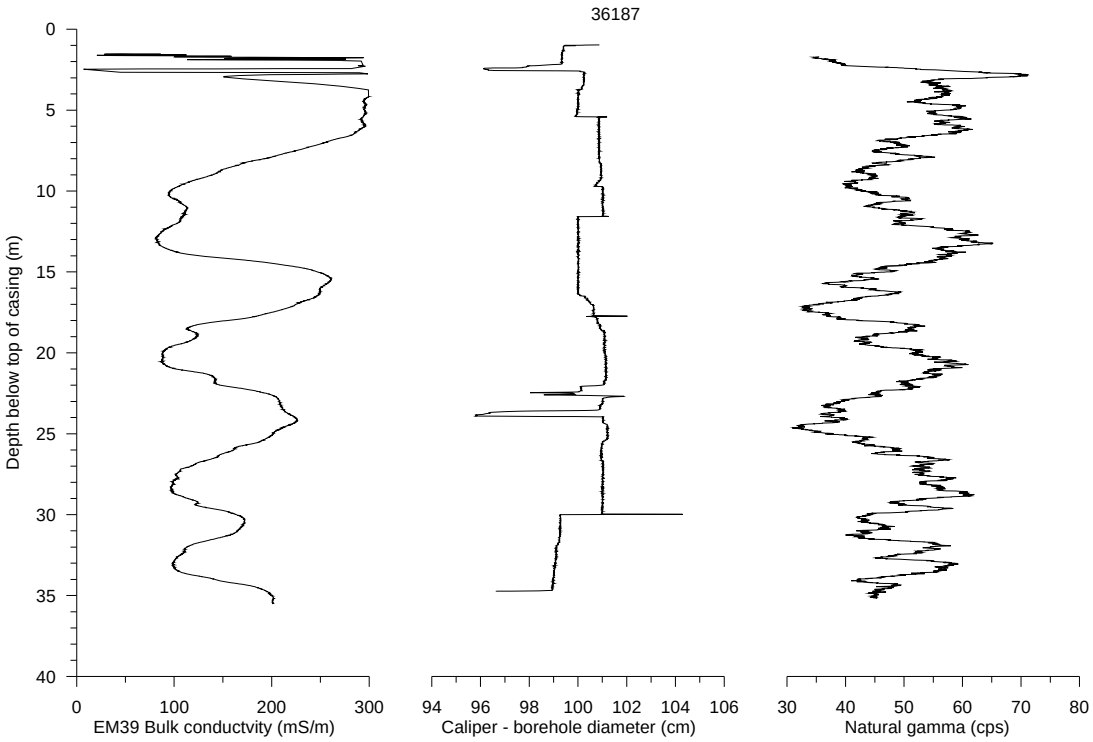
36187
Depth below top of casing (m)
0
5
10
15
20
25
30
35
40
0
100
200
300
EM39 Bulk conductvity (mS/m)
94
96
98
100
102
104
106
Caliper - borehole diameter (cm)
30
40
50
60
70
80
Natural gamma (cps)

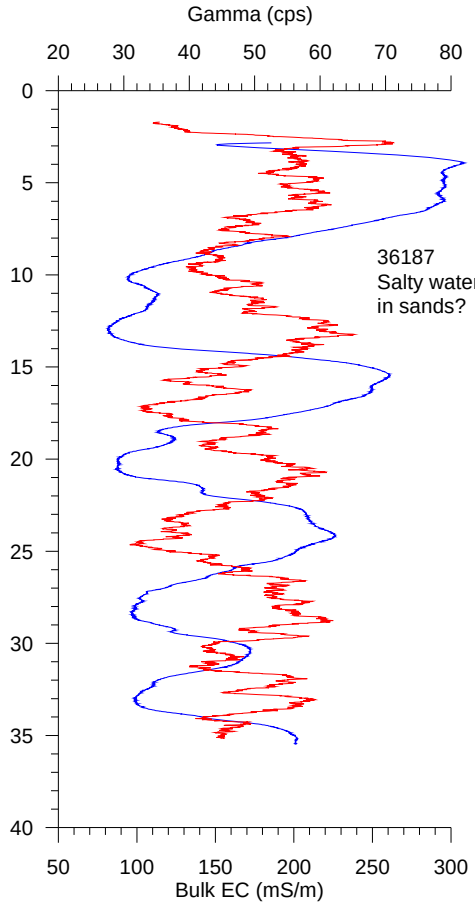
Gamma (cps)
20
30
40
50
60
70
80
0
5
10
15
20
25
30
35
40
36187
Salty water
in sands?
50
100
150
200
250
300
Bulk EC (mS/m)

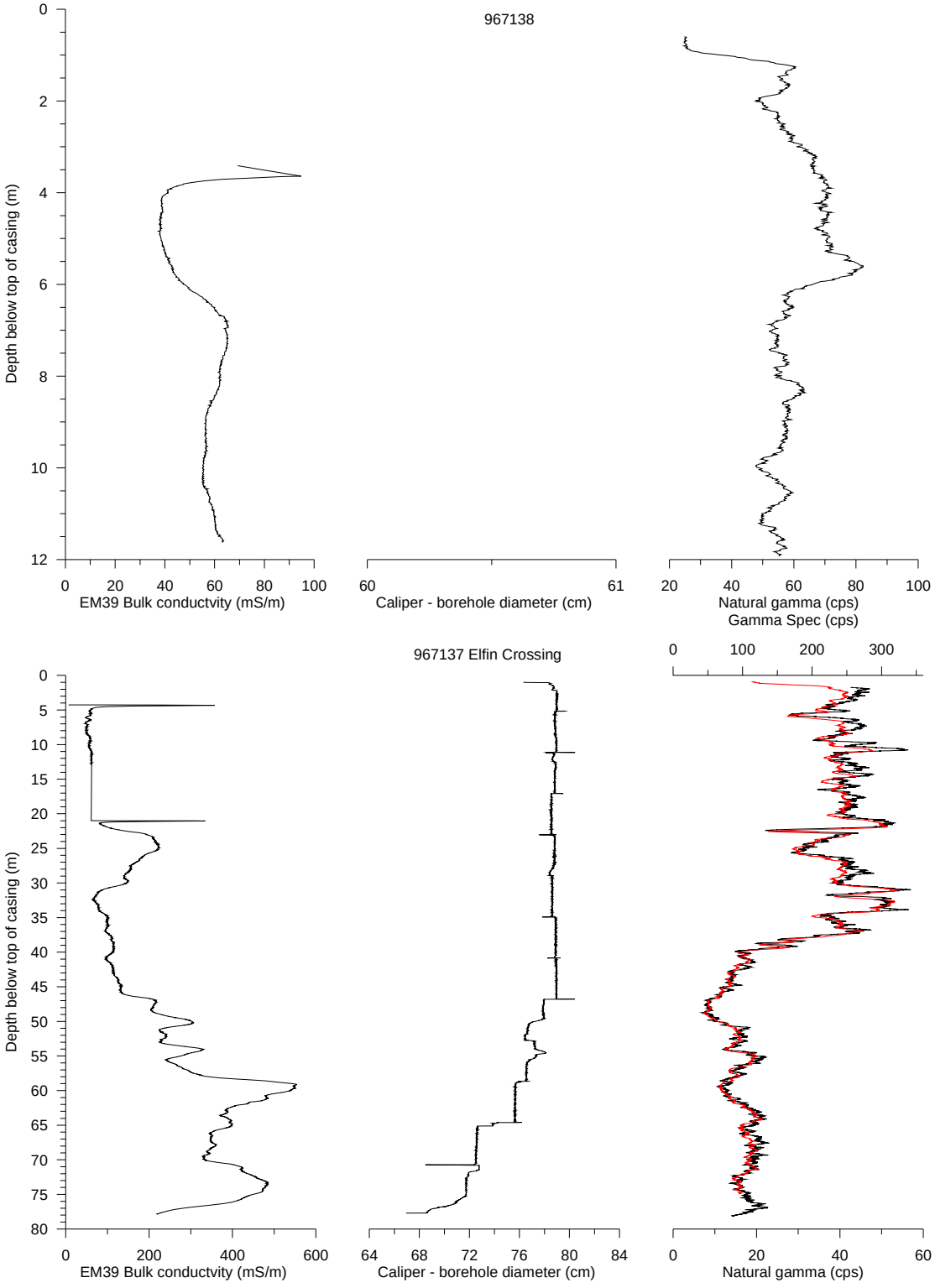
967138
Depth below top of casing (m)
EM39 Bulk conductvity (mS/m)
Caliper - borehole diameter (cm)
Natural gamma (cps)
Gamma Spec (cps)
967137 Elfin Crossing
Depth below top of casing (m)
EM39 Bulk conductvity (mS/m)
Caliper - borehole diameter (cm)
Natural gamma (cps)

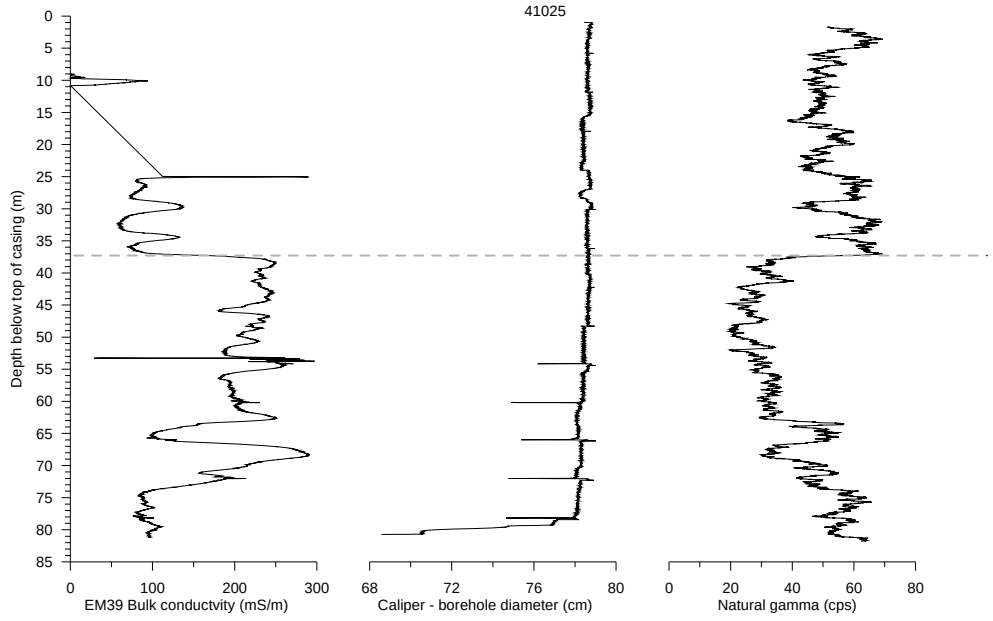
41025
Depth below top of casing (m)
EM39 Bulk conductvity (mS/m)
Caliper - borehole diameter (cm)
Natural gamma (cps)

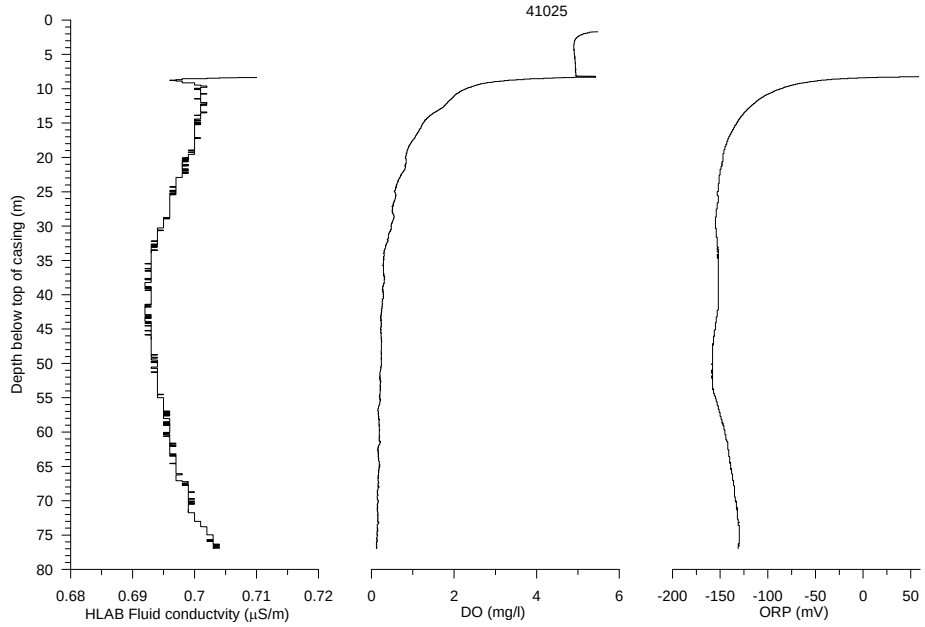
41025
Depth below top of casing (m)
HLAB Fluid conductvity (µS/m)
DO (mg/l)
ORP (mV)

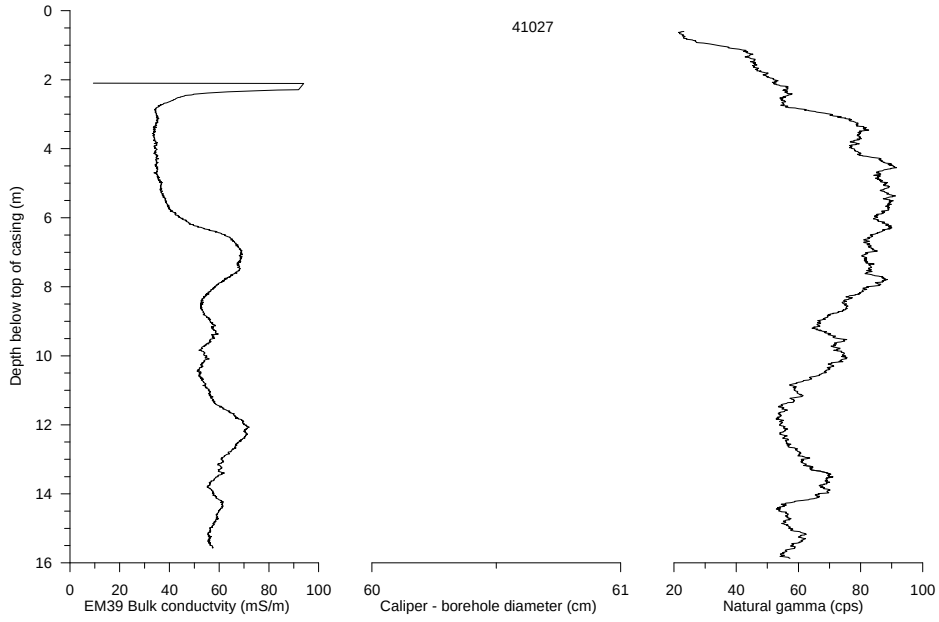
41027
Depth below top of casing (m)
EM39 Bulk conductvity (mS/m)
Caliper - borehole diameter (cm)
Natural gamma (cps)

Appendix 4. Resistivity Images near the Namoi River on the Property of Darren Eather

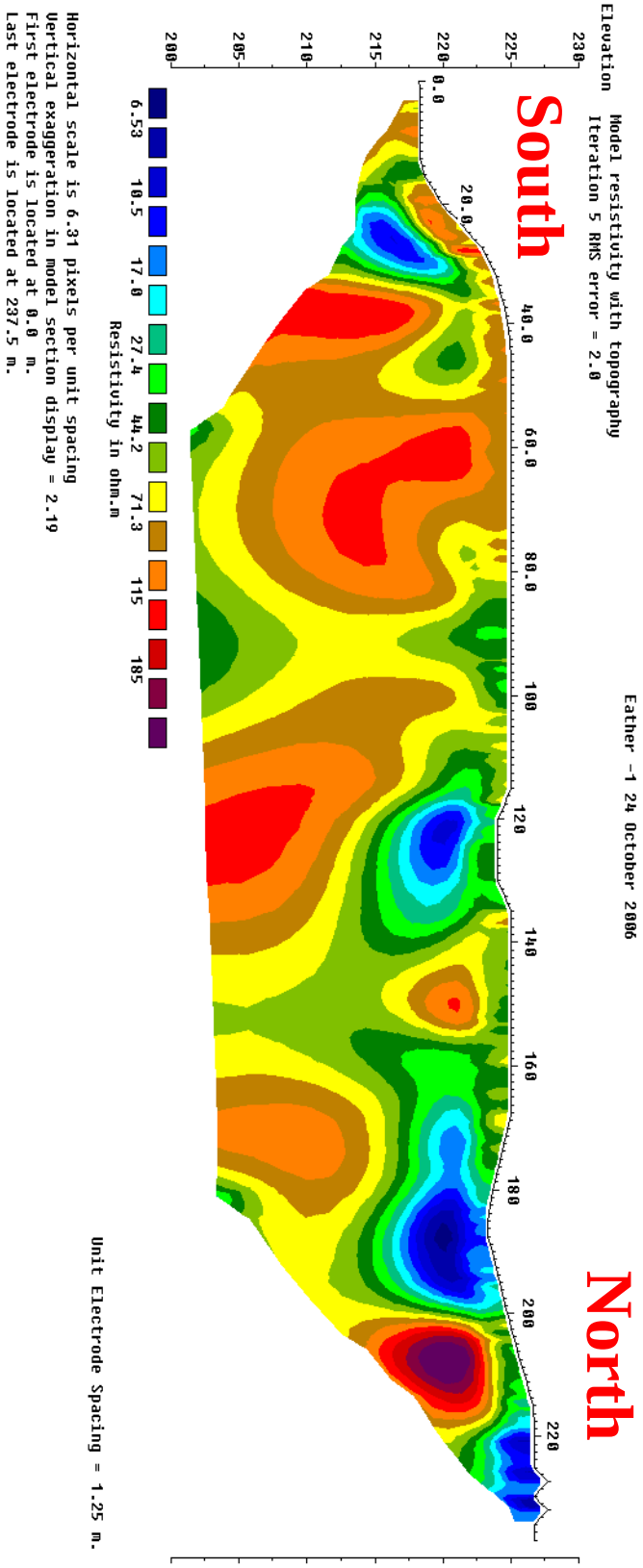

Fig. A.4-1: North-south trending resistivity image (on Darren Eathers property). The Namoi River is located immediately to the south. An irrigation bore is located at about 220 m with irrigation ditch located at about 230 m.

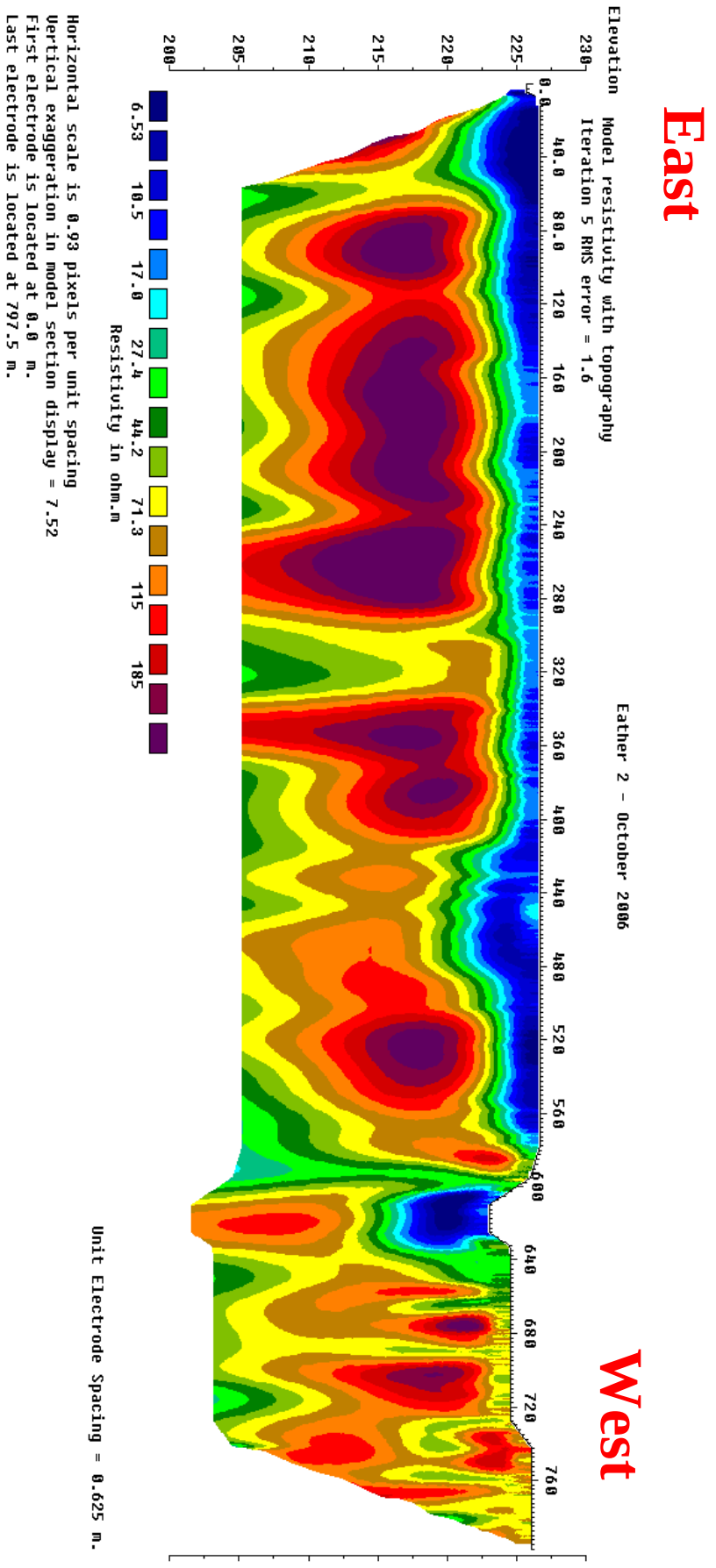

Fig A.4-2. East-west trending resistivity image (on Darren Eathers property). Wheat field from 0 to 560 m. The Namoi River is located about 50 m off the profile to the west.

Appendix 5. Head Distributions in the Upper, Middle and Lower Aquifer in August 2006

a) Hydraulic head upper aquifer (< 30 m)

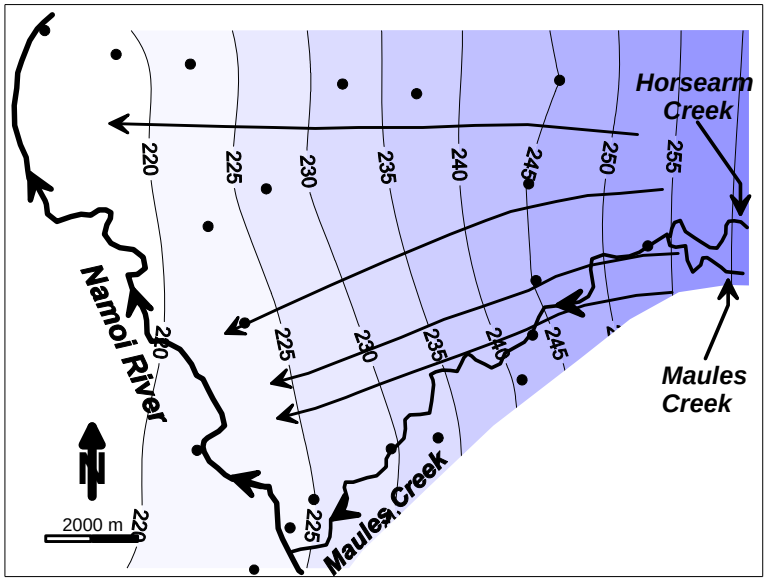

b) Hydraulic head middle part of aquifer (30-60 m)

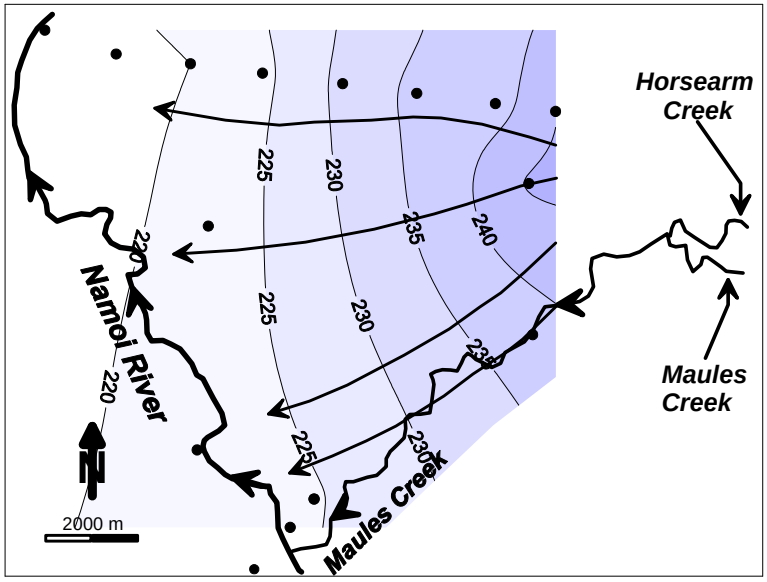

c) Hydraulic head lower part of aquifer (> 60 m)

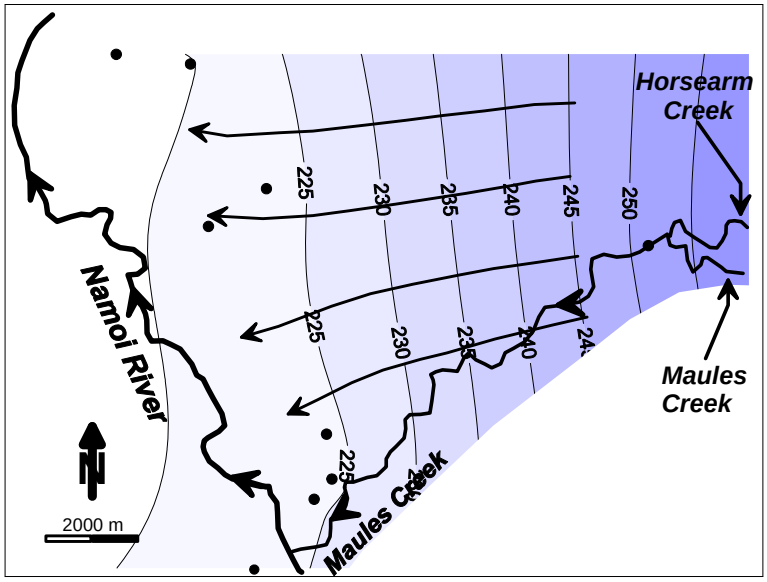

Appendix 6. Head Distributions in the Upper, Middle and Lower Aquifer in October 2006

a) Hydraulic head upper part of aquifer (< 30 m)

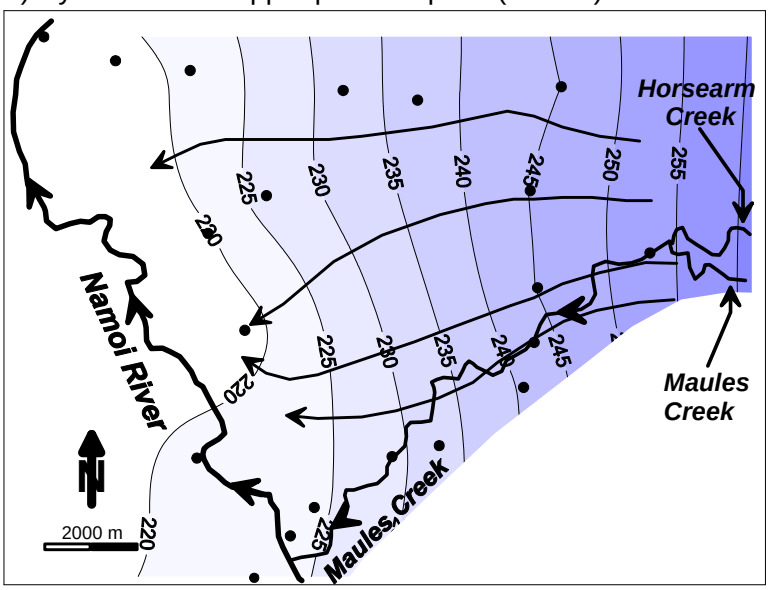

b) Hydraulic head middle part of aquifer (30-60 m)

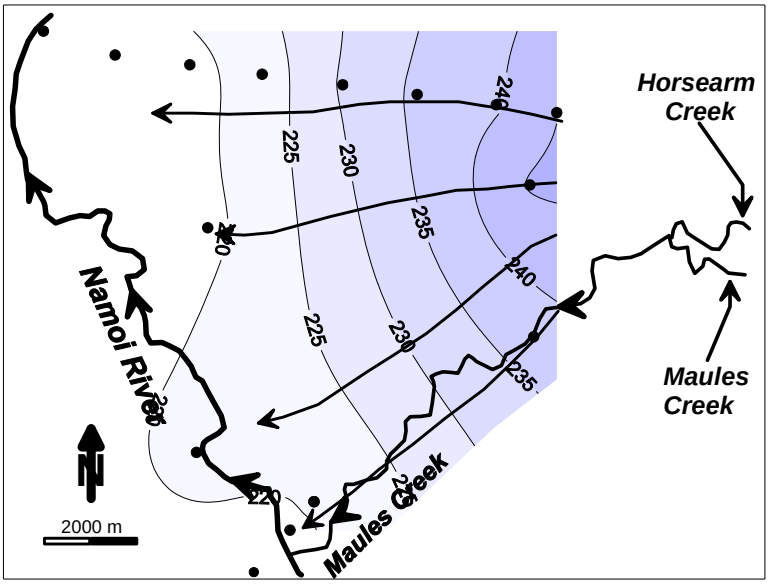

c) Hydraulic head lower part of aquifer (> 60 m)

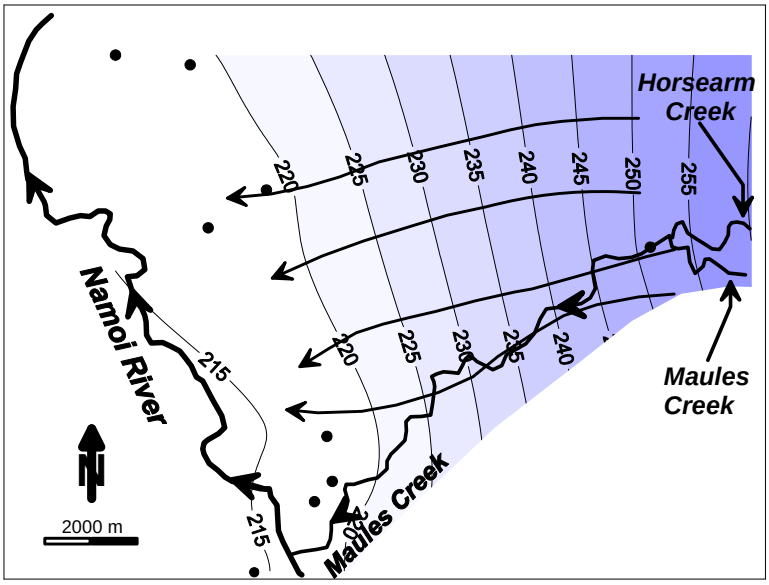

Appendix 7. Comparison of Groundwater Hydrograph GW036093 and Stream Flow in Maules Creek and the Namoi River

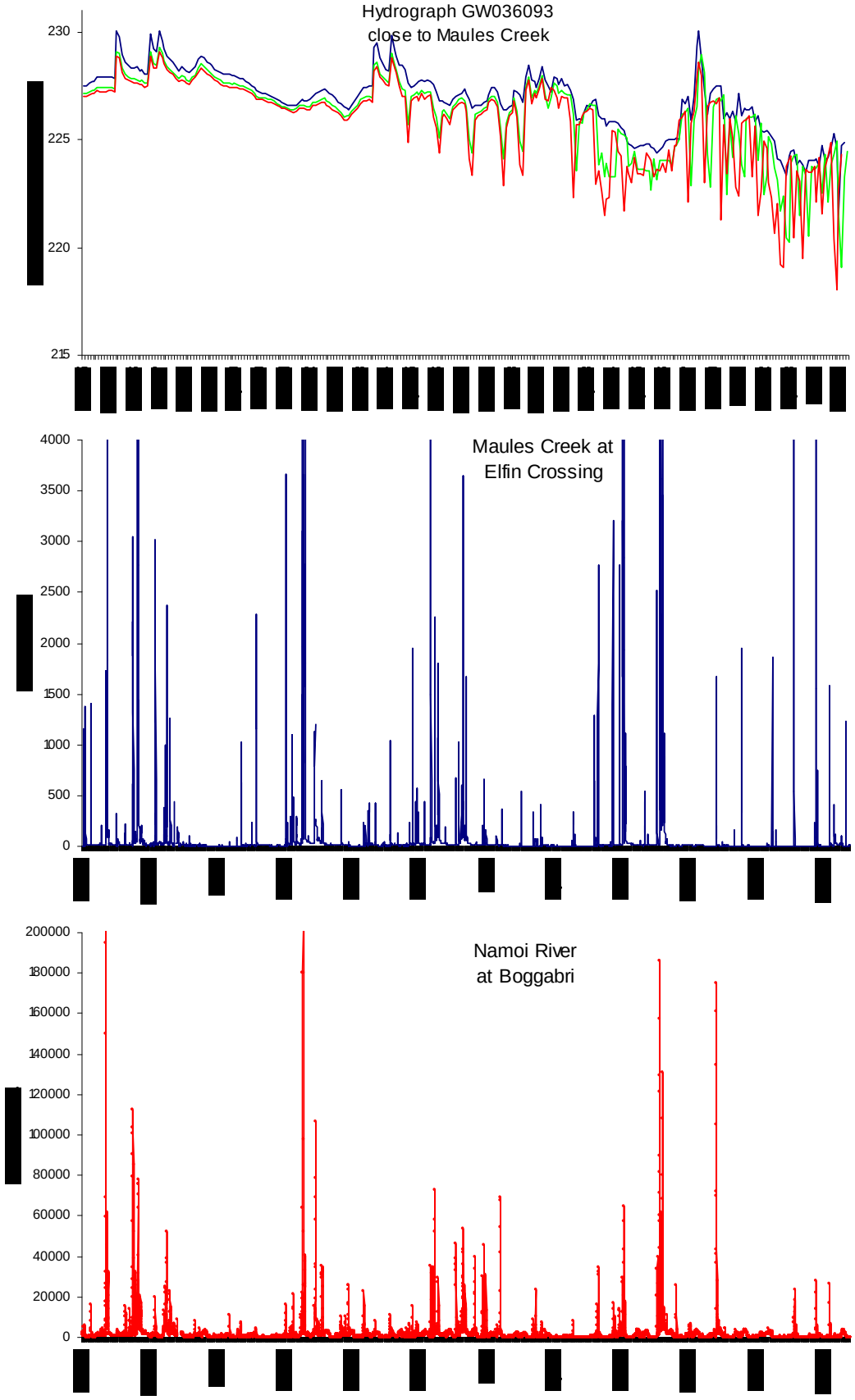

Appendix 8. Plots of Surface Water Chemistry

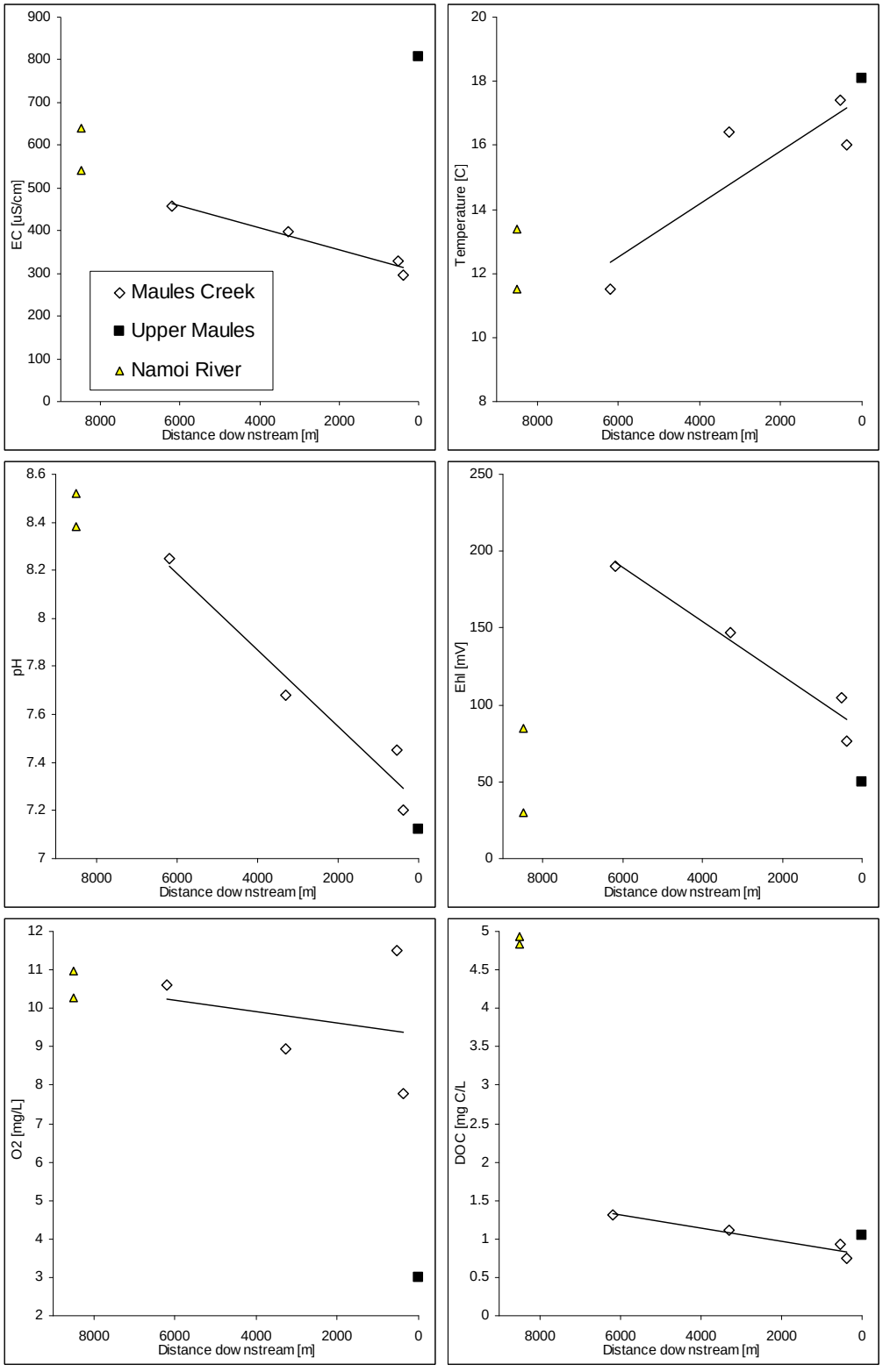

Fig. A.8-1. Water quality parameters: Electrical conductivity (EC), Temperature, pH, Redox potential (Eh), dissolved oxygen (DO), dissolved organic carbon (DOC).

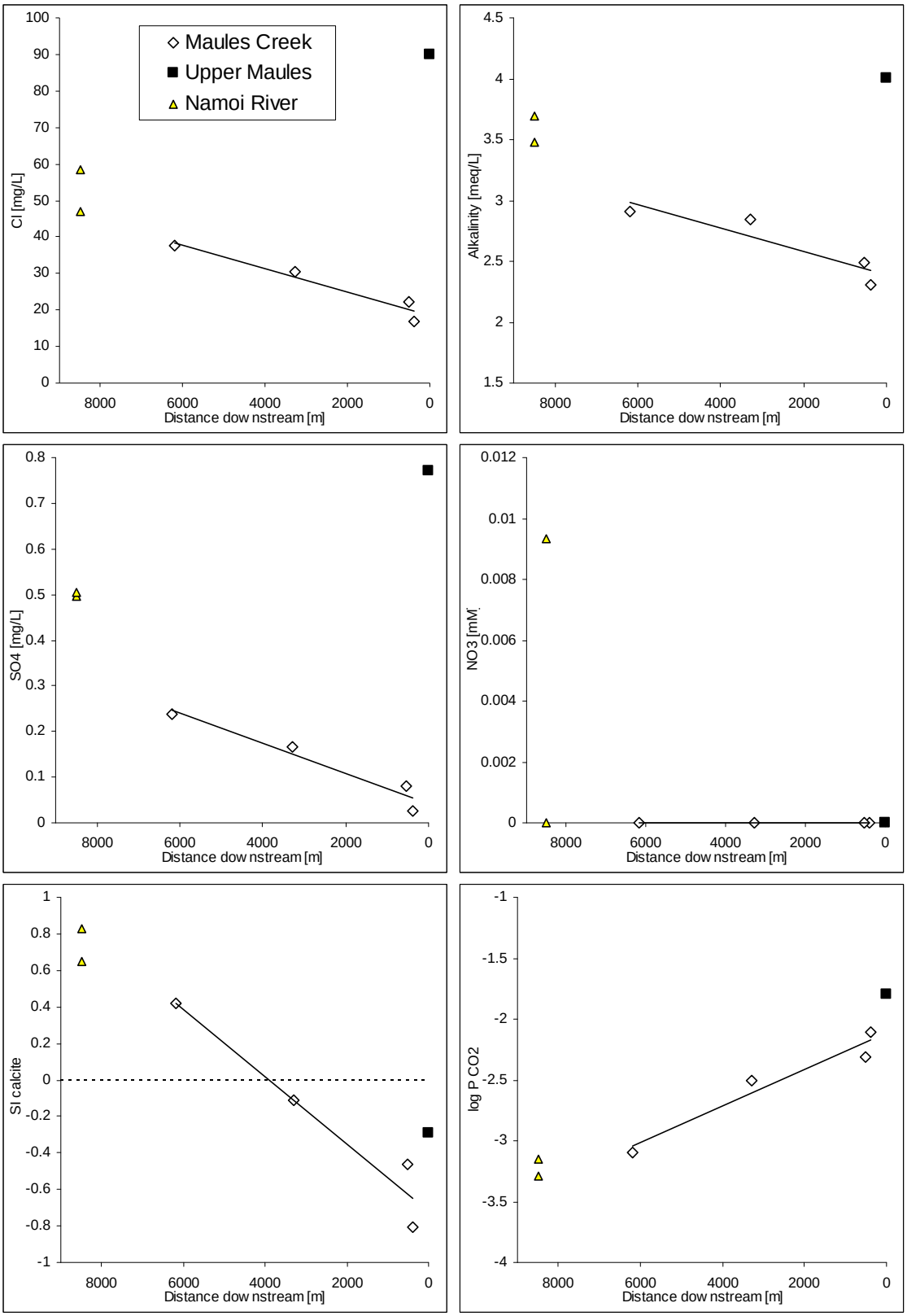

Fig. A.8-2. Anions: Cl^-, Alkalinity (HCO_3^-), SO_4^{2-}, NO_3^-; Saturation index (SI) for calcite and $\log P_{CO2}$.

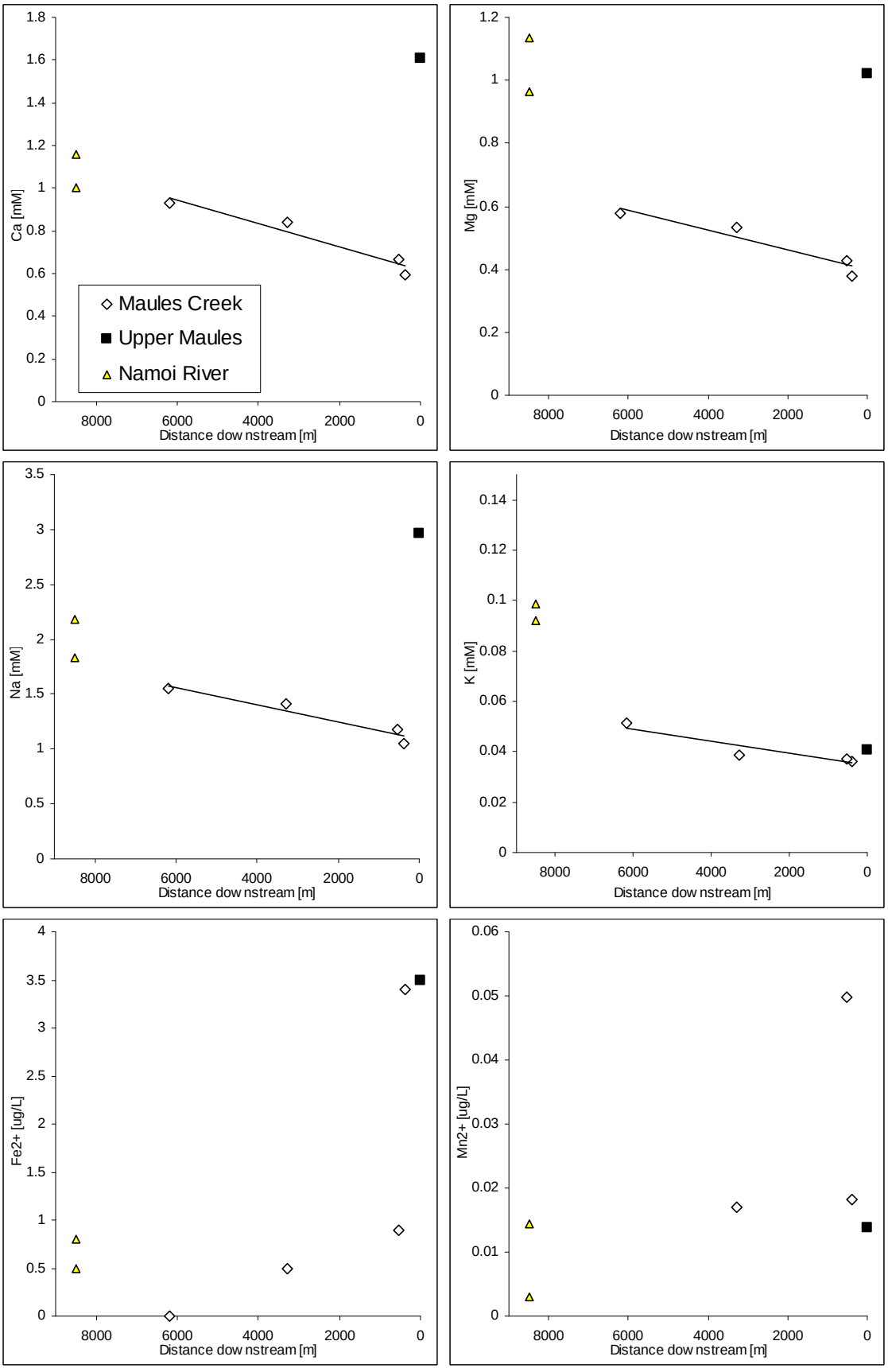

Fig. A.8-3. Major cations: Ca^{2+}, Mg^{2+}, Na^{+}, K^{+}; and Fe^{2+} and Mn^{2+}.

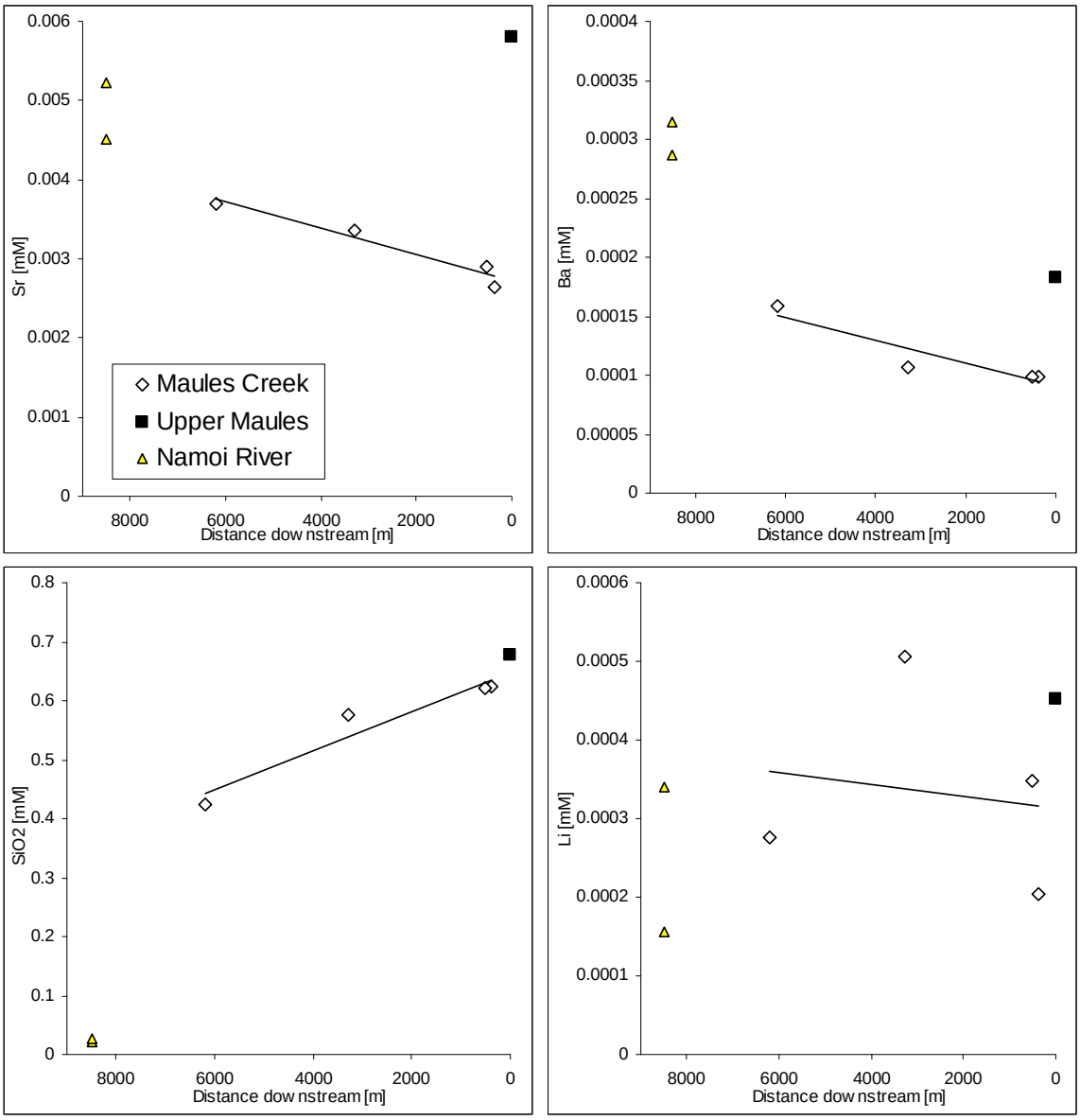

Fig. A.8-4. Trace elements: Sr^{2+}, Ba^{2+}, Silica and Li^{+}.

Appendix 9. Surface Water Ion Ratios

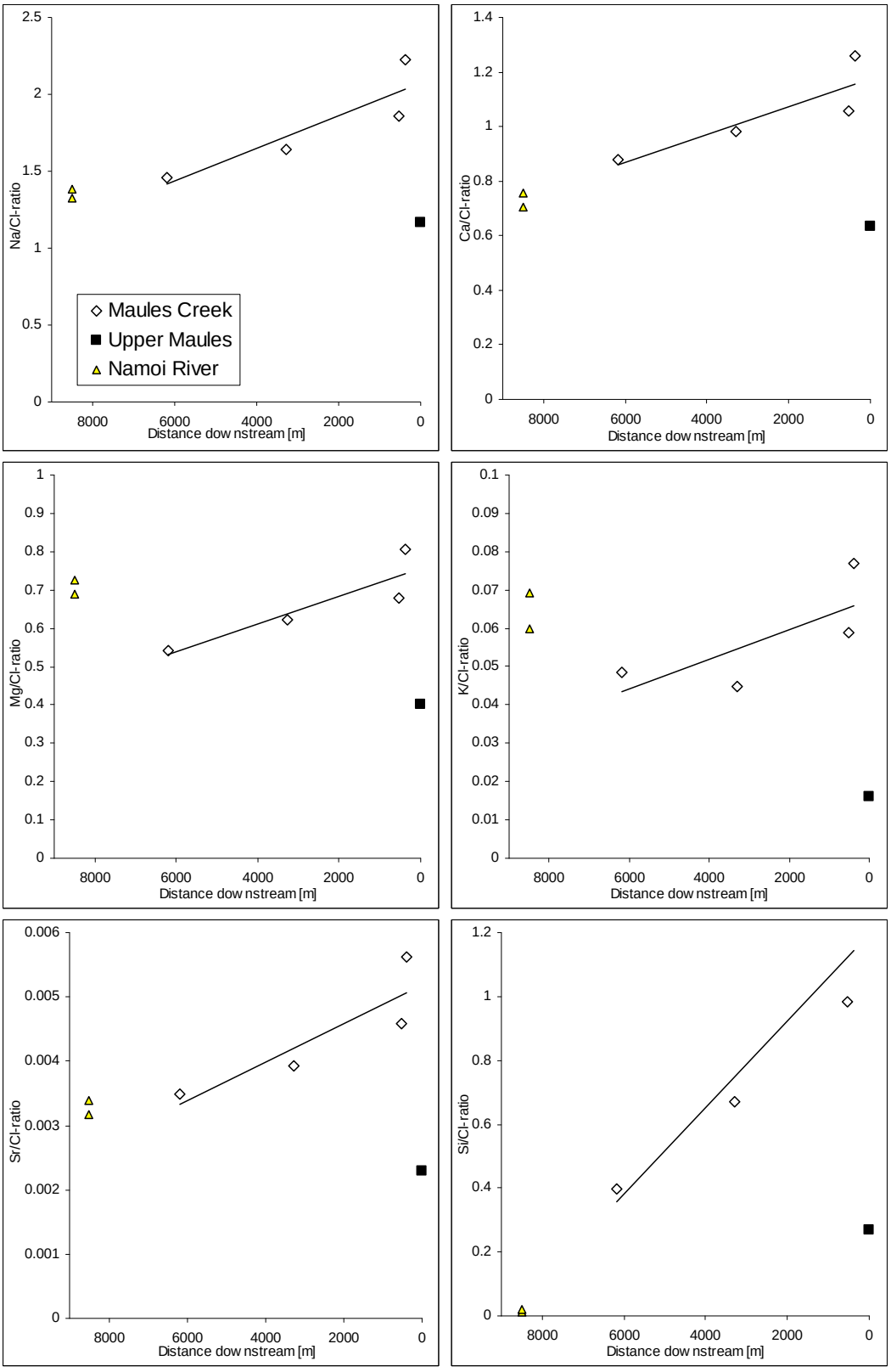

Fig. A.9-1. selected ion/Cl^- ratios.

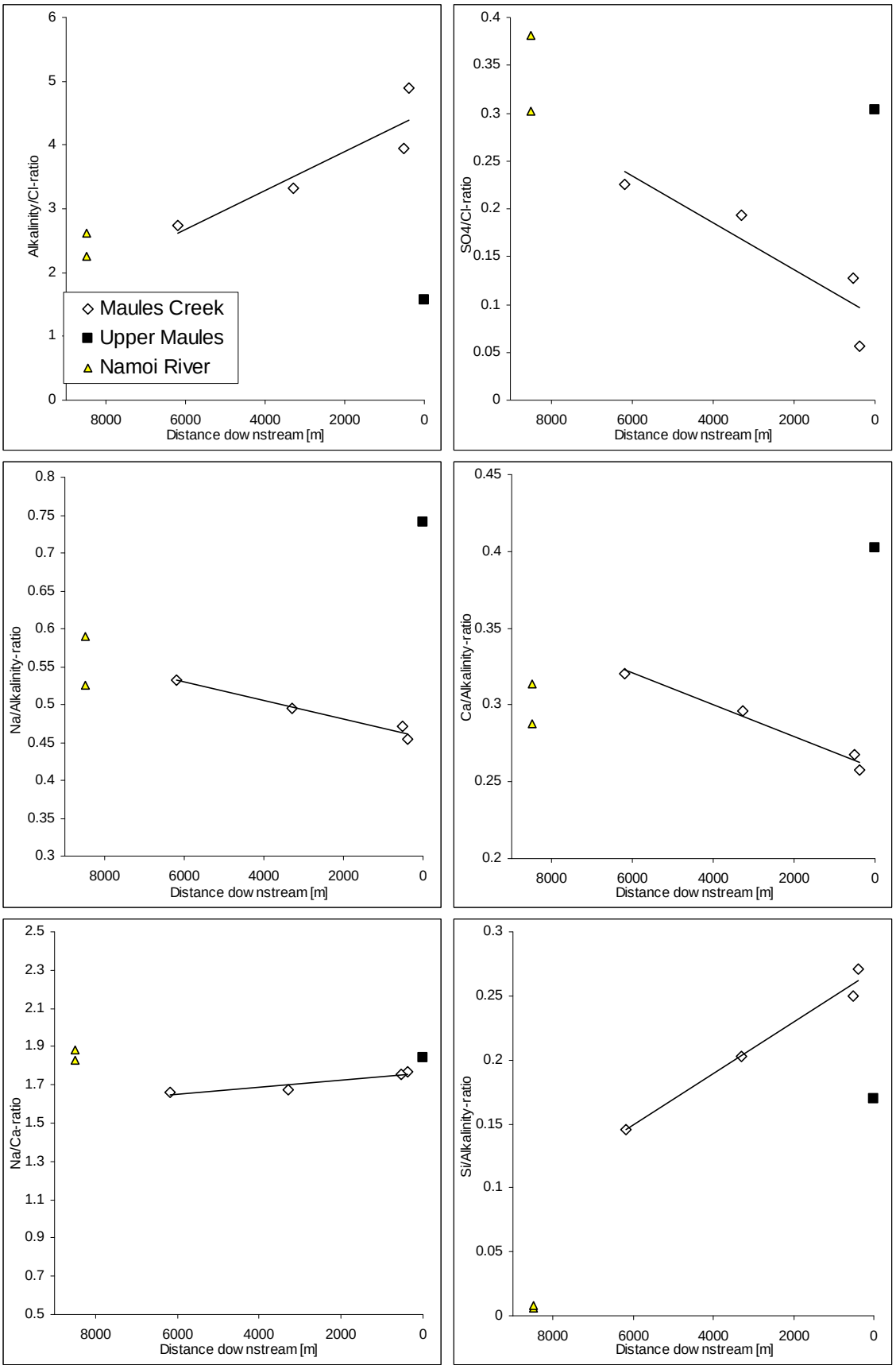

Fig. A.9-2. Additional ion ratios.

Appendix 10. Cross-section plots of Redox-chemistry along the Narrabri-Maules Creek Rd

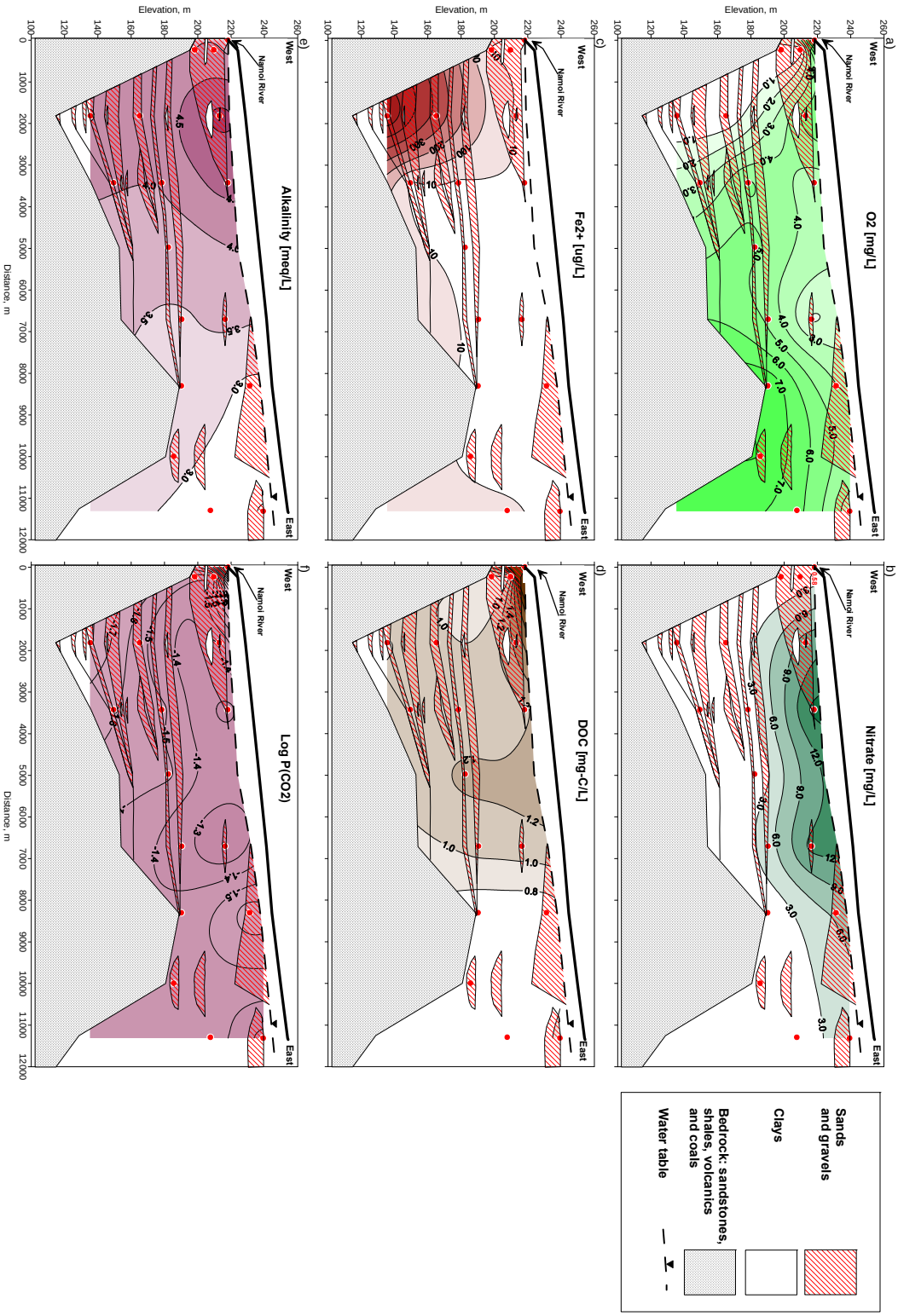

Fig. A.10-1. Cross-section of redox sensitive species along the Narrabri-Maules Creek Rd (for location see Fig. 3) showing a) Dissolved oxygen (O_2) [mg/L]; b) Nitrate (NO_3^-) [mg/L]; c) Ferrous iron (Fe^{2+}) [ug/L]; d) Dissolved Organic Carbon (DOC) [mg/L]; e) alkalinity (HCO_3^-) [meq/L]; and f) Log (P_{CO2}) calculated in PHREEQC.